Investigation of the LRRC8 subunit composition and the activating signal transduction of the volume-regulated anion channel (VRAC)

Inaugural-Dissertation

to obtain the academic degree

Doctor rerum naturalium (Dr. rer. nat)

submitted to the Department of Biology, Chemistry, Pharmacy

of Freie Universität Berlin

by

Sumaira Pervaiz

From Gujrat, Pakistan

Berlin, 2021

This work was prepared under the supervisor of Prof. Dr. Tobias Stauber at the

Freie Universität Berlin from May 2017 until July 2021.

The work entitled “Investigation of the LRRC8 subunit composition and the activating signal transduction of the volume-regulated anion channel (VRAC)” was solely undertaken by myself and no help was provided from other sources as those allowed. I have cited all sections of the thesis that use quotes or describe an argument or concept from another author, including all secondary literature used, to demonstrate that my argument is based on this material.

1st Reviewer: **Prof. Dr. Tobias Stauber**

BCP, Freie Universität Berlin

2nd Reviewer: **Prof. Dr. Helge Ewers**

BCP, Freie Universität Berlin

Date of defense: **10th December 2021**

Preface

Part of this work has been published in:

Pervaiz, S.; Kopp, A.; von Kleist, L.; Stauber, T. Absolute Protein Amounts and Relative Abundance of Volume-regulated Anion Channel (VRAC) LRRC8 Subunits in Cells and Tissues Revealed by Quantitative Immunoblotting. *Int. J. Mol. Sci.* 2019, *20*, 5879. https://doi.org/10.3390/ijms20235879

Part of the experiments in the thesis were performed by others, as depicted in the results section.

Acknowledgements

I would like to express my deepest and sincere gratitude to my supervisor, Prof. Dr. Tobias Stauber, for providing me the great opportunity of working in his lab and providing me with endless support, patience, and enthusiasm throughout this time. His guidance helped me a lot in all the time of research and writing of this thesis. I could not have imagined a better advisor and mentor for my Ph.D. study.

I would like to thank Prof. Dr. Helge Ewers for reviewing my PhD thesis.

I would also like to thank all of my former colleagues; Lisa von Kleist, Antje Buttgereit, Benjamin König, Tianbao Liu and Lingye Chen for their help, encouragement and support. Special thanks to Lingye Chen for introducing me to all the lab protocols and techniques and sharing her experiences about VRAC and Benjamin König for introducing me to the microscopy. I would like to thank Shroddha Bose for the delightful lunch discussions and her valuable suggestions on my project. I would also like to thank Yulia Kolobkova for proof-reading my thesis.

My thanks go to my parents, Pervaiz Iqbal and Naghmana Nargis for their prayers and support. Special thanks to my Father who always supported me to pursue my passion to become a scientist and for believing in me. **I dedicate my work to my Father** who helped me become who I am!

A special thank you goes to my Husband Hamid Raza, who is my biggest supporter, and who has provided me with unconditional love, motivation, and encouragement that helped me successfully complete my Ph.D. study. Life has been a rollercoaster, and is worth riding with you!

My journey would not be the same without my lifeline, my son Azaan. It was fun explaining to you what I do in my lab and listening to how you perceived it; "MAMA, I know, you work with germs!!

Last but not the least, I would like to thank rest of my family especially my parents-in-law for their continuous support, encouragement and prayers, my brother Sufyan, all my friends, and colleagues of AG Ewers, AG Stricker, AG Freund, and AG Knaus for letting me use their laboratory equipment and devices.

Table of Contents

List of Figures

List of Tables

List of Abbreviations

AC	adenylyl cyclase
ANOVA	analysis of variance
ATP	adenosine triphosphate
AVD	apoptotic volume decrease
BRET	bioluminescence resonance energy transform
C2	two-fold rotational symmetry
C3	three-fold rotational symmetry
C6	six-fold rotational symmetry
CFP	cyan-fluorescent protein
CFTR	cystic fibrosis transmembrane conductance regulator
cGAMP	2′3′cGMP-AMP
ClC-2	chloride channel 2
DAG	diacylglycerol
DCPIB	4-(2-butyl-6,7-dichloro-2-cyclopentyl-indan-1-on-5-yl) oxybutyric acid
DDA	2′,3′-dideoxyadenosine
DMR	dynamic mass redistribution
DMSO	dimethyl sulfoxide
DNA	deoxyribonucleic acid
DPBS	Dulbecco's phosphate-buffered saline
EAA	excitatory amino acids
EAT	Ehrlich ascites tumor cells
ECD	extracellular domain
EDTA	ethylenediaminetetraacetic acid
EL	extracellular loop
ER	endoplasmic reticulum
ERK	extracellular signal-regulated kinase
ESD	extracellular subdomain
FADD	fas-associated death domain protein
FBS	fetal bovine serum
FRET	fluorescence resonance energy transfer
GAPDH	glyceraldehyde 3-phosphate dehydrogenase
GM130	Golgi matrix protein 130
GPCR	G protein-coupled receptor

GPCR5A	G protein-coupled receptor 5A
GST	glutathione-S-transferase
GTP	guanosine-5'-triphosphate
HEPES	4-(2-hydroxyethyl)-1-piperazineethanesulfonic acid
HRP	horseradish peroxidase
I^{AA}	intensity measured with acceptor excitation and acceptor emission, acceptor channel
$ICl_{(swell)}$	swelling-induced chloride conductance
I^{DA}	intensity measured with donor excitation and acceptor emission, FRET channel
I^{DD}	intensity measured with donor excitation and donor emission, donor channel
IL	intracellular loop
IP3	inositol trisphosphate
IPTG	isopropyl β-D-1-thiogalactopyranoside
LPA	lysophosphatidic acid
LRR	leucine-rich repeat
LRRC8	leucine-rich repeat-containing protein family 8
LRRCT	leucine-rich repeat C terminus
LRRD	leucine-rich repeat domain
LRRNT	leucine-rich repeat N terminus
LUT	look-up table
MAPK	mitogen-activated protein kinase
MLC	megalencephalic leukoencephalopathy with cysts
NADPH	nicotinamide adenine dinucleotide phosphate
NKCC	Na-K-Cl cotransporter
NOX	NADPH oxidase
NTC	N-terminal coil
NTH	N-terminal helix
PA	phosphatic acid
PBS	phosphate buffer saline
PCR	polymerase chain reaction
PDGF	platelet derived growth factor
PI3K	phosphatidyl-inositol 3-kinase
PIP2	phosphatidylinositol-4,5-bisphosphate
PIP3	phosphatidylinositol-3,4,5-triphosphate
PKA	protein kinase A

PKC	protein kinase C
PKD	protein kinase D
PLC	phospholipase C
PTP	protein tyrosine phosphatase
PTX	pertussis toxin
Raig2	retinoic acid-inducible orphan G protein-coupled receptors
ROI	region of interest
ROS	reactive oxygen species
RVD	regulatory volume decrease
RVI	regulatory volume increase
s.e.m	standard error of mean
S1P	sphingosine-1-phosphate
S1P1	sphingosine-1-phosphate receptor 1
S1PR	sphingosine-1 phosphate receptor
SCOS	sertoli cell-only syndrome
seFRET	sensitized emission FRET
siRNA	small interfering RNA
TMH	transmembrane helix
TNF	tumor necrosis factor α
TNFR	tumor necrosis factor α receptor
TRADD	tumor necrosis factor receptor type 1-associated DEATH domain
VRAC	volume-regulated anion channel
VSOAC	volume-sensitive organic osmolyte/anion channel
VSOR	volume-sensitive outwardly rectifying anion channel
WT	wild-type
YFP	yellow-fluorescent protein

Abstract

The volume-regulated anion channel (VRAC) plays a key role in the regulation of osmotic cell volume as well as in various physiological processes such as apoptosis, insulin secretion, cell differentiation, and purinergic signaling. It is formed by hetero-hexamers of members of the leucine-rich repeat-containing protein family 8 (LRRC8), which consists of five members, LRRC8A-E. LRRC8A is the obligatory subunit, and its heteromerization with at least one other LRRC8 paralogue, LRRC8B-E, determines VRAC's biophysical properties. Subunit stoichiometry of VRAC is of physiological importance and largely influences its activation mechanism, as well as its response to regulatory inputs. However, the endogenous tissue-specific subunit composition of VRAC remains unknown. Furthermore, despite extensive research on VRAC's possible physiological functions, there is little consensus on its activation mechanism.

In this thesis, I developed and applied a quantitative immunoblot method to quantify the five VRAC LRRC8 subunits in various mouse cell lines and tissues, using glutathione-S-transferase (GST)-tagged recombinant fusion proteins for signal calibration. The subunits showed tissue-specific expression patterns, with relatively low expression of the obligatory LRRC8A subunit. Based on the co-immunoprecipitation of LRRC8B-E in excess with LRRC8A, I concluded that non-LRRC8A subunits predominate in native hetero-hexamers. In light of this information, I estimated ~10,000 VRACs per cell in the tested cell lines, which is consistent with an earlier calculation from the comparison of single-channel and whole-cell currents.

Furthermore, I assessed VRAC activity by a Förster-resonance energy transfer (FRET)-based approach upon induction of apoptosis, sphingosine-1-phosphate (S1P)-induced signaling, and glucose feeding in pancreatic β-cells. I found that the pharmacological inhibition of protein kinase D (PKD) impaired the apoptotic-induced VRAC activation. Interestingly, signaling via S1P appeared to be mediated by an alliance between S1P receptors, specifically the Gq-coupled S1P receptors. I proposed that the Gq family of heterotrimeric G-proteins served as central mediators of the diacylglycerol (DAG)-PKD mediated VRAC activation induced by S1P in HeLa cells. PKD may phosphorylate VRAC, thereby activating it. This notion is supported by the observation that hypotonic activation of phospho-ablative LRRC8A mutant 8A-T169A is diminished due to the loss of the putative phosphorylation site. Lastly, I showed that an orphan G protein-coupled receptor (GPCR), GPCR5B, adversely modulated the VRAC activity in rat pancreatic β-cells, which may affect β-cell survival and insulin secretion. All in all, these results indicate a possible signaling pathway of VRAC activation, highlighting the importance of membrane-localized GPCRs and G-proteins in signal transduction.

Zusammenfassung

Die volumenregulierten Anionenkanäle (VRAC) spielen eine Schlüsselrolle bei der osmotischen Regulation des Zellvolumens sowie bei verschiedenen physiologischen Prozessen wie Apoptose, Insulinsekretion, Zelldifferenzierung und purinerger Signalübertragung. Es wird von Hetero-Hexameren der *Leucine-Rich Repeat-Containing Protein Family 8* (LRRC8) gebildet, die aus fünf Mitgliedern, LRRC8A-E, besteht. LRRC8A ist die obligatorische Untereinheit, und ihre Heteromerisierung mit mindestens einem anderen LRRC8-Paralog, LRRC8B-E, bestimmt biophysikalische Eigenschaften von VRAC. Die Untereinheiten-Stöchiometrie von VRAC ist von physiologischer Bedeutung und beeinflusst weitgehend seinen Aktivierungsmechanismus sowie seine Reaktion auf regulatorische Signale. Die endogene gewebespezifische Untereinheitenzusammensetzung von VRAC ist jedoch weitestgehend unbekannt. Darüber hinaus gibt es trotz umfangreicher Forschung über die möglichen physiologischen Funktionen von VRAC wenig Konsens darüber, wie er aktiviert wird.

In dieser Arbeit habe ich eine quantitative Immunoblot-Methode entwickelt und angewandt, um die fünf VRAC LRRC8-Untereinheiten in verschiedenen Maus-Zelllinien und -Geweben zu quantifizieren, wobei rekombinante Fusionsproteine mit Glutathion-S-Transferase (GST)-Markierung zur Signalkalibrierung verwendet wurden. Die Untereinheiten zeigten gewebespezifische Expressionsmuster, mit relativ geringer Expression der obligatorischen Untereinheit LRRC8A. Basierend auf der Co-Immunpräzipitation von LRRC8B-E im Überschuss mit LRRC8A schloss ich, dass Nicht-LRRC8A-Untereinheiten in nativen Hetero-Hexameren überwiegen. In Anbetracht dieser Informationen berechnete ich das Vorkommen auf ~10.000 VRACs pro Zelle in den getesteten Zelllinien, was mit einer früheren Berechnung aus dem Vergleich von Einzelkanal- und Ganzzellströmen übereinstimmt.

Darüber hinaus habe ich die VRAC-Aktivität mittels Förster-Resonanz-Energie-Transfer (FRET)-basiertem Ansatz bei der Induktion von Apoptose, Sphingosin-1-Phosphat (S1P)-induzierter Signalgebung und Glukose-Stimulation in pankreatischen β-Zellen untersucht. Ich fand heraus, dass die pharmakologische Hemmung der Proteinkinase D (PKD) die apoptose-induzierte VRAC-Aktivierung beeinträchtigte. Interessanterweise wird die Signalisierung durch S1P über eine Allianz zwischen S1P-Rezeptoren, speziell den Gq-gekoppelten S1P-Rezeptoren, vermittelt. Dies deutet darauf hin, dass die Gq-Familie der heterotrimeren G Proteine als zentrale Vermittler der durch S1P induzierten Diacylglycerol (DAG)-PKD-vermittelten VRAC-Aktivierung in HeLa-Zellen dienen. PKD kann VRAC phosphorylieren und ihn dadurch aktivieren. Diese Vorstellung wird durch die Beobachtung unterstützt, dass die hypotone Aktivierung der phospho-ablativen

LRRC8A-Mutante 8A-T169A aufgrund des Verlustes der möglichen Phosphorylierungsstelle vermindert ist. Schließlich habe ich gezeigt, dass einn *orphan* G Protein-gekoppelten Rezeptor (GPCR), GPCR5B, die VRAC-Aktivität in pankreatischen β-Zellen der Ratte negativ moduliert und damit das Überleben der β-Zellen und die Insulinsekretion beeinflusst. Alles in allem weisen diese Ergebnisse auf einen möglichen Signalweg der VRAC-Aktivierung hin und unterstreichen die Bedeutung von membranständigen GPCRs und G Proteinen in der Signaltransduktion.

1. INTRODUCTION

1.1. Cell volume regulation and the regulatory mechanisms

With only a few exceptions, animal cell membranes are highly permeable to water. Water permeability is several orders of magnitude higher as compared to the cell's main inorganic osmolytes, Na^+, K^+ and Cl^-. Hence, the cellular water content and the cell volume depends on the concentration of intracellular osmolytes and extracellular tonicity (Hoffmann et al, 2009). Cells are constantly challenged by osmotic perturbations leading to cell volume fluctuations even under steady state physiological conditions. However, most of the cells can counteract these alterations through restoration processes. Cells facing swelling due to extracellular hypotonicity undergo regulatory volume decrease (RVD) by loss of K^+, Cl^-, non-essential osmolytes and water; and under hypertonic shrinkage they restore their original volume by regulatory volume increase (RVI) by a net gain of K^+, Cl^-, organic osmolytes and osmotically obliged water (Hoffmann et al, 2009; Hoffmann & Simonsen, 1989; Okada et al, 2001). During regulatory volume decrease, most cells extrude K^+ ions through K^+ channels (Chen & Simard, 2001; Farrugia & Rae, 1993; Okada et al, 2001; Sandford et al, 1992). In order to maintain electroneutrality, following K^+ efflux there should be a concomitant anion efflux. This anion efflux can be carried out by volume-sensitive chloride channels that have been reported in various cell types (Doroshenko & Neher, 1992; Jentsch, 1996; Nilius et al, 1994; Strange et al, 1996). One such ubiquitously expressed (Chen et al, 2019b; Nilius et al, 1997a; Nilius et al, 1994; Pedersen et al, 2016; Strange et al, 1996; Strange et al, 2019) and volume-stimulated channel is called volume-regulated anion channel (VRAC) alternatively named as volume-sensitive outward rectifying anion channel (VSOR) (Okada, 1997) or volume-sensitive osmolyte/anion channel (VSOAC) (Strange et al, 1996).

1.2. The volume-regulated anion channel (VRAC)

The first electrophysiological measurements of VRAC-mediated anion currents date back to the late 1980s (Cahalan & Lewis, 1988; Hazama & Okada, 1988). Soon after, these VRAC currents were reported to have several common functional characteristics such as mild outward rectification, variable inactivation at inside positive potentials (Jackson & Strange, 1995; Voets et al, 1997), and high selectivity of anions over cations (Kubo & Okada, 1992; Lewis et al, 1993) wherein the anionic permeability sequence is according to Eisenman's sequence I with $I^- > NO_3^- > Br^- > Cl^- > F^-$ (Akita & Okada, 2014; Nilius & Droogmans, 2003; Strange et al, 2019). In addition to these anions, VRAC also conducts large structurally diverse organic osmolytes such as taurine

and *myo*-inositol (Hand et al, 1997; Jackson & Strange, 1993; Kirk et al, 1992; Qiu et al, 2014; Voss et al, 2014). Though VRAC's biophysical properties had been extensively studied for nearly three decades, its molecular identity remained enigmatic until 2014, when two groups simultaneously identified LRRC8A, a member of leucine-rich repeat-containing (LRRC8) proteins, as being crucial for channel formation. Both groups conducted genome-wide siRNA screens and found that siRNA targeting LRRC8A reduced the yellow fluorescent protein (YFP) quenching caused by hypotonicity-induced I^- influx through VRAC (Qiu et al, 2014; Voss et al, 2014). Knock-down of LRRC8A also markedly suppressed the swelling induced chloride current mediated by VRAC, $ICl_{(swell)}$ (Qiu et al, 2014; Voss et al, 2014), suggesting it is indispensable for volume-sensitive channel formation. The LRRC8 protein family comprises five members, LRRC8A-LRRC8E. Interestingly, overexpression of LRRC8A in HEK cells decreased the $ICl_{(swell)}$ indicating VRAC contains LRRC8A as a part of a heteromer and its overexpression leads to incompatible subunit stoichiometry with respect to channel activity (Qiu et al, 2014; Voss et al, 2014). Without LRRC8A, LRRC8B-LRRC8E are stuck in the endoplasmic reticulum (ER) when expressed alone, but reach the plasma membrane when co-transfected with LRRC8A (Voss et al, 2014). For functional and conducting VRAC channels, LRRC8A must heteromerize with at least one other LRRC8 subunit (Gaitán-Peñas et al, 2016; Syeda et al, 2016; Yamada & Strange, 2018).

1.3. The structure of VRAC channel

Abascal and Zordaya suggested that LRRC8 proteins form hexameric channels because of their sequence similarities with connexins, pannexins, and innexins (Abascal & Zardoya, 2012). A few years later, this notion was supported by the high-resolution cryo-EM structure of LRRC8A (Deneka et al, 2018; Kasuya et al, 2018; Kefauver et al, 2018; Kern et al, 2019) and LRRC8D homomers (Nakamura et al, 2020) and a low-resolution cryo-EM structure of LRRC8A/C heteromers (Deneka et al, 2018). The homo-hexamer and every subunit in the channel consist of four regions, the extracellular region, membrane-spanning transmembrane region (TM), an intracellular region in the N-terminal part, and a leucine-rich repeat (LRR) region in the C-terminal part with both N and C-terminus facing the cytoplasmic side of the cell (Figure 1 A, B). The transmembrane region (TM) consists of four TM helices (TMH1-TMH4). In the extracellular region, these helices are connected by two extracellular loops (ELs): EL1 connecting TMH1 and TMH2, and EL2 connecting TMH3 and TMH4. In the intracellular region, TMH2 and TMH3 are connected by an intracellular loop (IL1). IL2 connects the TMH4 with the N-terminus of the LRR region (Figure 1A). Recently, Nakamura and colleagues have discovered an additional N-terminal helix (NTH) formed by the N-terminal residues proceeding the TMH1 in LRRC8D homomers that

protrudes into the channel pore (which will be discussed shortly hereafter), which was not previously discovered in the LRRC8A homomers (Nakamura et al, 2020).

The EL1 has one α-helix (EL1H) and one β strand (EL1β), part of a glycosylated amino acid stretch (Voss et al, 2014) between EL1H and EL1β is still unresolved in all the reported structures. EL2 has two β-strands EL2β1 and EL2β forming an antiparallel β-sheet with EL1β. On the intracellular side, the intracellular loop IL1 has three α helices (IL1H1-ILH3) with an unresolved stretch between second and third helices that has several putative phosphorylation sites (Abascal & Zardoya, 2012) while IL2 consists of four α helices (ILH1-ILH4) (Figure 1A).

1.3.1. Channel pore and LRR domains

Along the central axis of the membrane, the homomers form a channel pore that is perpendicular to the membrane and is divided into three domains. The long central domain consisting of the transmembrane part (TM) and two flanking subdomains: one on the extracellular side called the extracellular subdomain (ESD) and the other towards the cytoplasm termed as the cytoplasmic sub domain (CSD) (Figure 1C). The extracellular loops EL1 and EL2 form the extracellular domain (ESD) of the channel pore and are stabilized by three disulfide bonds representing the constricted region of the pore domain with a diameter of 2.9 Å at its constriction (Deneka et al, 2018). This narrowing, located at the N-terminus of the α-helix E1H, has an arginine (R103), whose side chain points in the direction of the pore axis and forms a highly electropositive selectivity filter for the size and charge of anions during permeation in anion-selective channels. Mutation of this arginine to phenylalanine, in LRRC8A-R103F+LRRC8C heteromeric channels, resulted in altered selectivity for Cl^- and insensitivity to external ATP block (Kefauver et al, 2018). Furthermore, three residues, K98, Y99, and D100 located in the loop preceding the EL1H, face the extracellular side of the channel pore. Electrophysiological analysis involving the single and combination mutants reported that these residues are crucial in voltage-dependent channel inactivation and anion selectivity (Ullrich et al, 2016).

According to sequence alignment, an aromatic ring of phenylalanine Phe143 forms the most constricted site of the pore domain in LRRC8D homomers, with a diameter of 11.5 Å (Nakamura et al, 2020). This value is close to the pore diameter of native VRACs i.e., 11.4-14.2 Å (Droogmans et al, 1999; Ternovsky et al, 2004). The pore diameter ranges from 7.6-9.6 Å in the LRRC8A homomers (Deneka et al, 2018; Kasuya et al, 2018; Kefauver et al, 2018; Kern et al, 2019), meaning that the pore diameter at the most constricted extracellular side is narrower in LRRC8A than in LRRC8D homomers (Nakamura et al, 2020). Assuming the possibility of different

LRRC8 protein-containing heteromers under physiological conditions, this can be a plausible structural explanation of the increased permeability of LRRC8D heteromers toward larger osmolytes (Lee et al, 2014; Lutter et al, 2017; Planells-Cases et al, 2015). In the membrane, this pore widens and consists of residues from TM1 and TM2 on its intracellular side (Deneka et al, 2018). Additionally, within this region, the interface between subunits is less tightly packed and contains gaps that are probably glued together by lipids (Deneka et al, 2018). The presence of these lipids might be useful for channel assembly or/and in stabilizing the upper transmembrane domains against the movements in the LRR domains (Kern et al, 2019). For instance, in the case of Innexin-6, lipid molecules in the inter-subunit space are thought to stabilize the conformation of the helix bundles (Oshima et al, 2016). Two threonines of the TMH1 constitute the channel pore at positions 44 and 48 (T44 and T48). In one study, mutating the T44 to cysteine altered the I^- vs Cl^- anion selectivity (Qiu et al, 2014). A similar alteration in I^- permeability was found for the equivalent threonines in LRRC8C, LRRC8D, and LRRC8E (Syeda et al, 2016). Following this, another threonine at position 48 (T48) contributes to the selectivity filter. TMH3 and TMH4 face the lipid environment of the membrane. Moving down toward the boundary of the TM region and the intracellular region, the first 14-17 amino-terminal residues are not resolved in any of the reported structures, but as with the structurally closely related connexins and innexins, an N-terminal coil (NTC) projects into the channel pore (Maeda et al, 2009; Oshima et al, 2016). It is therefore likely that in the VRAC channel, these undefined disordered amino acid stretches may form the NTC.

Below the TM domain, is the cytoplasmic subdomain (CSD) which is formed by a meshwork of IL α-helices and constitutes the channel exit leading to the cytoplasmic LRRD. The LRRD consists of a leucine-rich repeat N-terminal helix (LRRNT), 15 leucine-rich repeats (LRR1-LRR15), and a leucine-rich repeat C-terminal helix (LRRCT). Each LRR repeat consists of a β-strand followed by an α-helix on the N-terminal side, which contributes to the interaction with LRRDs of neighboring subunits at the C-terminus (Figure 1 A, C).

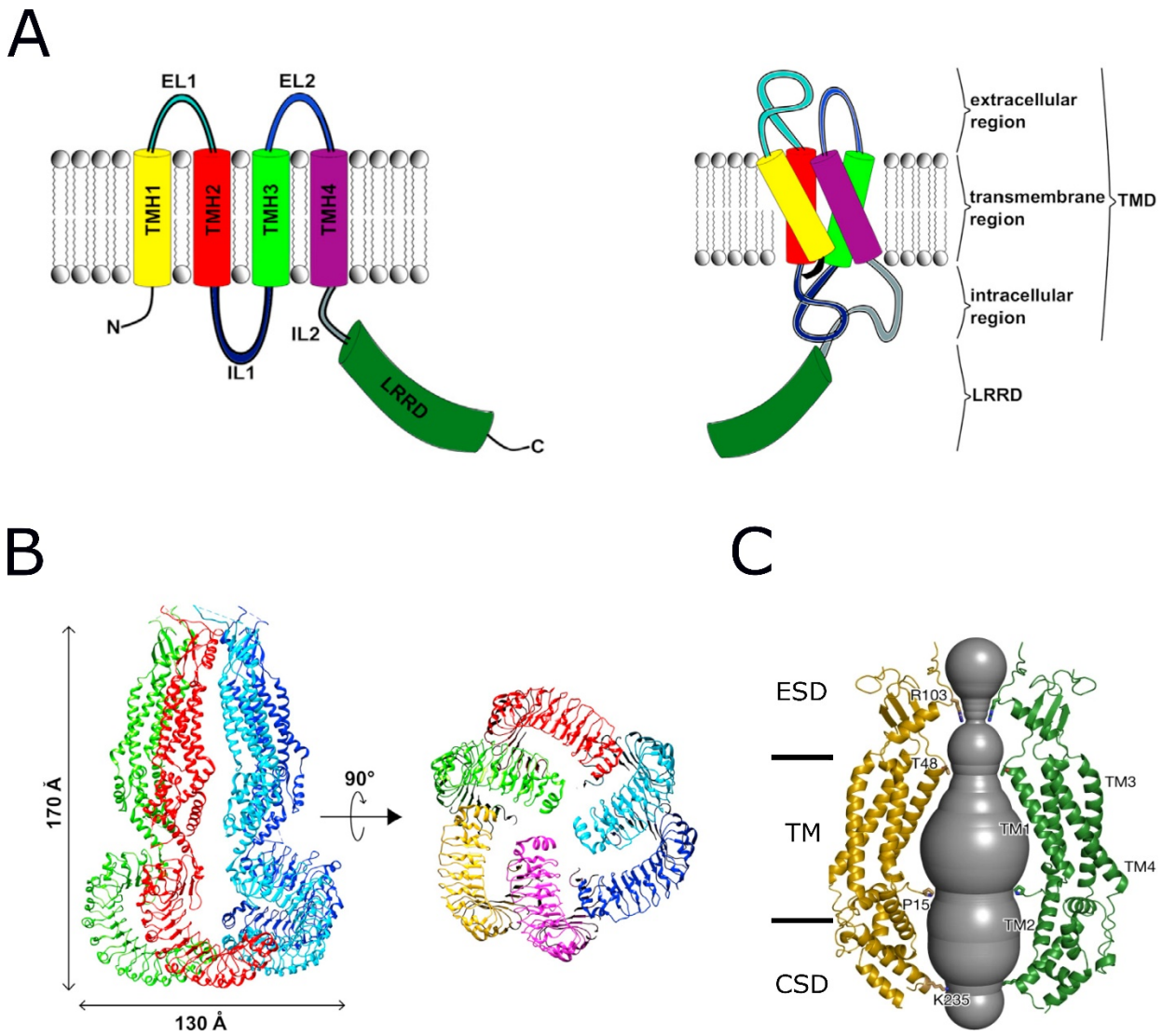

Figure 1. Structure of VRAC. (A) Schematic diagram of a single LRRC8 protein (left) and of the structure of a single LRRC8 subunit within a hexamer (right). (B) Ribbon representation of the hexameric LRRC8A channel structure (PDB 5ZSU (Kasuya et al, 2018)) viewed parallel to the membrane (two subunits in the back not shown for clarity, left) and from the intracellular side (right). Dashed lines represent loop regions of unsolved structure. Figure adapted from (Chen et al, 2019b). (C) LRRC8A pore domain as seen from the side of two opposite subunits, with selected resides shown (Deneka et al, 2018).

1.3.2. Channel symmetry

The hexameric LRRC8A structure was reported to be 170-180 Å long and 110-130 Å wide with all the subunits arranged around an axis of symmetry. Three of the reported structures showed a six-fold rotational (C6) symmetry for all the regions, including the extracellular, TM, and the intracellular region, except the LRR domain (Deneka et al, 2018; Kefauver et al, 2018; Kern et al,

2019), however, one study reported a C3 “trimer of dimer” symmetry in which the subunits have tight interactions with adjacent and a loose interaction with the neighboring subunit (Kasuya et al, 2018). One possible explanation of this difference in symmetry is due to the differences in the reconstitution of the channels. In nanodisc reconstituted structures, the hexamer adopts a conformation in which all the subunits are evenly spaced and the subunit gaps are filled by lipid moieties; however, in the structures solved in the lipid bilayer, the channel is forced to adopt a more compact conformation with smaller gaps that are incapable of lipid binding (Kern et al, 2019). Recently, the structure of human LRRC8D (HsLLRC8D) homomers was solved, showing a twofold symmetry “dimer of trimers” for LRRC8D, which is in contrast to the C3 or C6 symmetrical arrangement of previously reported LRRC8A homomers (Nakamura et al, 2020).

The symmetry of LRRDs is ambiguous as compared to the other regions in the solved structures. Three studies suggested a C3 symmetry, in which the interacting pairs of LRRDs are tightly packed with each other and more loosely with the LRRDs of the neighboring subunit. As a result, these pairs are oriented by 42 Å relative to each other, and all of them are tilted towards the membrane by approximately 30-40 Å. In simpler words, the LRR domains of each subunit in a hexamer can be visualized as having a horseshoe shape facing the pore axis. Although interacting, these LRR domains are quite flexible as indicated from the heterogenous LRRD arrangement in a subset of particles (Deneka et al, 2018; Kasuya et al, 2018; Kefauver et al, 2018). Due to the heterogeneous and disordered arrangement of LRRDs (Kasuya et al, 2018; Kern et al, 2019), it is plausible to assume different conformational rearrangements of LRRDs within a VRAC channel during gating. However, there is still ambiguity about the potential ligands for LRRDs, (Bryan-Sisneros et al, 2000), the role of phosphorylation events (Bryan-Sisneros et al, 2000; Okumura et al, 2009; Voets et al, 1998) and their impact on the channel activation.

1.4. Physiological and pathophysiological implications of VRAC

VRAC was initially analyzed using unspecific pharmacological inhibitors in order to determine its involvement in cellular processes. Therefore, defining the physiological significance of VRAC based on these preliminary findings is too vague. Nonetheless, with the molecular architecture of VRAC discovered recently, it should now be possible to assign specific functions to VRAC under cellular physiological and pathological states.

1.4.1. Electrogenesis

Cells have a basal K^+ and Cl^- conductance contributing to the resting membrane potential, with K^+ conductance higher than the Cl^- conductance. Small changes in the Cl^- conductance can induce drastic shifts in the membrane potential shifting it from a value close to K^+ equilibrium potential to the Cl^- equilibrium potential. Such changes in membrane potential due to the modulation of volume-sensitive Cl^- conductance influence the electrochemical gradient of ions across the cell membrane and the activity of various electrogenic transporters (Nilius et al, 1997a). One such effect can be seen in cardiac myocytes. Indeed, the swelling induced Cl^- conductance mediated by VRAC is important in the repolarization of cardiac myocytes, after a depolarizing action potential, during normal heart functioning (Vandenberg et al, 1994). Moreover, VRAC has also been involved in membrane depolarization contributing to insulin release from pancreatic β-cells (Stuhlmann et al, 2018). Pancreatic β-cells secrete insulin in response to a rise in serum glucose levels. Cellular uptake and metabolism of glucose resulted in high intracellular ATP levels, which inhibits the ATP-sensitive K^+ channels causing membrane depolarization and activation of voltage-dependent Ca^+ channels. Ca^+ then enters the cell transiently and triggers the exocytosis of insulin granules (Ashcroft & Rorsman, 2013; Rorsman & Braun, 2013). Consistent with a long-standing hypothesis, (Best et al, 2010) two independent studies simultaneously showed that in pancreatic β-cells, hypotonicity-induced or glucose-induced swelling activates LRRC8A-dependent VRAC currents, which causes membrane depolarization and subsequent electrical excitation. Notably, mice with β-cell specific LRRC8A genomic disruption had normal serum glucose levels, but reduced glucose tolerance (Kang et al, 2018; Stuhlmann et al, 2018).

1.4.2. Epithelial cell volume regulation

Animal cells are subjected to transmembrane osmotic gradients under a range of physiological conditions, including metabolic activities generating or requiring osmotically active substances, transport of ions/nutrients followed by osmotically obliged water, or during altered extracellular osmolarity (Hoffmann et al, 2009). In this respect, epithelial cells are of particular interest. Due to the frequent secretion and absorption of osmolytes, these cells face a constant need for volume regulation. Notably, in the case of absorptive epithelia, there is a Na^+-coupled uptake of glucose and amino acids leading to differential osmolyte concentration and eventually to cell swelling. This must be contracted by extrusion of K^+ and Cl^-, mainly over the basolateral membrane. These anionic extrusions are thought to be mediated by VRAC in epithelial cells, which helps to maintain their integrity (Pedersen et al, 2013).

1.4.3. VRAC in cell proliferation and migration

VRAC has also been involved in fundamental cellular processes such as proliferation and migration. During cell proliferation, there is a temporary cell swelling as a parent cell divides into cells of smaller size. The swelling is caused by the disinhibition of a NHE Na^+/H^+ exchanger and/or a NKCC Na^+, K^+, $2Cl^-$ transporter, followed by transient activation of Cl^- channels, which lead to a decrease in the cell volume. VRAC is one of the key mediators of this decrease in cell volume after an initial increase (Lang et al, 2006). Furthermore, differences in VRAC currents were noted during different phases of the cell cycle in a variety of cell types (Doroshenko et al, 2001; Klausen et al, 2007; Shen et al, 2000). For example, in Ehrlich Lettre ascites, $ICl_{(swell)}$ was high in the G0, less in the G1 phase, and increased again in the early S1 phase to a higher level as compared to the G0 phase (Klausen et al, 2007). Some of the studies using (rather non-specific) pharmacological inhibitors of VRAC showed inhibition of proliferation in many different cell types including human carcinogenic glioblastoma cells (U251 and U87) (He et al, 2012; Klausen et al, 2007; Liang et al, 2014; Maertens et al, 2001; Voets et al, 1995; Wong et al, 2018). In particular, siRNA-mediated knock-down of LRRC8A in glioblastoma cells inhibited their proliferation (Rubino et al, 2018). This pointed out the pathophysiological significance of VRAC in regulating tumor growth; on the other hand, some studies showed that VRAC might not be essential for cell proliferation (Chen et al, 2019a; Sirianant et al, 2016; Xue et al, 2018), including one study from our lab on various cancer cell lines (Liu & Stauber, 2019).

Cell migration is crucial to tissue homeostasis in health and disease. Cell motility is driven by directed membrane transport and cytoskeletal rearrangements. Notably, a repetitive cycle of protrusion at the leading edge of the cell followed by retraction at the trailing end causes a cell to migrate with local volume changes (Schwab et al, 2012). These volume fluctuations are caused by the differential activity of several ion channels and transporters, e.g., the locally active Na^+-K^+-$2Cl^-$ cotransporter (Haas & Sontheimer, 2010) and the Na^+/H^+ exchanger at the cell front causing uptake of inorganic ions and water leading to (RVI), and K^+ and Cl^- channels that cause a regulatory volume decrease (RVD) at the rear side via extrusion of K^+ and Cl^- followed by osmotically obliged water (Schwab et al, 2012). Since VRAC is a key player in RVD so we cannot exclude the possibility of its involvement in counteracting volume fluctuations during cell migration. Experimental findings confirmed this as well (Mao et al, 2007). For example, in microglial cells, glycine-induced cell swelling causes cell migration (Kittl et al, 2018). Consistently, 4-(2-butyl-6,7-dichloro-2-cyclopentyl-indan-1-on-5-yl) oxybutyric acid (DCPIB) that inhibited $ICl_{(swell)}$ also significantly reduced the migration of glioblastoma cell lines (Wong et al, 2018) and

siRNA knock-down of LRRC8A resulted in impaired migration in human colon cancer HCT116 cells (Zhang et al, 2018). Moreover, in an artificially confined microenvironment, cell migration was driven by osmotic water permeation and osmolyte flux even when actin polymerization was inhibited (Stroka et al, 2014). Despite these findings, a recent study conducted by our group showed that VRAC is not only dispensable for cell proliferation, but also migration (Liu & Stauber, 2019).

1.4.4. Apoptosis and apoptotic volume decrease (AVD)

Another cell process that contributes to the physiological significance of VRAC is the apoptotic volume decrease (AVD) during programmed cell death. Cell shrinkage is an early prerequisite of apoptosis (Ernest et al, 2008; Maeno et al, 2000) not strictly though, but often associated with progression of apoptosis (Bortner & Cidlowski, 1998; Lang & Hoffmann, 2012; Orlov et al, 2013). VRAC can indeed be activated under isotonic conditions by inducers of mitochondrion-mediated apoptosis such as staurosporine, death receptor-mediated apoptosis-inducers such as Fas-ligand (Okada et al, 2006; Shimizu et al, 2004), and platinum-based anticancer drugs such as cisplatin (Gradogna et al, 2017a; Ise et al, 2005; Planells-Cases et al, 2015). Further studies showed that pharmacological inhibition of VRAC impaired the apoptosis induced by the bacterial alkaloid staurosporine (STS) in HeLa cells (Hasegawa et al, 2012) or sodium butyrate-triggered apoptosis in murine colonic epithelial cells (Shimizu et al, 2015). Various cancer lines that were resistant to anti-cancer drug cisplatin also displayed an impaired VRAC activity (Lee et al, 2007; Min et al, 2011; Poulsen et al, 2009). In addition, in cisplatin-mediated apoptosis, VRAC not only contributes to the progression of apoptosis through its role in AVD but also mediates approximately half of the cellular uptake of cisplatin under isotonic conditions. The cisplatin uptake is mediated by LRRC8A/D heteromers. Notably, both LRRC8A and LRRC8D were identified in a genome-wide screen for carboplatin resistance. Genomic disruption of LRRC8A or LRRC8D strongly reduced cellular uptake of cisplatin and carboplatin under isotonic conditions, and low expression levels of LRRC8D correlated with a significantly reduced survival rate of ovarian cancer patients treated with platinum-based drugs (Planells-Cases et al, 2015).

1.4.5. Regulatory volume decrease (RVD) and signaling in the brain

Ischemic events in the heart and brain often lead to pathological cell swelling. VRAC is reported to have both physiological and pathological roles in the brain (Akita & Okada, 2014; Chen et al, 2019b; Elorza-Vidal et al, 2019; Mongin, 2016). Several studies demonstrated that astrocytes and

microglia release excitatory amino acids (EAAs) like glutamate via VRAC in response to hypotonic stimulation, or bradykinin which is released after brain injury, or in response to purinergic signaling (Akita et al, 2011; Benfenati et al, 2009; Harrigan et al, 2008; Kimelberg et al, 1990; Liu et al, 2009; Liu et al, 2006; Mongin & Kimelberg, 2002; Roy, 1995). The EAA release from astrocytes is important for astrocyte-neuron communication, neuronal excitability, and synaptic transmission. However, excessive release from swollen astrocytes during ischemic brain injury leads to excitotoxicity causing neuronal cell death (Lai et al, 2014). In fact, numerous studies described that pharmacological inhibition of VRAC reduces ischemic damage to the brain (Feustel et al, 2004; Inoue et al, 2007; Vakili et al, 2009; Zhang et al, 2008). Importantly, *Lrrc8a*$^{-/-}$ mice exhibited impaired glutamatergic transmission resulting in learning and memory deficits and provided neuroprotection from ischemic stroke (Yang et al, 2019).

1.4.6. VRAC and sperm development

Ion channels seem to play an important role in physiological sperm RVD, as during spermatogenesis, male germ cells encounter an osmotic shock from 350 mOsm in the seminiferous tubule to 290 mOsm in the rete testis (Yeung et al, 2006). Notably, a spontaneous mouse mutant *ébouriffé (ebo)*, that displayed infertility with a reduced number of spermatids having highly disorganized flagella and abnormal acrosomes (Lalouette et al, 1996), was recently found to have a mutation that truncated the cytoplasmic carboxyl terminus of LRRC8A (Platt et al, 2017) with virtually diminished VRAC activity. This mouse shared several phenotypic features with *Lrrc8a*$^{-/-}$ mice including abnormal wavy hair and curled vibrissae, infertility, tissue abnormalities, reduced postnatal survival but retained normal T-cell development and function not otherwise present in *Lrrc8a*$^{-/-}$ mice. Recently germ cell-specific, but not Sertoli-cell-specific disruption of *Lrrc8a* resulted in male infertility with malformed sperms having reduced motility. The cytoplasm of late spermatids was swollen and developed spermatozoa showed disorganized mitochondrial sheaths in the midpiece regions and flagellar coiling. The cytoplasmic swelling and the resulting phenotypes hint towards impaired volume regulation (Lück et al, 2018). Another study reported the same phenotypic features for germline-specific *Lrrc8a*$^{-/-}$ KO mice, constitutive *Lrrc8a*$^{-/-}$ and *ebo/ebo* mice (Bao et al, 2018). Importantly, this study also reported a human patient with a rare missense mutation in LRRC8A at R545H and possibly linked to Sertoli cell-only syndrome (SCOS), a male sterility disorder characterized by germ cell loss. However, it is doubtful that this mutation causes infertility, as R454H mutant reduced VRAC currents only by 25~30% when LRRC8A was expressed with LRRC8C or LRRC8D in *Xenopus* oocytes. Furthermore, the

mutation identified was heterozygous in patients of SCOS (Bao et al, 2018), while the heterozygous mouse model exhibited normal fertility (Kumar et al, 2014).

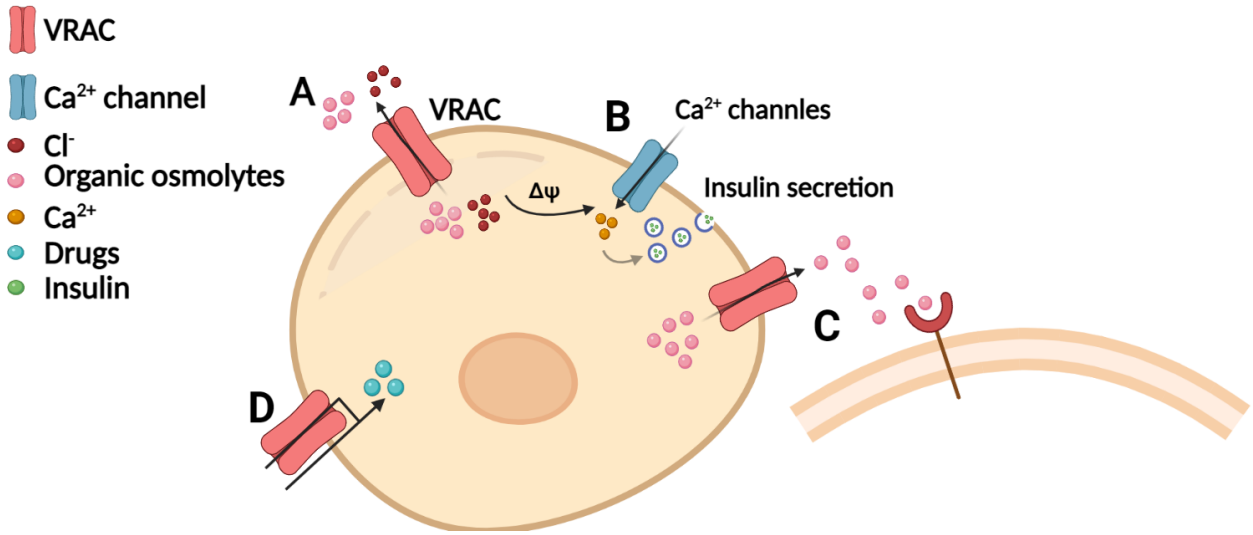

Figure 2. An illustration of VRAC's physiological functions. (A) Release of Cl^- and organic osmolytes leads to osmotic efflux of water and cell volume decrease. (B) VRAC opening shifts the plasma membrane potential towards the equilibrium potential of chloride, affecting the transport of other ions and the activity of ion channels. (C) VRAC conducted osmolytes act as signaling molecules. (D) Drug uptake (e.g., cisplatin) through LRRC8A/D heteromers causes VRAC activation, which leads to apoptotic volume decrease (AVD), and facilitates apoptosis. Figure modified from (Chen et al, 2019b).

1.5. VRAC's subunit composition and associated functions

As stated above, VRAC is formed by heteromers of LRRC8 proteins, with LRRC8A being indispensable (Qiu et al, 2014; Voss et al, 2014). Indeed, heteromerization of LRRC8A with the other family members has been shown by co-immunoprecipitation (Lee et al, 2014; Syeda et al, 2016; Voss et al, 2014) and by subcellular co-trafficking (Voss et al, 2014). The subunit stoichiometry is variable and depends on the relative expression levels of the LRRC8 paralogues (Gaitán-Peñas et al, 2016). Moreover, sequential co-immunoprecipitation showed that LRRC8A can combine with more than one other LRRC8 subunit in an individual VRAC complex (Lutter et al, 2017). Therefore, one can assume a large number of different VRACs having varying subunit compositions. Importantly, the differences in the subunit composition confer variability in the functional properties of the VRAC (Chen et al, 2019b; Syeda et al, 2016; Voss et al, 2014). For example, the single-channel conductance, depolarization-dependent inactivation, and extent of

rectification alter with the subunit that combines with the obligatory subunit LRRC8A in a functional channel (Syeda et al, 2016; Ullrich et al, 2016; Voss et al, 2014; Yamada & Strange, 2018). More important is the influence of the subunit composition in mediating the responses to regulatory mechanisms. Indeed, it was shown that VRAC channels are directly modulated by oxidation, with LRRC8A/E channels being activated and LRRC8A/C and LRRC8A/D channels being inhibited by oxidation of intracellular cysteines (Gradogna et al, 2017b). Subunit composition also affects substrate specificity. All subunit combinations of LRRC8A with LRRC8B-E mediate chloride currents, whereas the presence of LRRC8D in a heteromer makes it more specific and permeable towards larger organic osmolytes, such as taurine, myoinositol, lysine, anti-cancer drug cisplatin, and the antibiotic blasticidin (Lee et al, 2014; Lutter et al, 2017; Planells-Cases et al, 2015; Qiu et al, 2014; Voss et al, 2014). The negatively charged substrates like aspartate and glutamate are conducted by LRRC8A/C and LRRC8A/E other than LRRC8A/D heteromer (Lutter et al, 2017; Schober et al, 2017). Moreover, ATP is conducted far better by LRRC8A/E than LRRC8A/C (Gaitán-Peñas et al, 2016). Recently, LRRC8A/E containing VRACs were found to be important for the transport of cGAMP across the plasma membrane (Zhou et al, 2020). No substrate specificity has been assigned to LRRC8A/B heteromers so far.

The physiological importance of LRRC8A has been shown by the severe phenotype of the *Lrrc8a*$^{-/-}$ mice (Kumar et al, 2014) having increased prenatal and postnatal mortality, abnormal hair, growth retardation, sterility, tissue abnormalities, and defects in T-cell development and function (Kumar et al, 2014). Afterward, several studies using genomic disruptions or siRNA-mediated downregulation in a cell type-specific manner or in cell culture reported the physiological importance of LRRC8A (Chen et al, 2019a; Kang et al, 2017; Kumar et al, 2014; Lück et al, 2018; Yang et al, 2019; Zhang et al, 2017). LRRC8A is ubiquitously expressed in all vertebrates and was the first to be discovered among LRRC8 family, from a patient with congenital agammaglobulinemia who lacked circulating B cells and had minor facial anomalies (Sawada et al, 2003) So far, this is the only causative mutation identified in *Lrrc8a* and is associated with a human disease.

LRRC8B was reported to function as a Ca^{2+} leak channel in the endoplasmic reticulum (ER), as its overexpression and siRNA-mediated knock-down affected the ER Ca^{2+} dynamics in HEK cells (Ghosh et al, 2017). Nevertheless, this finding must be viewed cautiously in light of a previous finding by Voss and colleagues, who showed that LRRC8B localized to the ER when expressed alone and trafficked to the plasma membrane when co-transfected with LRRC8A (Voss et al, 2014). Furthermore, a recent proteomic study confirmed the plasma membrane localization of

LRRC8B (Orre et al, 2019). Conclusively, further studies need to validate the function of LRRC8B in ER.

LRRC8C was termed as the factor of adipocyte differentiation, *fad158* until the molecular identity of VRAC was identified in 2014, after which it was asserted to be a VRAC subunit (Tominaga et al, 2004). Surprisingly it was found that mice lacking LRRC8C gained less weight even when fed on a high-fat diet and knock-down of LRRC8C inhibited 3T3 adipocyte differentiation, while its overexpression promoted differentiation of NH-3T3 cells (Tominaga et al, 2004). Similar weight reduction in mice lacking adipocyte-specific LRRC8A was also observed, wherein it was associated with the affected insulin signaling (Zhang et al, 2017). Nonetheless, these findings point towards the involvement of VRAC in regulating adipocyte differentiation.

LRRC8D containing VRAC heteromers are well reported to have a diverse range of substrates, ranging from large organic osmolytes, amino acids, antibiotics, and neurotransmitters such as glutamate (Lee et al, 2014; Lutter et al, 2017; Schober et al, 2017). Thus, LRRC8A/D heteromers are likely to be involved in cell-to-cell communication and autocrine signaling. The involvement of LRRC8D in the uptake of the anti-cancer drug cisplatin in cancerous cells, followed by its reduced expression levels leading to a significant low survival rate of cancer patients makes it an interesting prognostic biomarker (Planells-Cases et al, 2015; Wang et al, 2018).

LRRC8E makes VRAC permeable for negatively charged substrates, such as glutamate, aspartate, and ATP (Gaitán-Peñas et al, 2016; Lutter et al, 2017; Schober et al, 2017). As these substrates can function as signaling molecules within cellular context, one can again speculate about LRRC8E being involved in cell-to-cell communication via VRAC. Recently two groups pointed an effective role of LRRC8A/E mediated bidirectional cGMP transport in innate immune response against viral infection (Lahey et al, 2020; Zhou et al, 2020).

1.6. VRAC activation and regulation

Many studies have been conducted to gain insight into the VRAC's regulatory mechanisms and the underlying players involved. However, most of them were compromised due to a lack of specific pharmacological tools and VRAC’s molecular nature. Many contradictions and misconceptions make it difficult to assign a generalized regulatory mechanism of VRAC in different cell types. All of the regulatory mechanisms being reported previously can be revised based on the recent structural models and molecular tools. The following section discusses the most important of these signaling cascades.

1.6.1. Mechanical activation

Cell volume itself, cannot be directly detected by the channel, there must be an intrinsic parameter that is altered upon volume change which eventually leads to channel activation. The idea of mechanical stretch in activating VRAC has been discarded, as several studies indicated that cell swelling is achieved without giving rise to a significant increase in membrane tension, at the expense of loss of multiple membrane infoldings or invaginations (Okada, 1997). Moreover, mechanosensitive Cl^- currents differed in their characteristics from VRAC currents, which could only be observed upon osmotic stimulus (Christensen & Hoffmann, 1992).

1.6.2. Actin cytoskeleton

Another hypothesis was the involvement of F-actin based cytoskeleton beneath the plasma membrane that maintains the integrity of membrane folds under isotonic conditions. The unfolding of these cytoskeletal elements under swelling conditions would result in a disruption of protein-protein interactions that could cause channel activation (Okada, 1997; Okada et al, 2019). Besides, disruption of the F-actin cytoskeleton has been reported to potentiate VRAC currents in some cell types (Morishima et al, 2000; Schwiebert et al, 1994).

1.6.3. Cholesterol content

The lipid bilayer of the plasma membrane is not homogeneous and consists of special membrane microdomains, e.g. caveolae that are enriched in particular lipids and proteins. Many membrane receptors are clustered in such domains of specific lipid composition. Changes in the membrane cholesterol content within these domains seem to modulate the functions of several transporters and channels (Simons & Toomre, 2000). For instance, changes in membrane cholesterol content change the fluidity of the membrane, the bilayer thickness, the stiffness, and the deformation energy. This influences the energy cost of channel opening/closing (Hoffmann et al, 2009). Additionally, cell volume perturbations have been shown to affect caveolae and lipid rafts (Kang et al, 2000; Volonté et al, 2001). The depletion of cholesterol potentiated VRAC in Ehrlich ascites tumor cells (EAT) (Klausen et al, 2006) and bovine aortic endothelial cells (BAE) cells (Levitan et al, 2000).

1.6.4. Ionic strength

Another well-studied mechanism of VRAC activation is the effect of ionic strength of the cell. Upon cell swelling, water influx dilutes the cytosolic ion content, thus reducing the intracellular ionic strength. Several studies reported direct activation of VRAC upon reduction in intracellular ionic strength (Sabirov et al, 2000; Voets et al, 1999). Notably, Syeda and colleagues reported activation of lipid droplet bilayer reconstituted LRRC8 complexes upon reducing the intracellular ionic strength but not by lowered osmolality (Syeda et al, 2016). On the contrary, VRAC was also reported to be activated isosmotically with constant ionic strength in some cell types (Best & Brown, 2009; Cannon et al, 1998; Zhang & Lieberman, 1996). Thus, the precise role of ionic strength in activating the VRAC should be reviewed critically. Recently, our lab was able to track VRAC activation, non-invasively in live cells using a FRET sensor fused to C-termini of LRRC8 subunits and showed that reduced intracellular ionic strength is neither sufficient to activate VRAC on intracellular compartments (ER- and Golgi localized VRAC) nor is it indispensable to maintain the plasma membrane-localized VRAC active (König et al, 2019). Moreover, using pharmacological inhibition of diacylglycerol (DAG), VRAC remained active in the isotonic buffer after activation by hypotonicity even though ionic strength was restored to normal levels (König et al, 2019). Also, the extents of ionic strength used to activate VRACs (Cannon et al, 1998; Deneka et al, 2018; Syeda et al, 2016) are not consistent with the physiologically relevant range of stimulus or during whole-cell current measurements normally used to study hypotonicity-induced VRAC currents (Strange et al, 2019).

1.6.5. Role of ATP

Numerous studies demonstrated the requirement of intracellular ATP in swelling induced VRAC activation (Jackson et al, 1994; Miley et al, 1999; Oiki et al, 1994; Patel et al, 1998). Replacement of intracellular ATP with non-hydrolysable analogues, while having no effect on channel activation, suggests that direct non-hydrolytic ATP binding to the channel is a prerequisite for channel activation (Akita & Okada, 2014). This further implicates that phosphorylation events are not important in the underlying cascade of signaling events causing VRAC activation (Bond et al, 1999; Jackson et al, 1996; Jackson et al, 1994; Oiki et al, 1994). However, Bryan and colleagues reported that even though substitution of ATP with its non-hydrolysable analogues does not impair VARC activation in mouse fibroblasts but pharmacological inhibition of protein tyrosine kinases does lead to a time-dependent inhibition of chloride current. One can conclude that ATP substitution was not complete i.e., some residual ATP remained in the dialyzed cells at levels

sufficient enough to support the protein tyrosine kinase (PTK) activity (Bryan-Sisneros et al, 2000).

1.6.6. Role of phosphorylation events

1.6.6.1. Protein tyrosine kinases (PTKs) and protein tyrosine phosphatases (PTPs)

The effect of tyrosine protein kinases on swelling-induced chloride current has been reported in many cell types. Using pharmacological inhibitors of PTK e.g. tyrphostin B46, tyrphostin A25, and genistein, prior to a hypotonic stimulus there was a time and concentration-dependent inhibition of VRAC current (Bryan-Sisneros et al, 2000; Okumura et al, 2009; Sorota, 1995; Tilly et al, 1993; Voets et al, 1998). While still, it is not clear which tyrosine kinase is responsible for swelling-induced phosphorylation events, nonetheless Lepple-Wienhues and colleagues reported a role of an Src family of tyrosine kinase $p56^{lck}$ in T-lymphocytes and showed that transfection of $p56^{lck}$ can restore the osmotic activation of $ICl_{(swell)}$ in $p56^{lck}$ deficient lymphocytes, which was otherwise defective (Lepple-Wienhues et al, 1998). In line with the activating effect of PTKs pharmacological inhibition of protein tyrosine phosphatases (PTPs) potentiated the $ICl_{(swell)}$ that was activated by mild hypotonicity (Tilly et al, 1993; Voets et al, 1998). On one hand, all this data suggests a reversible role of tyrosine phosphorylation that is a critical step in mediating VRAC activity; on the other hand, some studies reported no effect of PTK inhibitors on $ICl_{(swell)}$ (Gosling et al, 1995; Szücs et al, 1996). Furthermore, surprisingly PTP inhibitors prevented the activation of volume-sensitive chloride current in bovine chromaffin cells and mouse fibroblasts (Doroshenko, 1998; Thoroed et al, 1999). As a matter of fact, there is no conclusive statement that could sum up the role of tyrosine phosphorylation in activating VRAC (Bertelli et al, 2021).

There is a similarly confusing data set available for the regulation of VRACs by the protein kinase C (PKC) family (Bertelli et al, 2021). Several studies investigated the role of different isoforms of the PKC family, for example, Rudkouskaya and colleagues showed that conventional PKC isoforms α and β1 are involved in the ATP-dependent VRAC activation (Rudkouskaya et al, 2008). Additionally, PKCα was reported to be required for efficient regulatory volume decreases in HeLa cells (Hermoso et al, 2004). In a recent study, our lab reported that PKCμ, also known as protein kinase D (PKD), is responsible for hypotonicity-induced activation of VRAC (König et al, 2019). Others have, however, either observed that PKCs were deactivating (Ben Soussia et al, 2012) or that PKCs did not contribute to the regulation of $ICl_{(swell)}$ (Catacuzzeno et al, 2014; Zholos et al, 2005).

1.6.7. GPCR and G-proteins

G protein-coupled receptors (GPCRs) belong to the largest class of cell surface receptors. They are ligand-activated and are capable of initiating a plethora of cellular responses. However, despite the size and diversity of the GPCR superfamily, these proteins interact with a relatively small number of guanine nucleotide-binding proteins, the heterotrimeric G-proteins. The heterotrimeric G-proteins consist of an α subunit (with an intrinsic GTPase activity) and βγ subunit (Oldham & Hamm, 2008). Activation of the receptor catalyzes the exchange of GTP for GDP bound to the inactive Gα subunit, resulting in a conformational change and dissociation of the Gα-Gβγ complex. The G-protein α and βγ subunit are then able to regulate various cellular effectors such as phospholipases, adenylyl cyclase, and ion channels (Hurowitz et al, 2000). The Gα subunit is encoded by a multigene family and grouped into four classes, G_s, $G_{i/o}$, $G_{q/11}$, and $G_{12/13}$ based on the sequence homology, gene structure, and regulation of specific effectors (Hurowitz et al, 2000).

Many studies using toxins aimed to investigate the role of heterotrimeric and monomeric G-proteins such as Ras and Rho, and suggested the involvement of the Rho signaling pathway in activating VRAC. For example, Esteves and colleagues reported that the Rho GTPase inhibitor *Clostridium diffiicile* toxin B inhibited swelling induced activation of $ICl_{(swell)}$ in neuroblastoma cells (Estevez et al, 2001). Moreover, a Ras-related GTPase $p21^{rho}$ signaling cascade followed by actin reorganization was found to be involved in VRAC activation in human intestine 407 cells (Tilly et al, 1996). Also, Rho GTPases regulated VRAC currents in bovine endothelial cells (Nilius et al, 1999) and NIH3T3 mouse fibroblast (Pedersen et al, 2002). Notably, in various cell lines, intracellular application of GTPγS, a non-hydrolysable GTP analogue, induced isosmotic VRAC currents (Doroshenko, 1998; Estevez et al, 2001; Voets et al, 1998) while application of GDPβS, a GDP analogue known to inhibit G-proteins, inhibited the $ICl_{(swell)}$ in a time-dependent manner (Voets et al, 1998). Although extensively studied, a clear role of GPCR and G-protein signaling in VRAC activation remains elusive.

1.6.8. Sphingolipid signaling

The sphingosine-1-phosphate (S1P)-induced VRAC activation with concomitant ATP release in raw macrophages establishes a functional link between sphingolipid and purinergic singling in various pathological processes such as inflammation, phagocytosis, migration of white blood cells, and killing of intracellular bacteria (Burow et al, 2015). Indeed, it was shown in RAW 264.7

macrophages that application of a bioactive S1P resulted in isosmotic activation of outwardly rectifying anion currents similar to VRAC currents. S1P is known to bind to a family of G protein-coupled receptors, S1PR1-S1PR5 (Watters et al, 2011b) and the S1P receptors signal via heterotrimeric G-proteins (Hisano et al, 2012). Consistent with that the S1P-induced currents were significantly reduced by the intracellular application of GDPβS which blocks G-protein signaling. Furthermore, both S1P and hypotonicity-induced ATP secretion in RAW 264.7 were found to be sensitive to conventional VRAC blockers (Burow et al, 2015).

In addition to the above-mentioned regulatory mechanisms, VRAC has also been reported to be activated iso-volumetrically during apoptosis by pro-apoptotic drugs in cancer cells (Gradogna et al, 2017b; Planells-Cases et al, 2015; Shimizu et al, 2004), and by the reactive oxygen species in rat Hepatoma tissue culture (HTC) cells, (Varela et al, 2004), HeLa cells (Shimizu et al, 2004), and nodose ganglia (Wang et al, 2017). Furthermore, there is a multitude of studies that report the modulation of VRAC activity by confusingly diverse regulators such as tumor necrosis factor-alpha (TNF-α) (Choi et al, 2016), Ca^{2+} signaling (Akita et al, 2011; Netti et al, 2018; Trothe et al, 2018; Zholos et al, 2005), phosphatidylinositol-3,4,5-trisphosphate (PIP3) (Yamamoto et al, 2008) and phosphatidyl-inositol 3-kinase (PI3K)-Akt signaling (Bach et al, 2018). Overall, despite being extensively studied, the activating mechanism(s) of VRAC remain complex and poorly understood.

2. Aim of the work

VRAC is central to the osmotic regulation of vertebrate cell volume by mediating the extrusion of chloride and organic osmolytes during regulatory volume decrease. Aside from osmotic volume regulation, it plays additional roles in various physiological processes. It is formed by heteromers of the LRRC8 protein family. VRAC is made up of LRRC8A and another member of the LRRC8 family, and its biophysical characteristics are determined by the composition of its subunits. The variability in subunit composition within an individual complex depends on the relative expression levels of the subunits. As of yet, it is unclear what endogenous tissue-specific subunits make up VRAC. Additionally, many of the studies exploring the mechanisms of VRAC activation have to be viewed with caution since they were conducted before knowing VRAC's molecular identity, and used non-specific pharmacological inhibitors.

Therefore, in this thesis, I primarily sought to investigate the different cell-line and tissue-specific expression patterns of VRAC subunits using recombinant GST-tagged LRRC8 protein fragments and calibrated the immunoblot signals from murine cells and organs. Then, I evaluated the relative abundance of other LRRC8 paralogues, LRRC8B-E, in complex with LRRC8A, in mouse 3T3 and C2C12 cell lines using co-immunoprecipitation. Finally, I explored the ambiguous VRAC regulatory and activation mechanisms, particularly the G protein-associated GPCR signaling in S1P-treated HeLa cells and glucose-induced pancreatic β-cells. For this, I used an optical FRET sensor which is less invasive than electrophysiology. The FRET sensor not only allows real-time tracking of VRAC channel activity but also permits insights into the functional roles of different subunit combinations. Using FRET, I investigated hypotonicity-, S1P-, and apoptosis-induced VRAC activity in different cell types, including a genome-edited S1PR1 knockout cell line, and systematically assessed the involvement of GPCR and G protein-mediated signal transduction in channel activation.

3. Results

3.1. Determination of VRAC subunit abundance by quantitative immunoblotting

3.1.1. Expression of recombinant GST-tagged LRRC8 fragments

The modular architecture of VRAC with varying biophysical properties has been discussed in section 1.5 (recently in (König & Stauber, 2019). Importantly, in *Xenopus* oocytes, it was shown that the variable subunit stoichiometry corelates with the relative expression levels of the subunits (Gaitán-Peñas et al, 2016). Given the lack of understanding of the subunit stoichiometries of native, endogenous VRACs, I first determined the absolute abundance of LRRC8A-E in mouse embryonic fibroblast (3T3-L1) and myoblast (C2C12) cell lines and various tissues using quantitative immunoblotting. Such an approach would require explicit calibration with proper absolute standards on the same immunoblot. For the appropriate standards, recombinant GST-tagged LRRC8 fragments (generated by Anja Kopp in the Stauber group) were used. These recombinant proteins contain the respective peptide sequence, against which the antibody (used for immunostaining) was produced (Table 1). The epitope peptide of LRRC8A and LRRC8B is from an intracellular loop between transmembrane helices TM1 and TM2, while the peptides of LRRC8C-E represent the intracellularly localized carboxy-terminal ends of the proteins. To confirm the purity of the recombinant fusion proteins and to determine the specificity of the antibodies, all five GST-tagged LRRC8 fragments were probed against antibodies raised against LRRC8A-E, respectively. I used a GST fusion construct of the amino-terminal domain of ClC-6 protein (Stauber & Jentsch, 2010) as a control alongside the recombinant proteins in all blots and probed with an anti-GST antibody. As shown in Figure 3, the blots confirmed the purity of the GST-tagged fragments and the specificity of the antibodies used, since there were no unspecific bands.

Table 1. LRRC8 fragments containing the peptide sequence

Target	Epitope peptide (reference)	LRRC8 protein fragment fused to GST
LRRC8A	QRTKSRIEQGIVDRSE (Voss et al, 2014)	EESDPKPAFSKMNGSMDKKSSTVSEDVEATVPML**QRTKSRIEQGIVDRSE**TGVLDKKEGEQAK
LRRC8B	QSLPYPQPGLESPGIESPT (Planells-Cases et al, 2015)	LSKSKTLLSTSGGSADIDASK**QSLPYPQPGLESPGIESPT**SSVLDKKEGEQAK
LRRC8C	EDALFETLPSDVREQMKAD (Planells-Cases et al, 2015)	FEVLPPELGDCRALKRAGLVV**EDALFETLPSDVREQMKAD**
LRRC8D	LEVKEALNQDVNVPFANGI (Planells-Cases et al, 2015)	QCRMLKKSGLVVEDQLFDTLP**LEVKEALNQDVNVPFANGI**

LRRC8E	LYEGLPAEVREKMEEE (Voss et al, 2014)	TLPEELGDCKGLKKSGLLVEDT**LYEGLPAEVREKM EEE**

The peptide sequence is marked in bold letters within the protein fragment sequence, against which the antibodies were raised in rabbit. The peptides for the generation of anti-LRRC8C, -D and -E antibodies localize at the carboxy-termini of the proteins.

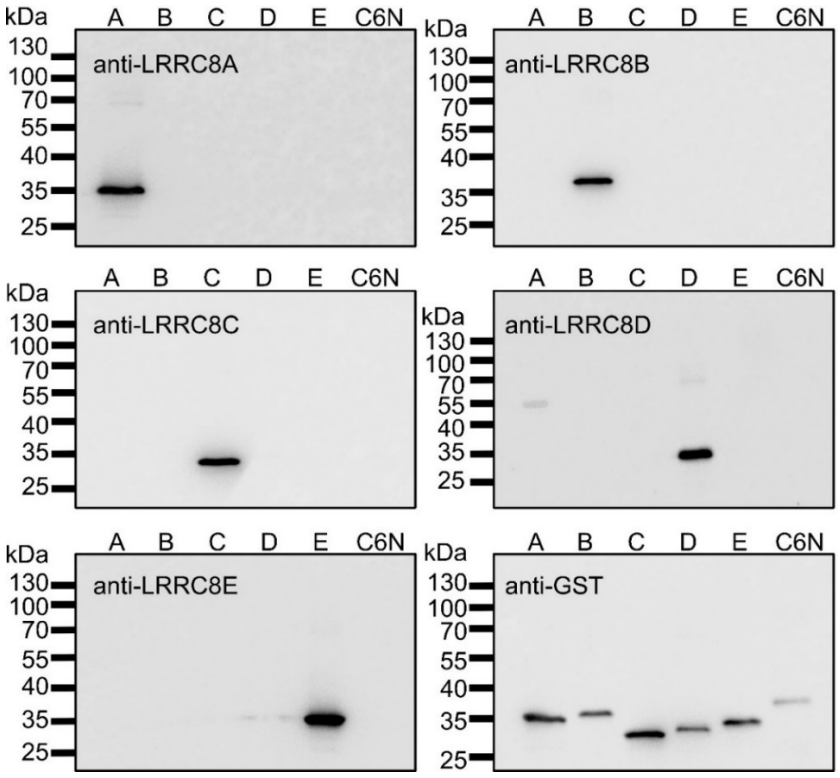

Figure 3. Characterization of anti LRRC8A-E antibodies and purity of GST-tagged LRRC8 fragments. Equal amounts (10 ng/lane) of purified recombinant GST fusion proteins LRRC8A-LRRC8E and an amino terminal domain of ClC-6 (C6N) were probed with anti LRRC8A-E and anti-GST antibody. The presented blots are illustrative for three independent experiments.

3.1.2. Knock-out-controlled immunoblotting of five LRRC8 proteins in various cell lines

I first carried out the probing of endogenous LRRC8 proteins against the anti-LRRC8A-E antibodies, in a variety of cell lines, including human cell lines such as HCT116, HEK293, and mouse myoblast C2C12 and fibroblast 3T3 cell line. As a control, I used CRISPR/Cas-9 genome-edited knock-out of LRRC8A ((Voss et al, 2014), and generated by Anja Kopp in the Stauber group, respectively). The sizes of all LRRC8 proteins can be estimated by comparison of the wild-type (WT) and LRRC8A-KO control in C2C12 and 3T3 cells and from the comparison of wild-type and quintuple LRRC8A-LRRC8E knock-out in HCT116 and HEK293 cells (Figure 4).

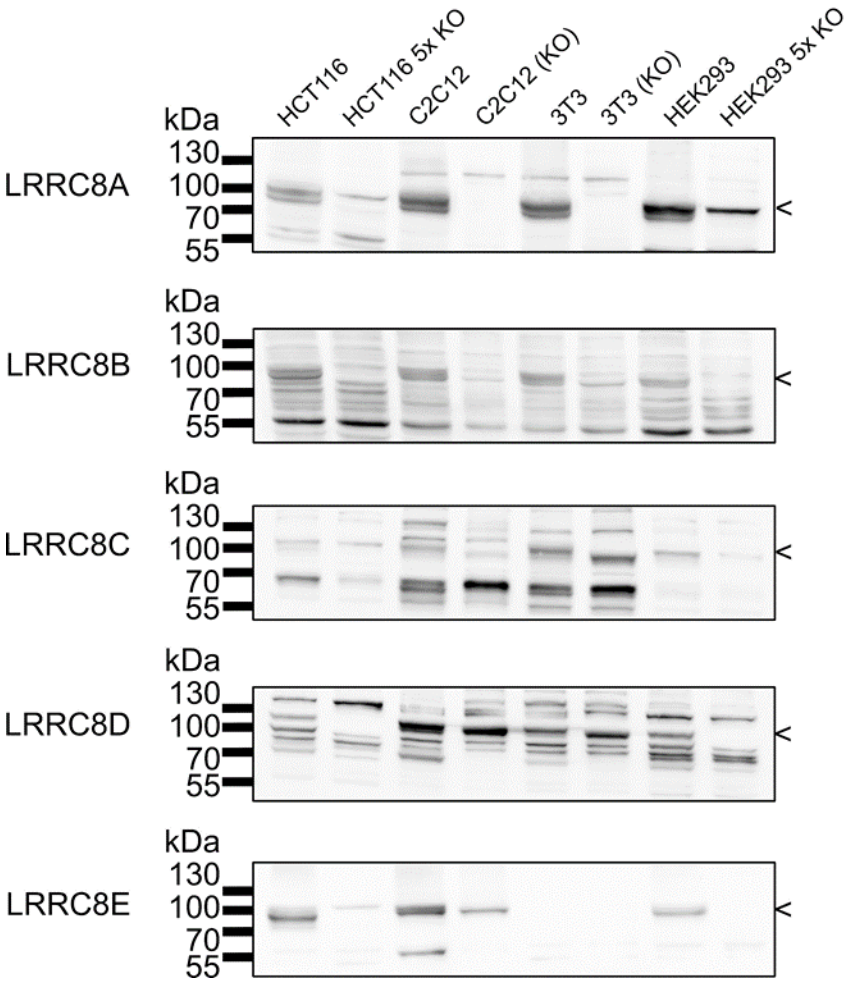

Figure 4. Western blot detection of five LRRC8 paralogues in human and mouse cell lines. 60 µg/lane of the whole cell lysates from different cell lines were separated by SDS-PAGE. The blots included human HCT116 and HEK293; each wild-type and quintuple knock-out of LRRC8A-LRRC8E (5x KO), murine C2C12 and 3T3; each wild-type and LRRC8A knock-out (KO), and are representative of three independent preparations. (<) indicates the size of the LRRC8 proteins.

3.1.3. Absolute quantification of LRRC8 proteins in murine cell lines

To determine the absolute amounts of LRRC8A-LRRC8E in murine C2C12 myoblast and 3T3 fibroblast cell lines, I established calibration curves from immunoblots in which serial dilutions of the recombinant LRRC8 fragments were loaded alongside 60 µg of the whole-cell protein and then probed with the respective antibodies. For calibration, the unknown samples must fall between the calibration samples that are well fit by linear regression analysis. Indeed, dilutions of the recombinant proteins ranging from 3 pg – 3 ng allowed for a calibration with a linear fit in the range of signal from the endogenous protein per blot, and hence the calculation of the absolute protein amounts for the five LRRC8 paralogues. Two independently prepared cell lysates for wild-

type cells (labelled as WT-1 and WT-2) were tested per immunoblot (with three independent blots per protein and cell type). Whole-cell lysate from LRRC8A knock-out (KO) cells were used as a control to identify the specific band for LRRC8A. Since, LRRC8A is required for other LRRC8B-LRRC8E paralogues to exit ER, (Voss et al, 2014) and hence for their normal glycosylation, so in its absence, there is an alteration in the apparent sizes of the other LRRC8 subunits (Planells-Cases et al, 2015), here for example seen for LRRC8C (Figure 5A, B). Interestingly in C2C12 the amount of LRRC8A was approximately five-fold lower than the levels of LRRC8B, LRRC8C, and LRRC8D; but similar to that of LRRC8E. In 3T3 cells, LRRC8A-LRRC8D were expressed at similar levels, and LRRC8E was not detectable.

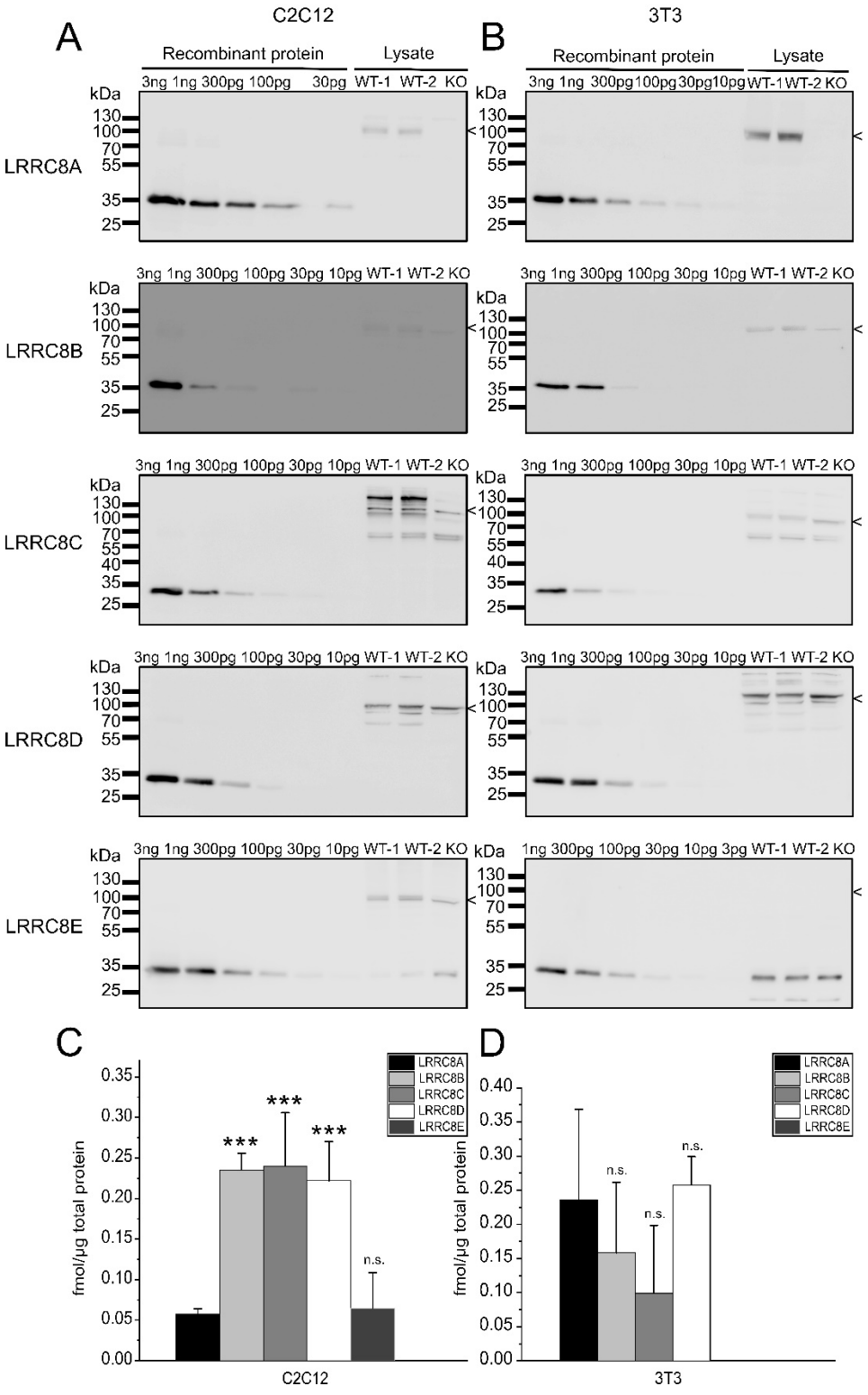

Figure 5. Quantification of LRRC8 protein amounts in mouse cell lines. Western blot analysis (A, B) and quantification (C, D) of LRRC8A-E protein levels in C2C12 and 3T3 cell lines. (A, B) 60 µg/lane of two whole-cell protein preparations from wild-type C2C12 (A) and 3T3 (B) (WT-1

and WT-2) cells alongside LRRC8A-deficient C2C12 and 3T3 (KO) cell line were separated by SDS-PAGE. Each blot was loaded with a dilution of recombinant GST fusion protein to calibrate for the respective antibody signal. (<) indicates the size of the LRRC8 proteins as determined from Figure 4. The blots are representative of three independent experiments. (C, D) Quantification of LRRC8A-E in C2C12 (C) and 3T3 (D) cells from three independent blots, with two lysates each. Data represent the mean from six lysates ± SD, ***p < 0.001, n.s.= not significant, compared with LRRC8A using one-way ANOVA with Bonferroni's post hoc test.

3.1.4. Expression patterns in mouse tissues

Next, I assessed the levels of LRRC8 protein expression in a subset of mouse tissues. To this end, lysate from different mouse tissues i.e., brain, kidney, lung, heart, and spleen containing 60 µg of protein from two 8-weeks old male mice was separated by SDS-PAGE. The tissue lysates were then loaded alongside dilution of recombinant fusion proteins, and the antibody signal from the lysates was calibrated.

VRAC subunit expression has been reported to vary between mouse tissues in some studies (Lück et al, 2018; Stuhlmann et al, 2018; Wang et al, 2017). Accordingly, I observed variable expression of LRRC8 proteins in the tested mouse tissues. It was, however, quite surprising to observe that the essential subunit LRRC8A was not the most abundant in any of the tested organs, as was the case in the C2C12 cell line. LRRC8B displayed the highest expression in the brain, while it was undetectable in the heart and spleen. LRRC8C displayed the strongest expression in the heart, where it was the most abundant LRRC8 paralogue. LRRC8D had approximately the same levels in all the tested organs, while LRRC8E had limited expression being only detectable in the spleen and lung, where it was present in similar amounts as LRRC8A (Figure 6,7). Equal loading of all the samples was ensured by Ponceau staining after SDS-PAGE and also by probing for GM130 and GAPDH as loading controls for each immunoblot as shown in Figure 8.

Indeed, the immunoblots with the tested cell lines and organs provided a direct comparison and confirmed the variable relative expression of LRRC8 proteins between tissues.

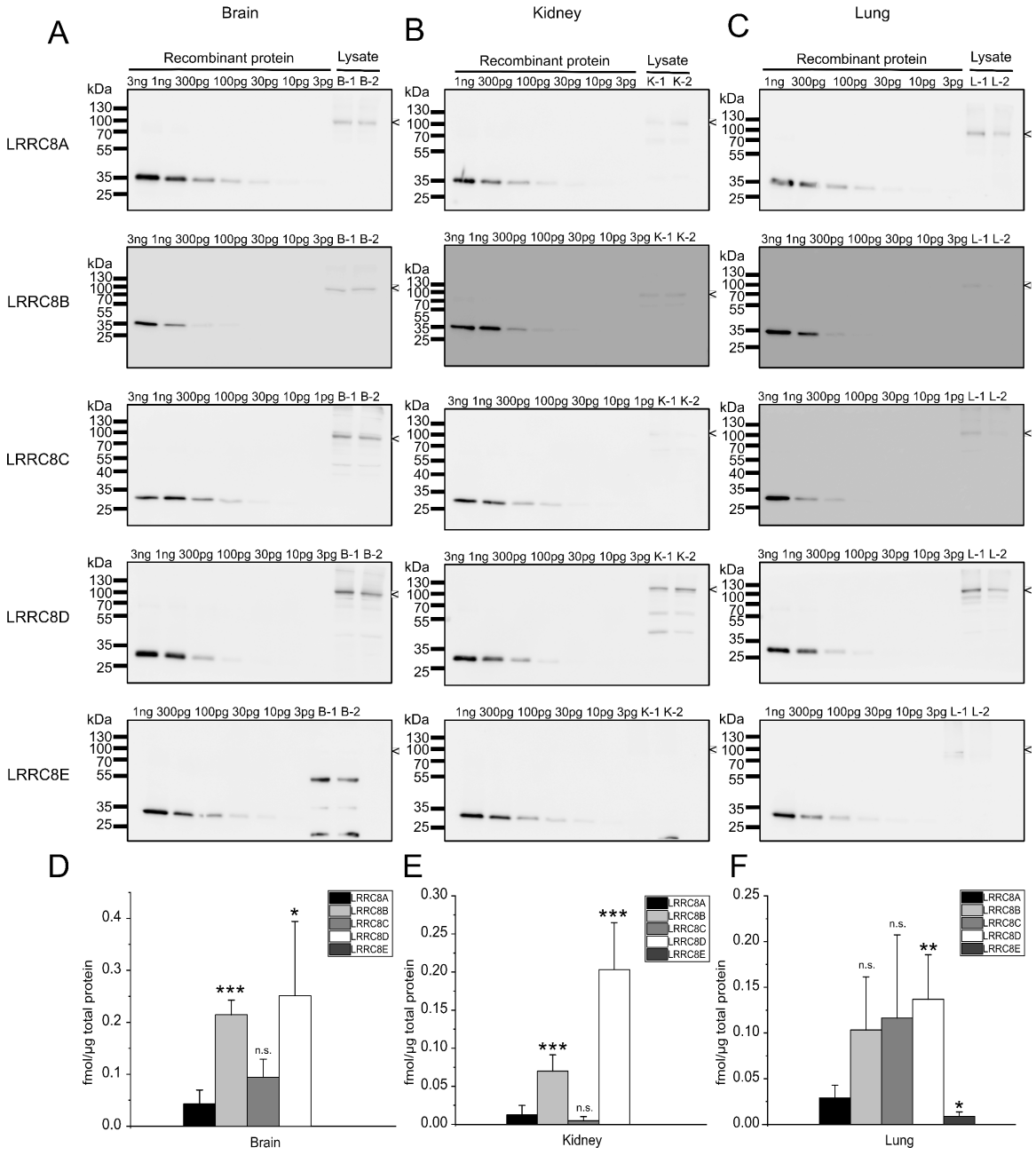

Figure 6. Quantification of LRRC8 protein amounts in mouse tissues. (A, B, C) western blot detection of LRRC8A-E proteins in mouse brain (A), kidney (B), and lung (C). 60 µg/lane of each tissue lysate from two 8-weeks old mice were separated by SDS-PAGE. Each blot was loaded with a dilution of recombinant GST fusion protein to calibrate for the respective antibody signal. (<) indicates the size of the LRRC8 proteins as determined from Figure 4. The blots are representative of three independent experiments. (D, E, F) Quantification of the protein amounts of LRRC8A-E in the brain (D), kidney (E), and lung (F). Data represent mean from three independent experiments (six measurements) ± SD. *p<0.05, **p<0.01, ***p<0.001, n.s=not significant, as compared to LRRC8A using one-way ANOVA with Bonferroni's post hoc test.

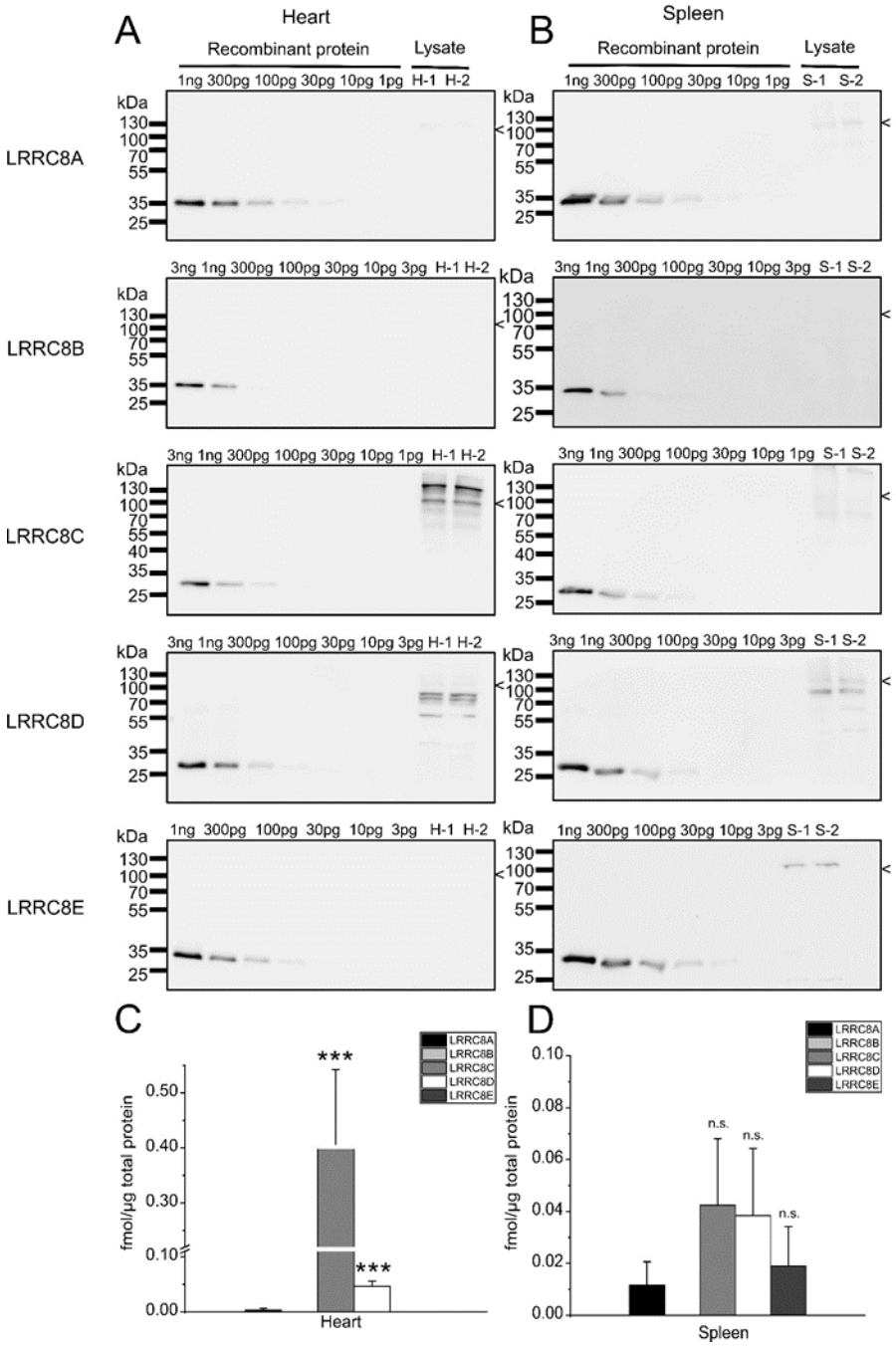

Figure 7. Quantification of LRRC8 protein amounts in heart and spleen. (A, B) Western blot detection and quantification (C, D) of LRRC8 proteins in the heart (A, C) and spleen (B, D). (A, B) 60 µg/lane of each tissue lysate from two 8-weeks old mice were separated by SDS-PAGE. Each blot was loaded with a dilution of recombinant GST fusion protein to calibrate for the respective antibody signal. (<) indicates the size of the LRRC8 proteins as determined from Figure 4. The blots are representative of three independent experiments. (C, D) Quantification of the protein

amounts of LRRC8A-E in the heart (C) and spleen (D). Data represent mean from three independent experiments (six measurements) ± SD. ***p<0.001, n.s=not significant, as compared to LRRC8A using one-way ANOVA with Bonferroni's post hoc test.

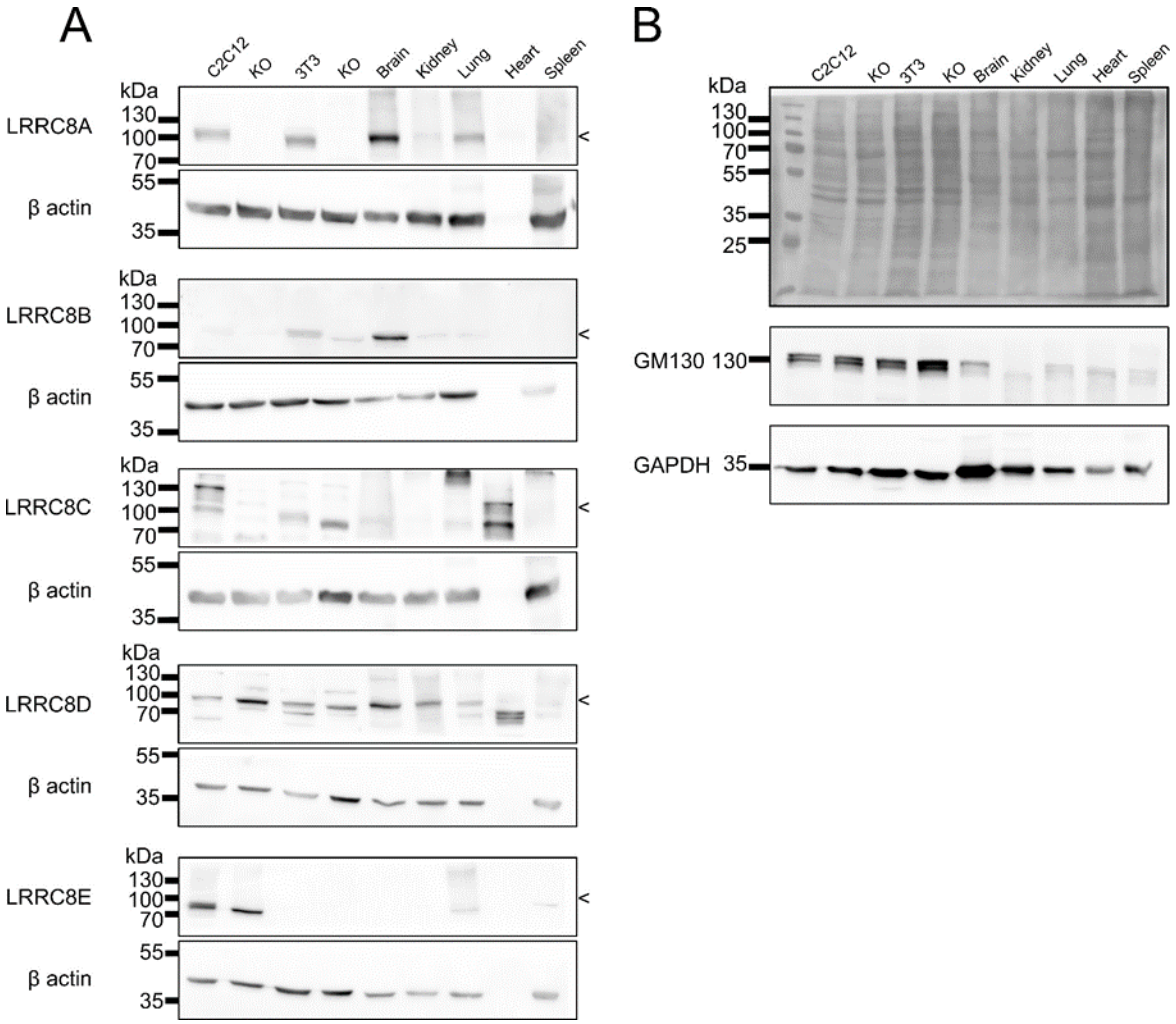

Figure 8. Immunoblotting of the LRRC8 proteins in different cell lines (including LRRC8A-KO of C2C12 and 3T3) and organs. (A) Equal amounts (60 µg protein/lane) of the whole-cell lysates and tissue lysates were separated by SDS-PAGE and probed for the LRRC8 proteins, β-actin served as a loading control (not expressed in the heart (Lin & Redies, 2012). The size of the LRRC8 proteins, as determined from Figure 4 is indicated (<). (B) Ponceau staining after SDS-PAGE, as well as probing for GM130 and GAPDH as loading controls, were used to ensure equal loading of all samples.

3.1.5. Co-Immunoprecipitation of the LRRC8 paralogues

Next, I determined if the ratios in protein levels in the tested cell lysates represent the subunit stoichiometries in LRRC8 complexes, containing LRRC8A, rather than the mere presence of

proteins that may not be incorporated in functional VRACs. To this end, I immuno-precipitated LRRC8A from C2C12 and 3T3 lysates and probed for co-immunoprecipitation of the other subunits. Indeed, I could show that LRRC8B-E efficiently precipitated with LRRC8A, but not from the LRRC8A-deficient cells used as negative controls. The Na^+, K^+-ATPase, tested as a negative control, did not co-precipitate with LRRC8A (Figure 9 A, B). Dilution of the recombinant fusion proteins was also loaded alongside the immunoprecipitated lysates to calibrate for LRRC8A-E in each immunoblot. I found that the relative abundance of LRRC8 paralogues in the immuno-precipitates from C2C12 cells (Figure 9C) was very similar to that of proteins in C2C12 lysate (Figure 5C). In the case of 3T3 cells, LRRC8A was not enriched relative to the other subunits and even reduced comparing to the protein levels in 3T3 lysate (Figure 5D). These findings suggested a relatively low abundance of LRRC8A in native VRAC complexes.

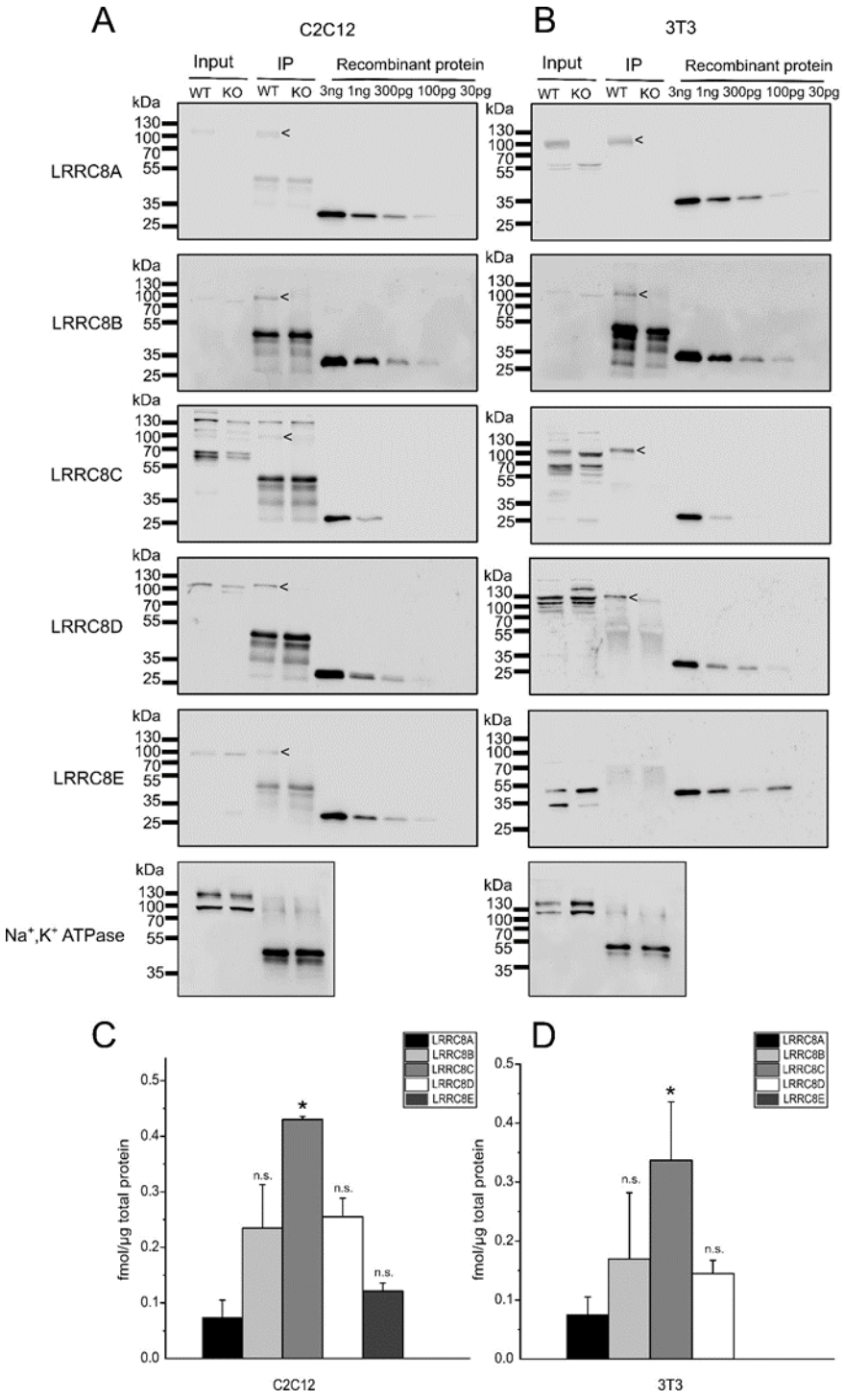

Figure 9. Quantification of the immunoprecipitated LRRC8 proteins in mouse cell lines. (A, B) LRRC8A co-precipitated LRRC8B-E in immunoprecipitations with an LRRC8A antibody from C2C12 (A) and LRRC8B-D in 3T3 cell lysates (B), but not from the respective LRRC8A-deficient cells. Notice, that Na+, K+-ATPase, being used as a negative control, did not co-precipitate. Lysate equivalent to 25% of input was loaded as a reference (input). Each blot was loaded with a dilution of recombinant GST fusion protein to calibrate for the respective antibody signal. (C, D)

Quantification of the immunoprecipitated LRRC8A-E in C2C12(C) and 3T3 (D) cells. Data represent mean ± SD from three independent experiments. *p<0.05, n.s.=not significant, compared with LRRC8A using one-way ANOVA with Bonferroni's post hoc test.

3.2. Mechanism of VRAC activation and regulation

Next, I investigated the mechanisms underlying VRAC activation and regulation. There are several techniques to study the activation mechanisms of VRAC. So far, electrophysiology has been considered the gold standard for evaluating the channel activity, either at the single-channel level or the whole-cell level (Akita & Okada, 2014; Nilius et al, 1997a; Strange et al, 2019). However, it suffers certain drawbacks, for example, investigating VRAC in excised membrane patches allows biophysical characterization of VRAC but in the absence of signaling context. Moreover, the effects of manipulating signaling pathways cannot be observed directly and precisely probably due to the dialysis of the critical signaling molecules in the whole-cell patch-clamp configuration. Using optical tools (fluorescence microscopy) can circumvent these problems. For example, the molecular events behind the slow-gating of Cl^- channels remained elusive until a spectroscopic microscopy FRET (Förster-resonance energy transfer) showed the movement of the C-terminus to be functionally linked to slow gating of the channel (Bykova et al, 2006).

3.2.1. FRET-based assessment of VRAC activity by osmotic swelling

FRET is a distance-dependent physical process in which energy is transferred non-radiatively from an excited molecule (donor) to another molecule (acceptor) having overlapping absorption and emission spectra respectively. It is a powerful tool to measure the molecular proximity at angstrom levels (10-100 Å) and is highly efficient when donor and acceptor are positioned within the Förster radius - the distance at which half of the excitation energy of the donor is transferred to the acceptor (Sekar & Periasamy, 2003). As the efficiency of FRET is dependent on the inverse sixth power of intermolecular separation (Stryer & Haugland, 1967), it has been used as a sensitive technique to investigate a variety of biological phenomena that produce changes in molecular proximity and conformational changes of proteins (Bykova et al, 2006; dos Remedios et al, 1987; König et al, 2019; Sekar & Periasamy, 2003; Zachariassen et al, 2016).

Our lab has developed a FRET sensor for monitoring VRAC activity. Fluorescent proteins (CFP (cyan fluorescent protein) or YFP (yellow fluorescent protein) were fused to the cytosolic C-terminus of LRRC8 proteins (either LRRC8A or LRRC8E), and VRAC activation with the

movement of the C-terminal domains was reflected by a drop in FRET efficiency (König et al, 2019). The donor used in this thesis was Cerulean and the acceptor was Venus. Cerulean and Venus are equivalent to CFP and YFP and will be referred to as LRRC8A-CFP and LRRC8E-YFP when fused to LRRC8A and LRRC8E subunits, throughout this thesis.

Utilizing the FRET sensor, I first monitored the hypotonicity-induced VRAC activation in living cells (Figure 10). HeLa cells were co-expressed with CFP tagged LRRC8A and YFP tagged LRRC8E, and bathed from isotonic (340 mOsm) to hypotonic (250 mOsm) solution, and the corrected FRET (cFRET) was measured. As illustrated in Figure 10B, switching the extracellular solution from 340 mOsm to 250 mOsm resulted in a significant decrease of the cFRET value by roughly 13% within 70 seconds. Moreover, the cFRET decrease was reversible and repeatable. This cFRET decrease is due to the movement of C-termini of the LRRC8 proteins in VRAC complexes and enabled me to track the VRAC activation in real-time experiments during VRAC gating.

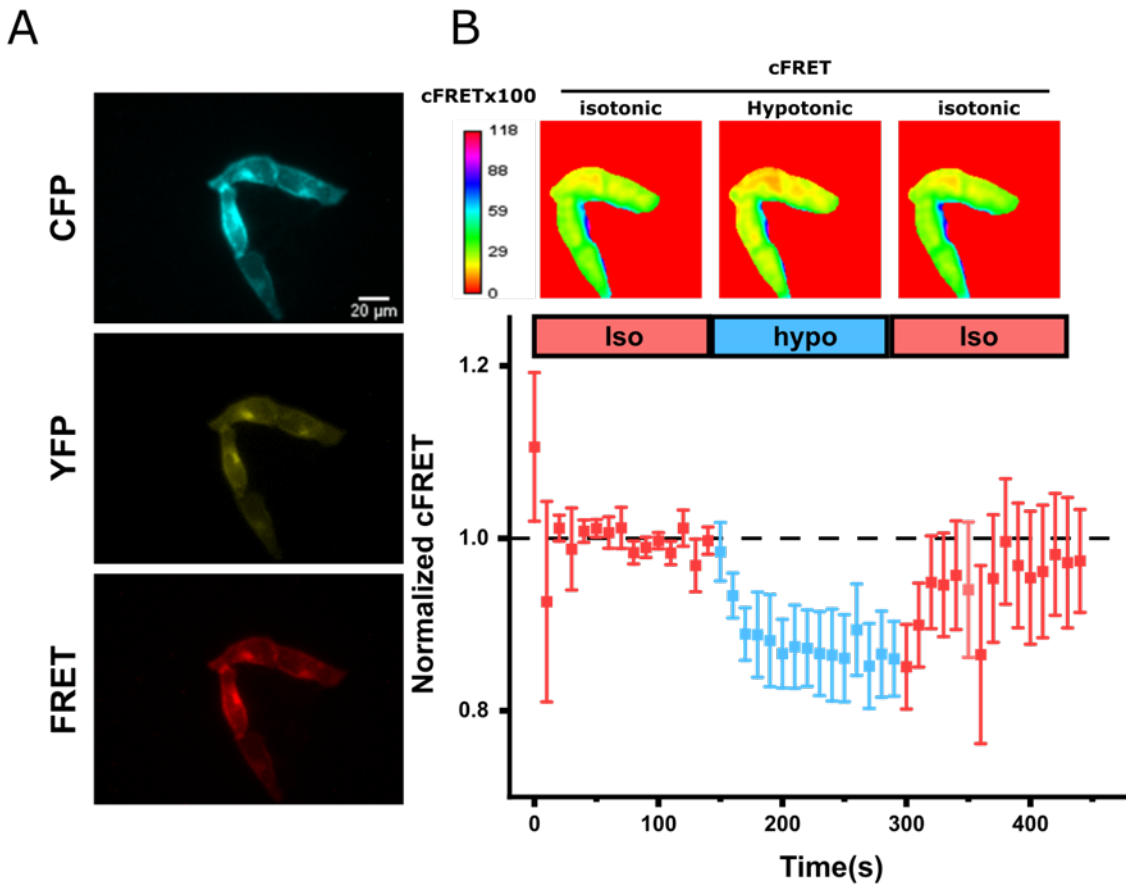

Figure 10. cFRET changes reflect VRAC activation by osmotic swelling. (A) Images of HeLa cells transfected with A-CFP/E-YFP. Shown are the three channels needed for cFRET calculation: CFP (donor), YFP (acceptor), and FRET channel. (B) Top panel: cFRET map of the transfected cells calculated from the three channels using pixFRET plugin of Image J, during buffer exchange experiments. Calibration bar left of cFRET map represents the cFRET values and their respective color codes in look-up-table (LUT). Bottom graph: cFRET normalized to the isotonic conditions of the cells shown in the top panel during switching from isotonic to hypotonic solution. Data represents mean ± SD of 7 cells.

Recently, the Stauber lab reported a putative role of PKD signaling in hypotonicity-induced activation of VRAC. Pharmacological inhibition of PKD using the inhibitor CRT0066101 resulted in no FRET decrease upon hypotonicity (König et al, 2019). I, therefore, evaluated whether PKD signaling contributed to VRAC activation in isosmotic conditions in the next set of experiments.

3.2.2. Isosmotic channel activation by death receptor-mediated apoptosis

VRAC activation without cell swelling was discovered initially in an effort to identify the chloride channels that caused cells to shrink during apoptosis (Maeno et al, 2000; Okada et al, 2001; Okada et al, 2006). Apoptosis is a physiological and pathophysiological form of cell death that is important in organ development, tissue homeostasis, somatic cell turnover, and pathogenesis of degenerative diseases (Okada et al, 2006). It is induced by two main apoptotic pathways, the extrinsic or death receptor pathway and the intrinsic or mitochondrial pathway (Elmore, 2007). Both types of stimulus can activate VRAC currents under isotonic conditions (Okada et al, 2006; Shimizu et al, 2004). The activation mechanism of VRAC elicited by mitochondrial-mediated apoptosis induced by staurosporine (STS) involves reactive oxygen species (ROS) generation by NADPH oxidase (NOX) (Shimizu et al, 2004). On the other hand, the mechanism triggered by stimulation of death receptors (for example by tumor necrosis factor receptors and Fas receptors) is suggested to involve tyrosine kinase-mediated signaling and Rho proteins in some cell types (Klausen et al, 2006; Nilius et al, 1999; Pedersen et al, 2002; Szabò et al, 1998b; Tilly et al, 1996). To this end, I investigated the isosmotic VRAC activation caused by death receptor-mediated apoptosis and the possible underlying mechanisms.

3.2.3. Pharmacological inhibition of PKD impaired the isosmotic death receptor-mediated VRAC activation

Some members of the TNF receptor family, initiate cell death in response to extracellular death signals and are characterized by an intracellular death domain that recruits some adaptor proteins (for example, TRADD and FADD) and cysteine proteases. Tumor necrosis factor receptor 1 (TNFR1) is one of the best-characterized death receptors (Okada et al, 2001; Smith et al, 1994; Wallach et al, 1999). An inflammatory polypeptide cytokine, TNF-α induces ligand-induced trimerization of the TNFR1 receptor and activates two opposing signaling pathways. The apoptotic pathway stimulating caspases and a cell-death protecting pathway that activates downstream nuclear factor-κB (NF-κB) and MAP kinases (Xia et al, 1999). Moreover, it was reported that in the presence of protein or RNA synthesis inhibitors such as cycloheximide or actinomycin D, TNFR stimulation resulted in apoptosis (Pohlman & Harlan, 1989). Therefore, to investigate the VRAC activity induced by death receptor-mediated apoptosis, I utilized the FRET optical sensor and tracked the VRAC activation in HeLa cells co-transfected with LRRC8A-CFP and LRRC8E-YFP. I monitored the cFRET changes in response to 2 ng/ml TNF-α +1 μg/ml CHX-containing isotonic buffer. Indeed, I could observe a cFRET drop indicating the isosmotic channel activation.

As isosmotically activated VRACs were previously shown to be closing when the bath solution is switched to hypertonic buffer (Mao et al, 2007; Shimizu et al, 2004), I could also notice cFRET values recovering to the initial baseline value in the isotonic buffer when bath solution is switched from TNF-α+CHX-containing isotonic to TNF-α+CHX-containing hypertonic solution (Figure 11A). So, the cFRET drop is likely due to the real conformational change of subunits leading to channel activation induced by inflammatory cytokine TNF-α. Importantly, the vehicle control of CHX, dimethyl sulfoxide (DMSO) did not affect cFRET under the same set of conditions. Moreover, the apoptotic inducers had no effect on cFRET of a cytosolic fusion construct (CFP-18A-YFP), used as a positive control for FRET (Elder et al, 2009; König et al, 2019) (Figure11B).

I then investigated how PKD signaling affects death receptor-mediated VRAC activation. As shown in Figure 11B, 15 minutes pre-incubation of HeLa cells with 5 µM of PKD inhibitor CRT006610, inhibited the cFRET drop caused by TNF-α+CHX, but rather surprisingly increased the cFRET. Since a decrease of cFRET reflects channel opening, an increase in cFRET might be due to the deactivation of already open VRAC. Conclusively, the pharmacological inhibition of PKD impaired the death receptor-mediated VRAC activation.

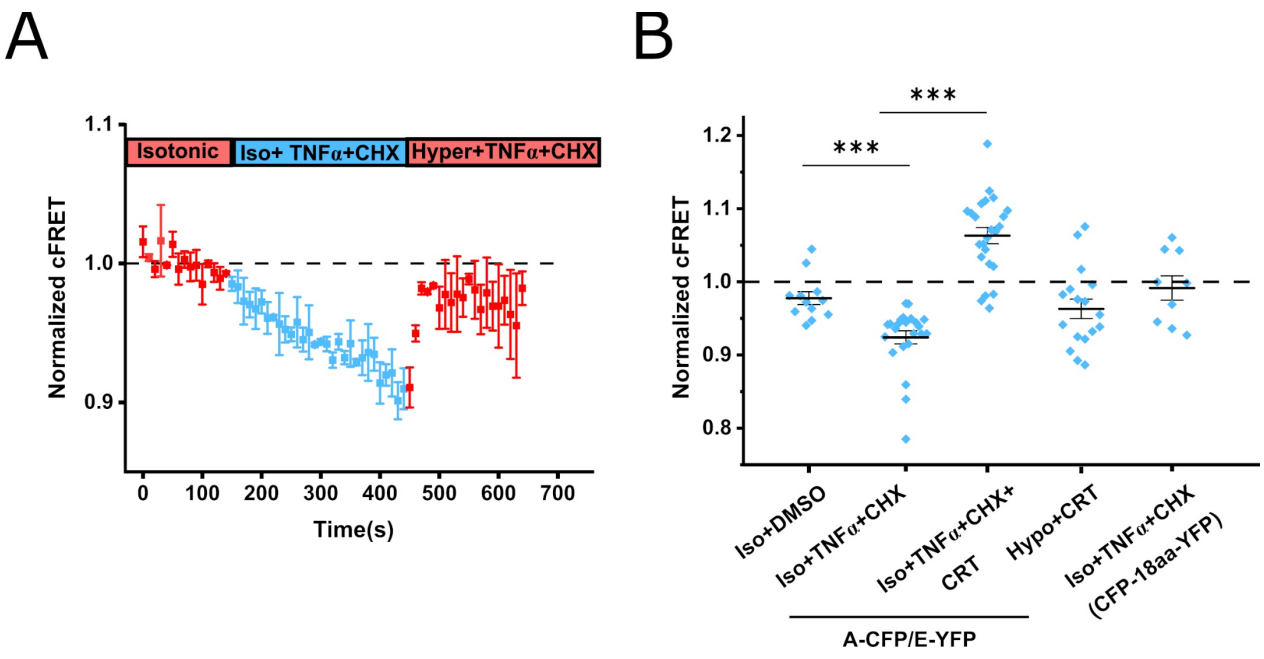

Figure 11. Isosmotic VRAC activation by death receptor-mediated apoptosis is affected by PKD signaling. (A) Normalized cFRET of HeLa cells expressing A-CFP /E-YFP (n=8 dishes,23 cells) during buffer exchange from isotonic to isotonic containing 2 ng/ml TNF-α+1 µg/ml CHX and finally to hypertonic containing 2 ng/ml TNF-α+1 µg/ml CHX. (B) Quantification of normalized cFRET values of HeLa cells expressing A-CFP/E-YFP challenged with different buffers; isotonic solution containing DMSO (as vehicle control for CHX) (n=5 dishes,12 cells); isotonic containing

apoptotic inducers (2 ng/ml TNFα+1 µg/ml CHX) (n=8 dishes,23 cells); isotonic containing apoptotic inducers and the PKD inhibitor CRT0066101(5 µM) (n=7 dishes,24 cells); hypotonic and 5 µM CRT (n=5 dishes,17 cells), and of the HeLa cells expressing the construct CFP-18aa-challenged with isotonic containing 2 ng/ml TNF-α+1 µg/ml CHX (n=3 dishes,9 cells). Note that the PKD inhibitor CRT0066101 diminished the hypotonicity-induced VRAC activation as reported in a previous study (König et al, 2019). Data represent mean of last ten time points in the respective challenging buffer of individual cells (blue diamonds) and mean of all cells ± s.e.m.***p<0.0005 by Students' t-test compared to vehicle DMSO.

3.2.4. Activation by sphingosine-1-phosphate (S1P)

Sphingolipids are the ubiquitous membrane lipids in eukaryotes that carry out numerous cellular critical functions. In most cells, different metabolites of sphingolipids act as intracellular mediators of enzyme functions and important signaling molecules (Hannun & Obeid, 2008; 2018; Pulli et al, 2018). One of the key mediators is the sphingosine-1-phosphate (S1P), which is identified as a critical regulator of many physiological and pathophysiological processes such as cancer, diabetes, and osteoporosis (Maceyka et al, 2012). It not only influences the complex reactions of the innate immune system during defense against infectious organisms but is also of significant importance during aberrant production of inflammatory cytokines in autoinflammatory disorders and sepsis (Burow et al, 2015; Chi, 2011). S1P is produced in cells by two sphingosine kinase isoenzymes, SphK1 and SphK2. Many cells secrete S1P which can then act in an autocrine or paracrine manner (Maceyka et al, 2012). Most of the known actions of S1P are mediated by a family of five specific GPCRs, termed S1PR1-S1PR5, and a majority of cells express one or more subtypes of S1P receptors. S1P binds to all of these receptors with high affinity and induces cellular responses. Recently, Markwardt lab (Burow et al, 2015; Zahiri et al, 2021) reported the activation of anion currents similar to VRAC currents by S1P in murine macrophage and microglial cells. Furthermore, using pharmacological VRAC inhibition and siRNA-mediated knock-down of LRRC8A, the S1P-induced currents were significantly abolished. Intrigued by this, I next assessed whether I can track the S1P-induced isosmotic VRAC activation using the non-invasive FRET optical sensor. To this end, I used murine macrophage cell-line RAW 264.7 and transfected it with LRRC8A-CFP and LRRC8A-YFP. Homomers formed by LRRC8A alone might be interesting to discover the mechanism of cell's native VRACs, as LRRC8A is the obligatory subunit needed, however, physiological relevance has not been reported yet for this homomer. Moreover, I choose to co-transfect the RAW 264.7 cells with this FRET pair, based on the observation that LRRC8A-CFP/LRRC8A-YFP is easily expressed in a difficult-to-transfect cell line. As shown in Figure 12B, I could indeed observe a FRET drop indicating channel activation in Raw 264.7 cells in the presence of 10 nM S1P in the bath solution. This cFRET drop is reversible, as I could observe

the cFRET values returning to initial baseline values in the isotonic buffer when the extracellular solution is switched to 10 nM S1P containing hypertonic solution (500 mOsm). Importantly, when the perfusion was switched from isotonic to hypotonic solution, the percentual reduction of cFRET was slightly more as compared to that induced by S1P.

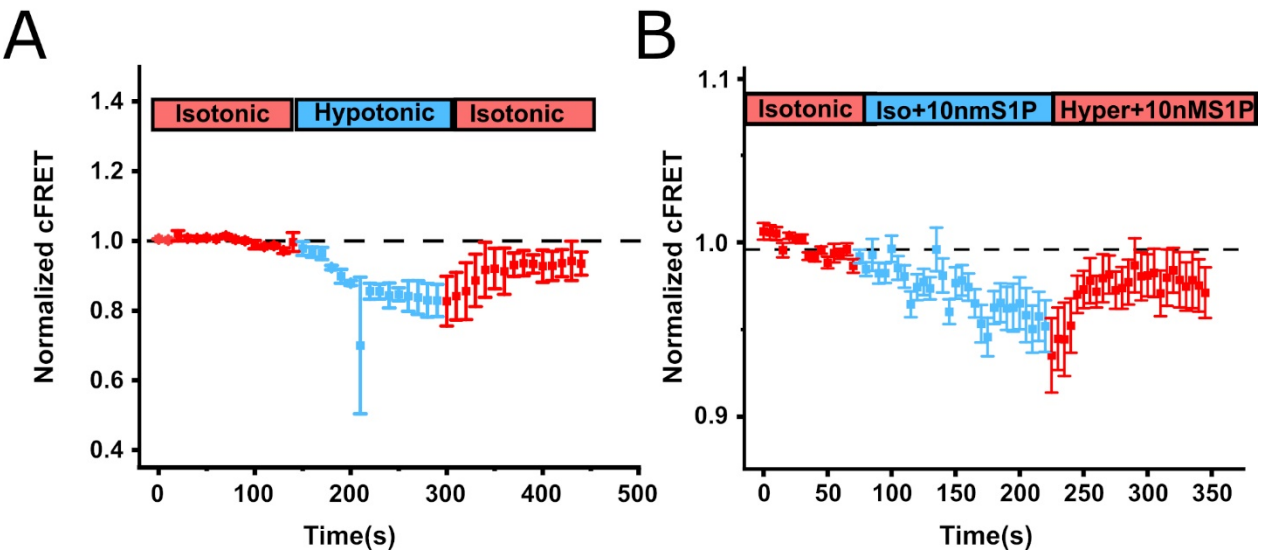

Figure 12. Hypotonicity and S1P-induced VRAC activation in RAW 264.7 cells. (A) Normalized cFRET of RAW 264.7 cells expressing LRRC8A-CFP and LRRC8A-YFP during buffer exchange from isotonic to hypotonic (n=3 dishes,11 cells) and (B) to 10 nM S1P containing isotonic buffer (n=4 dishes,15 cells). Data were acquired in 5 s intervals. cFRET values normalized to the respective cFRET values in the isotonic buffer for all the cells. All data are presented as mean ±SD.

3.2.5. Potential Mechanism of S1P-induced VARC activation

Next, I investigated the mechanisms by which S1P activates VRAC. Since S1P signals through five GPCRs, S1PR1-S1PR5, I sought to identify which receptor subtype is responsible for S1P-induced VRAC activation. S1PR1 (S1P receptor 1 or S1P1) signaling is important in RAW 264.7, as these cells only express the receptor subtypes S1PR1 and S1PR2 (Burow et al, 2015). In addition, S1PR1 antagonist abolished the S1P-induced VRAC currents, but the antagonist had no effect on the hypotonicity-induced VRAC current. Using the HeLa cell line, I investigated which receptor subtypes are responsible for mediating the stimulation effect of S1P, as well as the signaling pathway downstream of these receptor subtypes. The S1PR1-3 receptor subtypes are widely expressed in most organs, whereas S1PR4 is restricted to lymphatic and hematopoietic tissues and S1PR5 is expressed in the central nervous system (Takuwa et al, 2012; Wang et al, 2019a). In HeLa cells, all of the S1P receptors are expressed (Blom et al, 2010; Gandy et al,

2013). As shown in Figure 13A, when HeLa cells expressing LRRC8A-CFP and LRRC8E-YFP were bathed in 10 nM S1P isosmolar solution for 5 min, cFRET dropped by ~5-8%. Interestingly, pre-incubation of cells with the S1PR1 antagonist W123 reduced the S1P effect (Figure 13B) suggesting that S1P might activate VRAC in HeLa cells through the S1PR1 receptor. Importantly, the S1PR2 selective blocker JTE-013 had no effect on the S1P-induced cFRET reduction (Figure13C). The findings provide further support for the idea that S1P may activate VRAC via S1PR1 in HeLa cells. The cFRET was unaffected by S1P solubilizer methanol (Figure 13D).

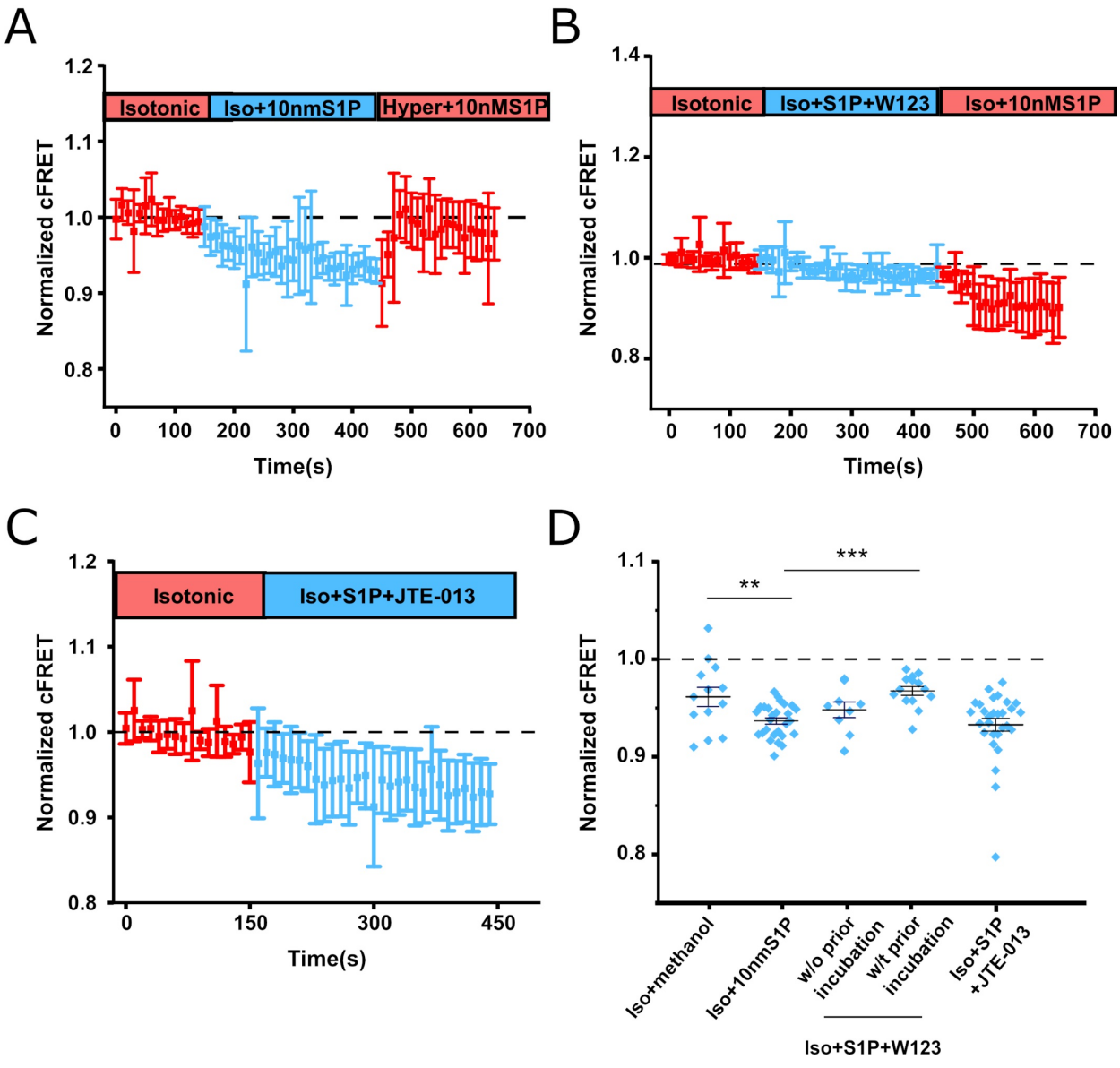

Figure 13. S1PR1 antagonist impaired the S1P-induced VRAC activation. (A) Typical cFRET drop in HeLa cells expressing LRRC8A-CFP and LRRC8E-YFP during buffer exchange from isotonic to 10 nM S1P isosmolar solution (n=5 dishes, 27 cells) (B, C) Effect of S1P receptor

(S1PR) blockers on the S1P-induced channel activation. Normalized cFRET of the HeLa cells during buffer exchange from isotonic to 10 nM S1P containing isotonic buffer and S1PR1 antagonist W123 (B) (n=4 dishes, 14 cell) and isotonic+S1P+S1PR2 blocker JTE-013 (C) (n=3 dishes,29 cells). Cells were preincubated for 20 minutes with 10 µM W123 and 0.1 µM JTE-013 prior to the FRET measurements. (D) Quantification of the normalized cFRET of HeLa cells challenged with different buffers; isotonic containing S1P solubilizer methanol; isotonic with 10 nM S1P; isotonic+S1P+S1PR1 blocker W123 and isotonic+S1P+S1PR2 blocker JTE-013. Data represents mean of last ten points per condition of individual cells and mean ± s.e.m. ***p<0.0005, **p<0.005 by Students' t-test.

When I next tested whether W123 had an effect on the non-isosmotic VRAC activation, I found that surprisingly prior incubation of cells with 10 µM W123 and W123 in hypotonic buffer abolished the cFRET reduction when cells were bathed from isotonic to the hypotonic solution. Neither the S1PR2 antagonist JTE-013 nor the solubilizer (ethanol) of W123 and JTE-013 affected the cFRET drop (Figure 14 A, B). Consequently, the hypotonicity-induced activation of VRAC was significantly diminished by S1PR1 receptor antagonist W123.

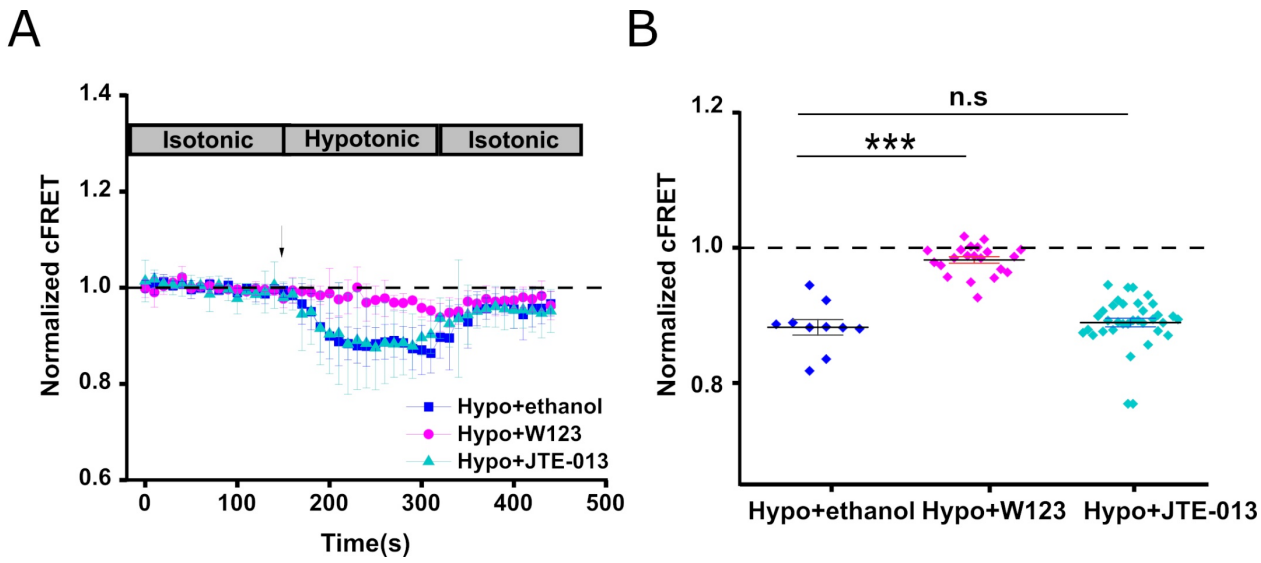

Figure 14. Hypotonicity induced VRAC activation is impaired by S1PR1 antagonist. (A) Normalized cFRET of HeLa cells expressing A-CFP/E-YFP during buffer exchange experiments from isotonic to hypotonic medium containing ethanol (—■—) (n=3 dishes,10 cells), hypotonic and 10 µM W123 (—●—) (n=4 dishes, 21 cells), and hypotonic containing 0.1 µM JTE-013 (—▲—)(n=3 dishes, 35 cells). (B) Quantification of normalized cFRET of the HeLa cells expressing A-CFP/E-YFP, in different hypotonic buffers. Data represents average cFRET of the last seven time points per condition of individual cells, and mean of all cells ±s.e.m. ***p<0.0005, n.s., not significant, by Student's t-test.

3.2.5.1. S1P1 receptor selective agonist cause isosmotic VRAC activation

To further confirm that S1PR1 mediates the S1P-signal and causes VRAC activation, I evaluated the effect of a selective S1PR1 agonist, SEW 2871 (Sanna et al, 2004). This agonist in nanomolar concentrations was capable of activating multiple downstream signals triggered by S1P including calcium flux, GTPγS binding, and Akt and ERK1/2 phosphorylation (Jo et al, 2005; Sanna et al, 2004). As shown in Figure 15 A, 500 nM SEW2871 was able to cause a cFRET decrease in HeLa cells expressing the FRET pair A-CFP/E-YFP when the extracellular isotonic solution was replaced by a SEW 2871 containing isotonic solution. The magnitude of channel activation was similar to that caused by 10 nM S1P. Moreover, the isosmotic channel activation could be reversed by the application of an extracellular hypertonic solution. In conclusion, the antagonist and agonist-based results showed that S1PR1 mediates S1P signaling and causes VRAC activation in HeLa cells. This led me to explore the downstream signaling pathway of S1PR1, which could potentially unlock a more general mechanism for VRAC activation.

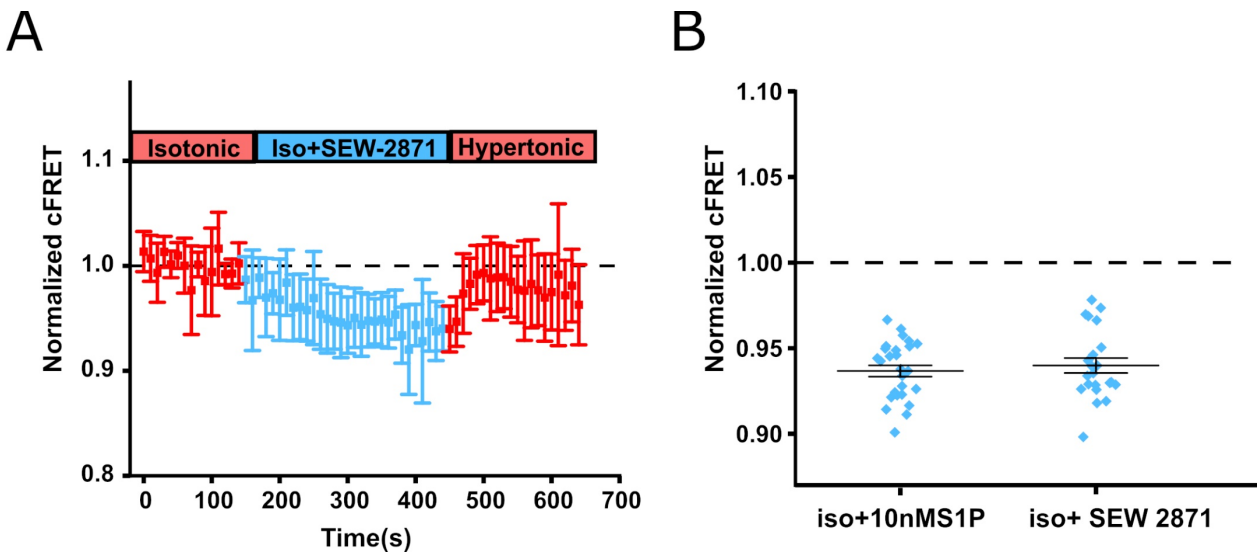

Figure 15. S1PR1 receptor selective agonist mimics the S1P-induced VRAC activation. (A) Time traces of HeLa cells expressing A-CFP/E-YFP during buffer exchange experiments from isotonic to isotonic containing 500 nM SEW-2871. Data represents average cFRET of 22 cells ± SD. (B) Quantification of normalized cFRET of HeLa cells challenged with different isotonic buffers; isotonic with 10 nM S1P (n=5 dishes,27cells) and isotonic with S1PR1 receptor agonist SEW-2871 (n=5 dishes, 22 cells). Data represents mean of last ten time points per condition of individual cells and mean of all cells ± s.e.m.

3.2.6. The role of heterotrimeric G-proteins in S1P and hypotonicity-induced VRAC activation

After ligand-induced activation, all GPCRs (including S1P receptors) employ heterotrimeric GTP-binding regulatory proteins (G-proteins) to regulate the activity of enzymes and effector molecules and initiate intracellular signaling cascades (Neves et al, 2002). As mentioned earlier in section 1.6.7, the G-proteins consist of three subunits α, β, and γ. The signal-transducing properties of various βγ combinations do not differ significantly, however, the G protein α subunit is divided into four distinct groups (G_s, $G_{i/o}$, $G_{q/11,}$ and $G_{12/13}$) based on the sequence similarity and downstream effector regulation (Siehler & Manning, 2002). The first class Gs (G_s and G_{olf}) is the stimulatory G protein that activates the downstream target adenylyl cyclase by catalyzing cAMP formation and induces activation of PKA. Gi is the inhibitory G protein (G_{i1}, G_{i2}, G_{i3}, G_{o1}, G_{o2}, G_z, G_t, and G_{gus}), which is structurally similar to Gs but inhibits adenylyl cyclase and lowers the cAMP production. The third class is the is Gq family (G_q, G_{11}, G_{14}, $G_{15/16}$) which activates the membrane-bound PLC, which leads to the cleavage of plasma membrane lipid phosphatidylinositol 4,5-bisphosphate to form inositol 1,4,5-trisphosphate (IP3) and diacylglycerol (DAG). The fourth class is the G12 (G_{12}, G_{13}) family of G-proteins, which is a family of Rho GTPases and targets the Rho-specific guanine nucleotide exchange factors (Neves et al, 2002; Siehler & Manning, 2002; Watters et al, 2011a).

Out of the five receptor subtypes of S1P, the signaling mechanisms of S1PR1-S1PR3 are better characterized as compared to S1PR4 and S1PR5. All of these receptors have unique as well as overlying signaling mechanisms. For example, S1PR2 and S1PR3 have overlapping yet distinctive intracellular signaling pathways in a variety of cell types, while S1PR1 couples exclusively to heterotrimeric Gi proteins to activate the downstream signaling molecules such as PI3K), PLC, Ras guanosine triphosphatase and deactivate adenylyl cyclase (AC) (Cuvillier, 2012; Xiao et al, 2019). The activation of these signaling molecules leads to subsequent stimulation of downstream signaling pathways including Rac GTPase, mitogen-activated protein kinase (MAPK), Akt, and mammalian target of rapamycin (mTOR). Moderate activation of PLC also induces Ca^{2+} mobilization (Lee et al, 1998; Okamoto et al, 1998; Wang et al, 2019b; Xiao et al, 2019). Due to the inhibitory effect of $G\alpha_i$ (with “i” referring to the inhibitory role) on adenylyl cyclase, there is a decreased production of cAMP from ATP, which in turn results in decreased activity of cAMP-dependent protein kinase (de Oliveira et al, 2019; Okamoto et al, 1998). The βγ subunit of Gi heterotrimer might also activate PLCβ isoforms and is responsible for GPCR dependent PIP2 hydrolysis (Smrcka, 2008).

3.2.6.1. The role of pertussis toxin (PTX)-sensitive and insensitive mechanisms in activating VRAC

To evaluate the role of heterotrimeric Gi proteins downstream of S1PR1 in mediating VRAC activation, I next monitored the cFRET of HeLa cells treated with pertussis toxin. PTX ADP ribosylates the α subunit of Gi protein, thus inactivating it by preventing or slowing down the dissociation of $G\alpha_i$ from Gβγ subunit. Thus, $G\alpha_i$ is unable to inhibit adenylyl cyclase (AC) which results in enhanced accumulation of cAMP (Mangmool & Kurose, 2011). HeLa cells co-transfected with A-CFP and YFP were incubated overnight with 500 ng/ml of the PTX. As shown in Figure 16A PTX had no significant effect on channel activation, induced by extracellular hypotonic solution, compared to untreated HeLa cells. Furthermore, the S1P-induced activation of VRAC does not differ between PTX-treated and untreated cells (Figure 16B). These results indicate that S1PR1 signaling had no influence on VRAC activation via the $G\alpha_{i/o}$ protein-dependent pathway.

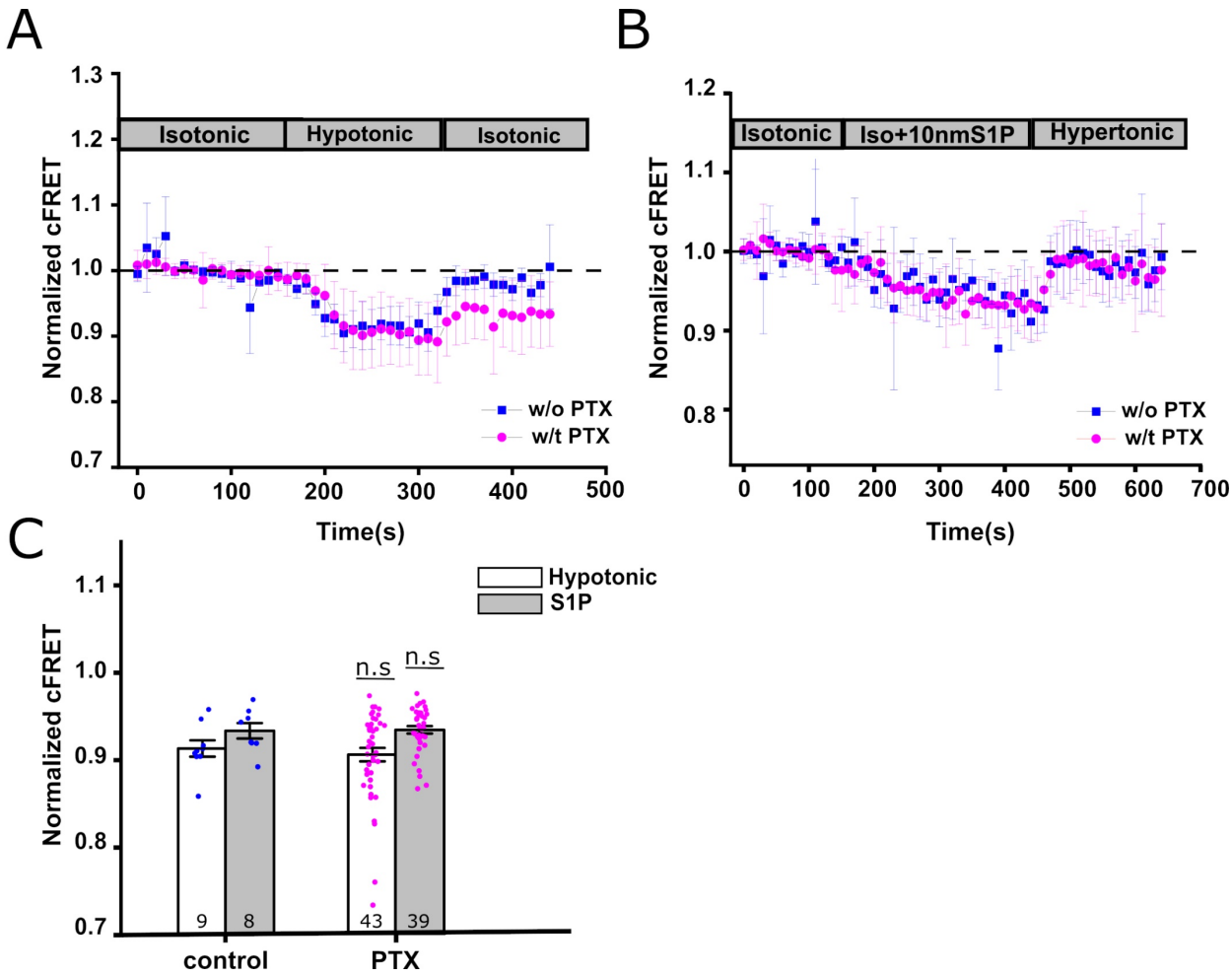

Figure 16. Hypotonicity and S1P-induced VRAC activation is not modulated by Gαi proteins. (A) Normalized cFRET of HeLa cells expressing A-CFP/E-YFP during buffer exchange experiments from isotonic to hypotonic medium (A) and isotonic to isotonic+10 nM S1P. (B) The untreated cells are represented by blue squares (—■—) (control), and the cells treated with 500 ng/ml PTX overnight are represented by magenta circles (—●—). (C) Quantification of normalized cFRET of the treated and untreated HeLa cells challenged with hypotonic and isotonic+10 nM S1P buffer i.e., from (A) and (B). The number in bars indicates the total number of cells for each treatment. Data represents the average cFRET of the last seven time points of individual cells in hypotonic media and the last ten time points in S1P containing isotonic media, and mean of all cells ±s.e.m. n.s., not significant, by Student's t-test compared to control cells**.**

Several studies have reported that many of the GPCR dependent physiological processes inhibited by PTX are mediated by the Gβγ subunits rather than the Gα subunit (Ikeda, 1996; Logothetis et al, 1987; Stephens et al, 1994). As well as the PTX-insensitive processes are also mediated by the βγ subunits (Stehno-Bittel et al, 1995) hence Gβγ can directly modulate downstream effector molecules either in a stimulatory or inhibitory manner. Due to the relatively

higher amounts of Gi families of G-proteins in cells, most of the Gβγ-dependent signaling arises from Gi proteins (Syrovatkina et al, 2016). Thus, to evaluate G-protein βγ signaling in VRAC activation, I next assessed the FRET measurements of HeLa cells treated with Gallein, a Gβγ subunit signaling inhibitor (Clapham & Neer, 1997; Lehmann et al, 2008). Gallein binds to the effector binding hot spots in Gβ (Davis et al, 2005) and effectively blocks the Gβγ subunit effector interactions (Siripurapu et al, 2017). As shown in Figure 17 (A, B) 30 minutes incubation of HeLa cells with 10 μM Gallein prior to FRET measurements did not significantly affect the cFRET reduction in comparison to untreated cells. Taken together, these results suggest that the Gi (Gα/βγ) family of G-proteins are not participating in VRAC activation.

Apart from the Gi family, adenylyl cyclase is also regulated by another heterotrimeric G protein family, called the Gs family. Gs is the stimulatory protein for AC enzyme, activated adenylyl cyclase converts ATP to cAMP. cAMP can modulate the swelling-induced currents in a stimulatory and inhibitory manner (Shimizu et al, 2000). So, I tested whether adenylate cyclase and cAMP are involved in mediating the S1P signal and hypotonicity-induced channel activation. Cholera toxin ADP ribosylates the alpha subunit of the Gs family of G protein, stabilizing the GTP bound conformation of α_s and decreases its intrinsic GTPase activity, as a result, there is increased stimulation of adenylyl cyclase and elevated intracellular cAMP levels (Chang & Bourne, 1989). HeLa cells were incubated overnight with 100 ng/ml of the cholera toxin and analyzed for cFRET reduction during buffer exchange experiments to hypotonic and S1P containing isotonic media (Figure 18 A, B). However, in both sets of experiments, I observed no significant difference in the cFRET decrease between treated and untreated cells. Even when the cells were pre-incubated 24 hours before the FRET measurement, the cFRET remained unaffected. Therefore, the Gs-mediated protein signaling does not mediate the hypotonicity and S1P-induced activation of VRAC.

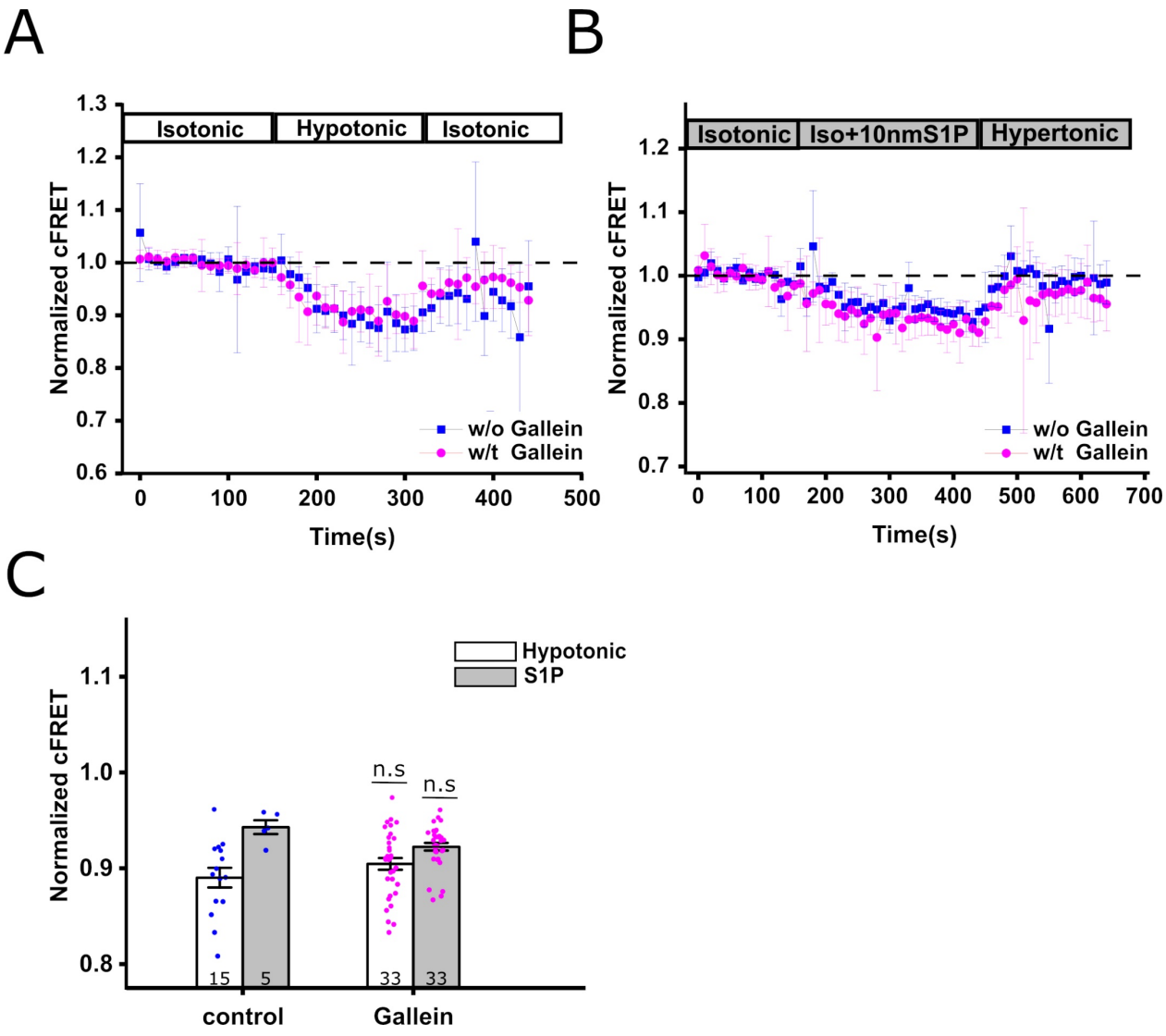

Figure 17. Gβγ signaling inhibitor Gallein had no effect on Hypotonicity and S1P-induced channel activation. Normalized cFRET of HeLa cells expressing A-CFP/E-YFP during buffer exchange experiments from isotonic to hypotonic medium (A) and isotonic to isotonic+10 nM S1P (B). Blue squares (—■—) (control) indicate the untreated cells whereas the cells incubated with 10 μM Gallein prior to FRET measurements are represented by magenta circles (—●—) (C) Quantification of normalized cFRET of the treated and untreated HeLa cells challenged with hypotonic and isotonic+10 nM S1P buffer i.e., from (A) and (B). The number in bars indicates the total number of cells for each treatment. Data represents average cFRET of the last seven time points of individual cells in hypotonic media and last ten time points in S1P containing isotonic media, and mean of all cells ±s.e.m. n.s., not significant, by Student's t-test compared to control cells.

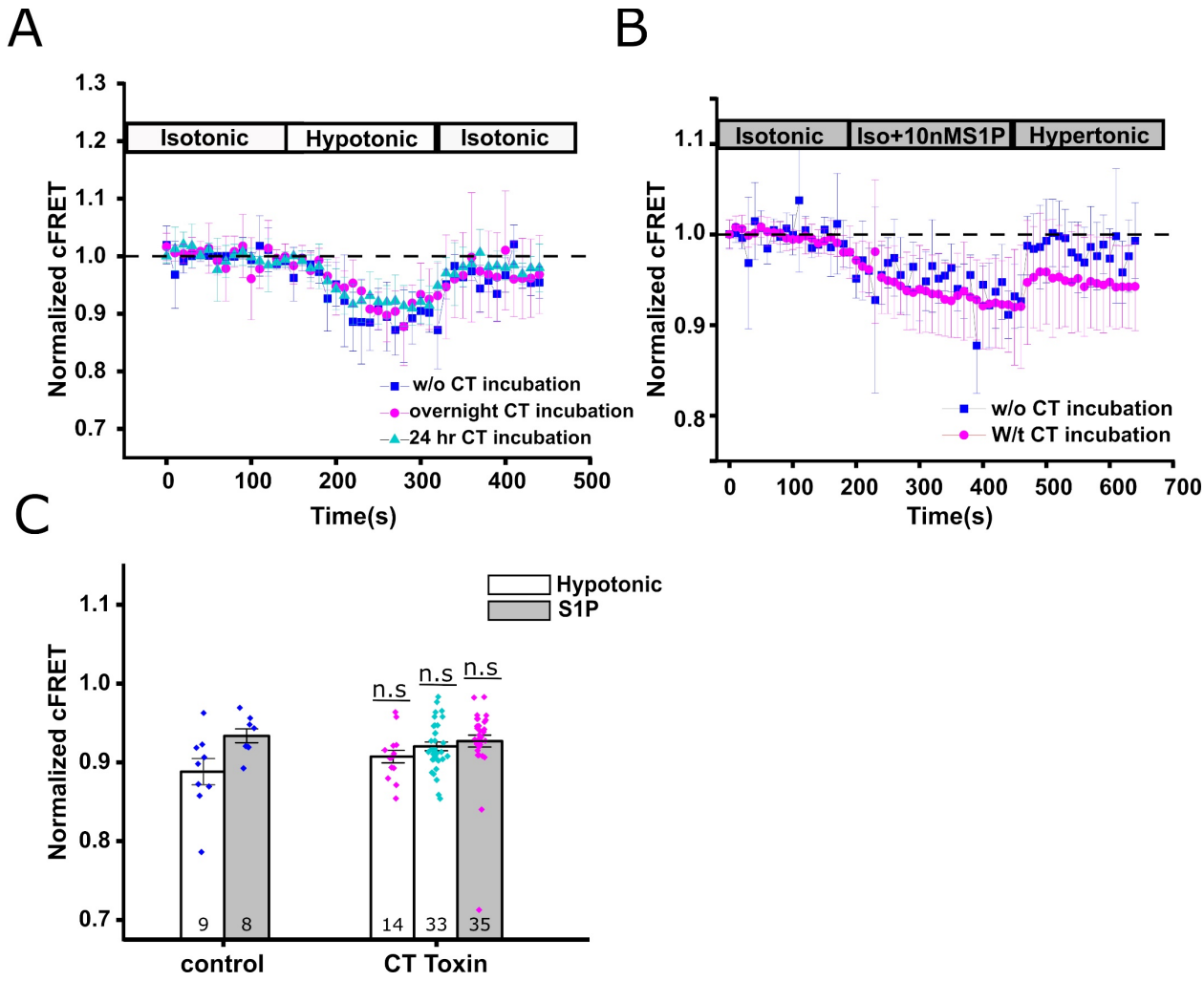

Figure 18. Gαs family do not regulate the S1P and hypotonicity induced VRAC activation. Normalized cFRET of HeLa cells expressing A-CFP/E-YFP during buffer exchange experiments from isotonic to hypotonic medium (A) and isotonic to isotonic+10 nM S1P (B). Blue squares (—■—) (control) indicate the untreated cells; cells incubated with 100 ng/ml of cholera toxin (CT) overnight are represented by magenta circles (—●—); (–▲–) indicate the cells incubated 24 hours with CT toxin prior to FRET measurements. (C) Quantification of normalized cFRET of the treated and untreated HeLa cells challenged with hypotonic and isotonic+10 nM S1P buffer i.e., from (A) and (B). The number in bars indicates the total number of cells for each treatment. Data represents the average cFRET of the last seven time points of individual cells in hypotonic media and the last ten time points in S1P containing isotonic media, and mean of all cells ±s.e.m. n.s., not significant, by Student's t-test compared to control cells.

Toxin-induced modulation of adenylyl cyclase activity revealed that the enzyme was not involved in S1P and hypotonicity-induced VRAC activation, so I wondered whether inhibiting its activity would be effective. To achieve this goal, one way is to use adenylyl cyclase inhibitors, such as 2′,3′-Dideoxyadenosine (DDA)(Estevez et al, 2001). The other way is to differentially modulate the heterotrimeric G-proteins (Gs and Gi) rendering them ineffective in stimulating the adenylyl

cyclase. Melittin, a natural peptide from bee venom, with a broad spectrum of biological activities has been reported to be a potent inhibitor of PKC activity (Raynor et al, 1991). Furthermore, it is considered to be the first metabostatic peptide that inhibits intrinsic Gs activity while stimulates Gi activity (Fukushima et al, 1998). Both of these mechanisms i.e., through the Gi stimulation and Gs inhibition, are involved in the melittin inhibition of adenyl cyclase (Fukushima et al, 1998). To investigate the effect of melittin-based adenylyl cyclase inhibition, I co-transfected HeLa cells with the FRET pair A-CFP/E-YFP and incubated overnight with 1 µg/ml of melittin at 37°C. The next day cells were analyzed in buffer exchange experiments from isotonic to hypotonic, as shown in Figure 19 A, melittin did not affect channel activation compared to control cells. However, in the absence of cell swelling, S1P-induced VRAC activation is significantly reduced in treated cells in comparison to untreated cells (Figure 19 B).

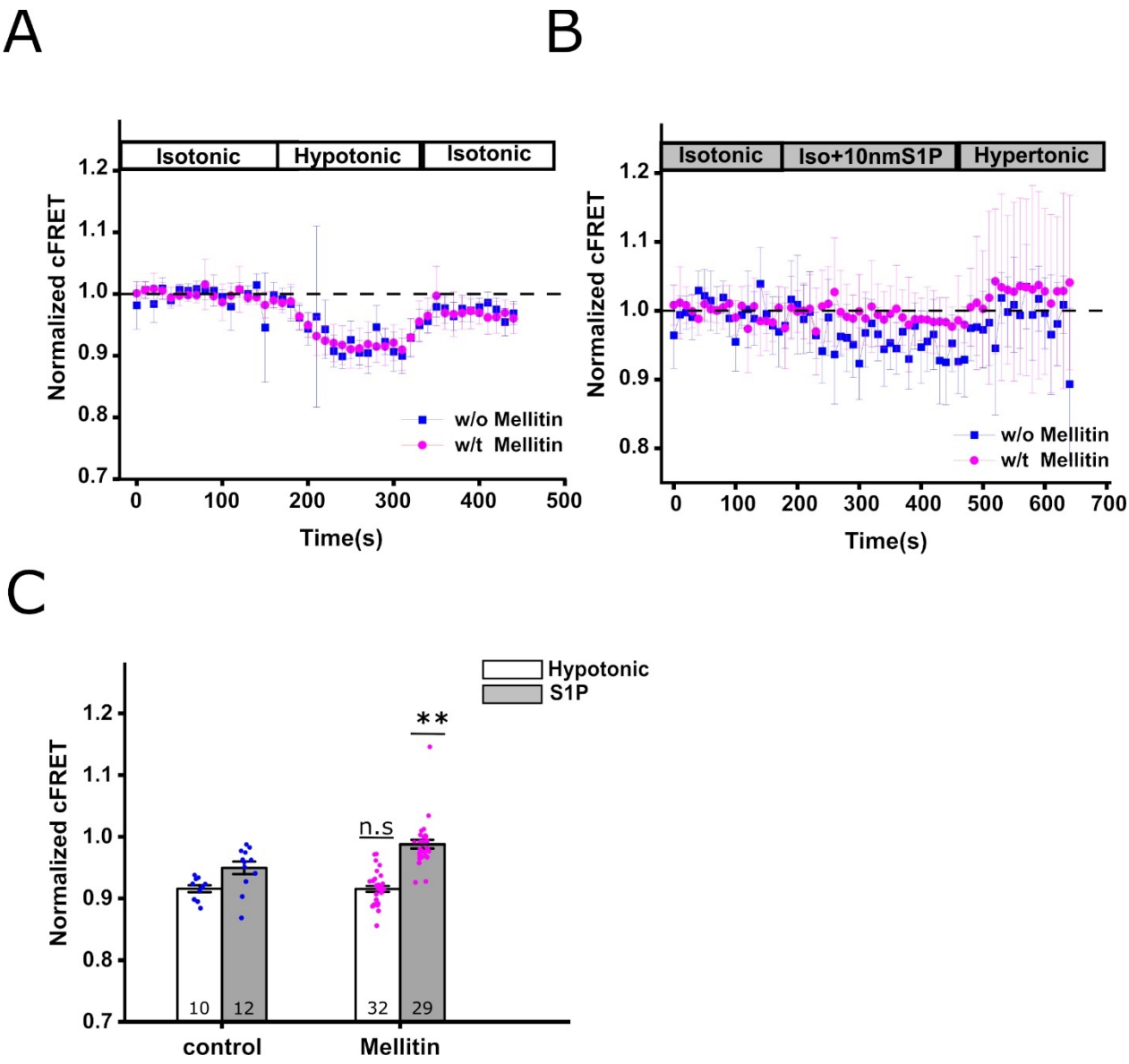

Figure 19. S1P-induced isosmotic VRAC activation is impaired by melittin. Normalized cFRET of HeLa cells expressing A-CFP/E-YFP during buffer exchange experiments from isotonic to hypotonic medium (A) and isotonic to isotonic+10 nM S1P (B). Blue squares (—■—) (control) indicate the untreated cells whereas the cells incubated with 1 µg/ml of melittin overnight prior to FRET measurements are represented by magenta circles (—●—). (C) Quantification of normalized cFRET of the treated and untreated HeLa cells challenged with hypotonic and isotonic+10 nM S1P buffer i.e., from (A) and (B). The number in bars indicates the total number of cells for each treatment. Data represents the average cFRET of the last seven time points of individual cells in hypotonic media and the last ten time points in S1P containing isotonic media, and mean of all cells ±s.e.m. n.s., not significant, **p<0.005 by Student's t-test compared to control cells.

3.2.6.2. VRAC activation is mediated by PTX-insensitive signaling

Since the PTX-sensitive Gi signaling modulated neither hypotonicity nor S1P-induced activation of the VRAC, I next investigated the PTX-insensitive signaling mechanisms. The PTX-insensitive pathways are mainly mediated by $G\alpha_q$-dependent activation of PLCβ or by pathways involving the Rho monomeric proteins and PLCε (Citro et al, 2007; Kelley et al, 2006; Singer et al, 1997). YM-254890 is a suitable inhibitor for studying Gq signaling. It is a cyclic depsipeptide produced by *Chromobacterium* sp. QS3666 and can modulate Gq pathway by inhibiting the guanine nucleotide exchange on $G\alpha_q$, thus rendering it in its inactive $G\alpha_q$-GDP form and inhibiting further effector molecule signaling (Mizuno & Itoh, 2009). Incubation of HeLa cells with 1 μM YM-254890 for 5 minutes at 37°C blocks the Gq heterotrimer dissociation by preventing GDP/GTP exchange (Takasaki et al, 2004) and Gq-mediated PIP2 hydrolysis. As shown in Figure 20 A incubation of HeLa cells with the selective Gq inhibitor YM-254890 before FRET measurements did not affect the cFRET drop between treated and untreated control cells, upon buffer exchange to the extracellular hypotonic solution. In contrast to the S1P-induced cFRET reduction in untreated HeLa cells, no significant cFRET decrease was observed in YM-254890 treated cells (Figure 20 B). It is important to note that S1PR2 and S1PR3 signal through different G-proteins, depending on the cell type and the stimulus, one of which is the Gq family of heterotrimeric G-proteins (Adada et al, 2013). Having observed that impaired Gq signaling modulates VRAC activation, the involvement of S1PR2 and S1PR3 cannot be totally ruled out.

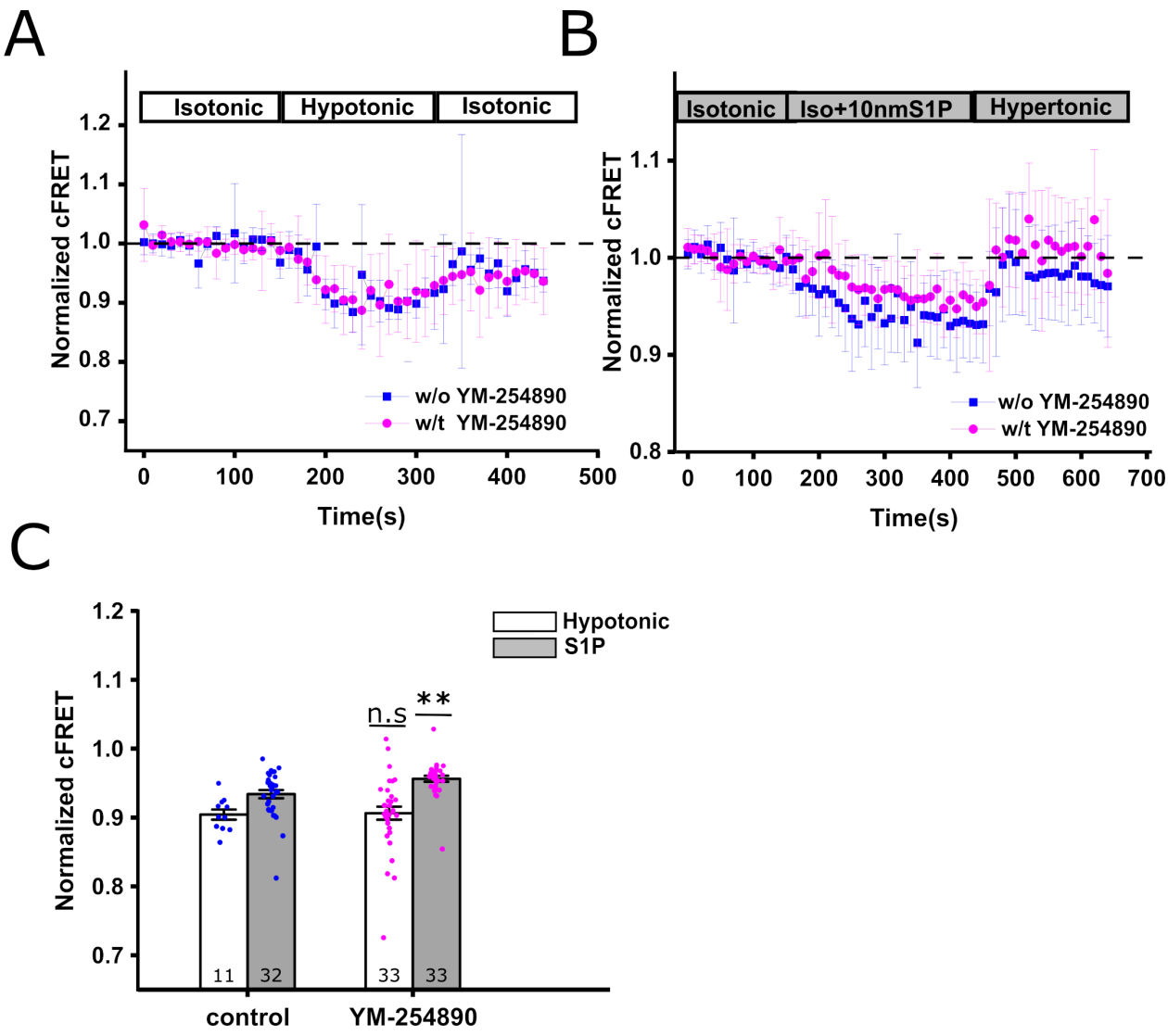

Figure 20. $G\alpha_q$-mediated protein signaling regulate S1P-induced VRAC activation. Normalized cFRET of HeLa cells expressing A-CFP/E-YFP during buffer exchange experiments from isotonic to hypotonic medium (A) and isotonic to isotonic+10 nM S1P (B). Blue squares (—■—) (control) indicate the untreated cells whereas the cells incubated with 1 μM YM-245890 prior to FRET measurements are represented by magenta circles (—●—). (C) Quantification of normalized cFRET of the treated and untreated HeLa cells challenged with hypotonic and isotonic+10 nMS1P buffer i.e., from (A) and (B). The number in bars indicates the total number of cells for each treatment. Data represents the average cFRET of the last seven time points of individual cells in hypotonic media and the last ten time points in S1P containing isotonic media, and mean of all cells ±s.e.m. n.s., not significant, **p<0.005., by Student's t-test compared to control cells.

3.2.7. The role of monomeric G-proteins

After assessing no involvement of PTX-sensitive signaling pathway in mediating VRAC activation, I next investigated the role of small monomeric G-proteins called the Rho family of GTPases which are downstream effectors of $G\alpha_{q/11}$ family, $G\alpha_{i}$ and $G\alpha_{12/13}$. To test for the involvement of Rho G-proteins, HeLa cells were co-transfected with A-CFP and E-YFP and incubated with 1ng/ml of *C. difficile* toxin B overnight and next day analyzed during FRET measurements in buffer exchange experiments. Toxin B catalyzes the UDP-glucosylation of the Rho family of G-proteins including Rho, Rac, and Cdc42. The glucosylation inactivates the Rho proteins, therefore, inhibiting the Rho signaling pathway (Aktories et al, 2000). As shown in Figure 21, the cFRET decrease caused by hypotonicity or S1P did not differ between control (untreated) and treated cells, thus indicating that Rho GTPase signaling pathways do not regulate the S1P and hypotonicity induced channel activation. Importantly, S1PR4 and S1PR5 are coupled to the $G\alpha_{i}$ and $G\alpha_{12/13,}$ which signal through the Rho GTPases. Hence, activation of VRAC by S1P signal is unlikely to involve this subset of receptors.

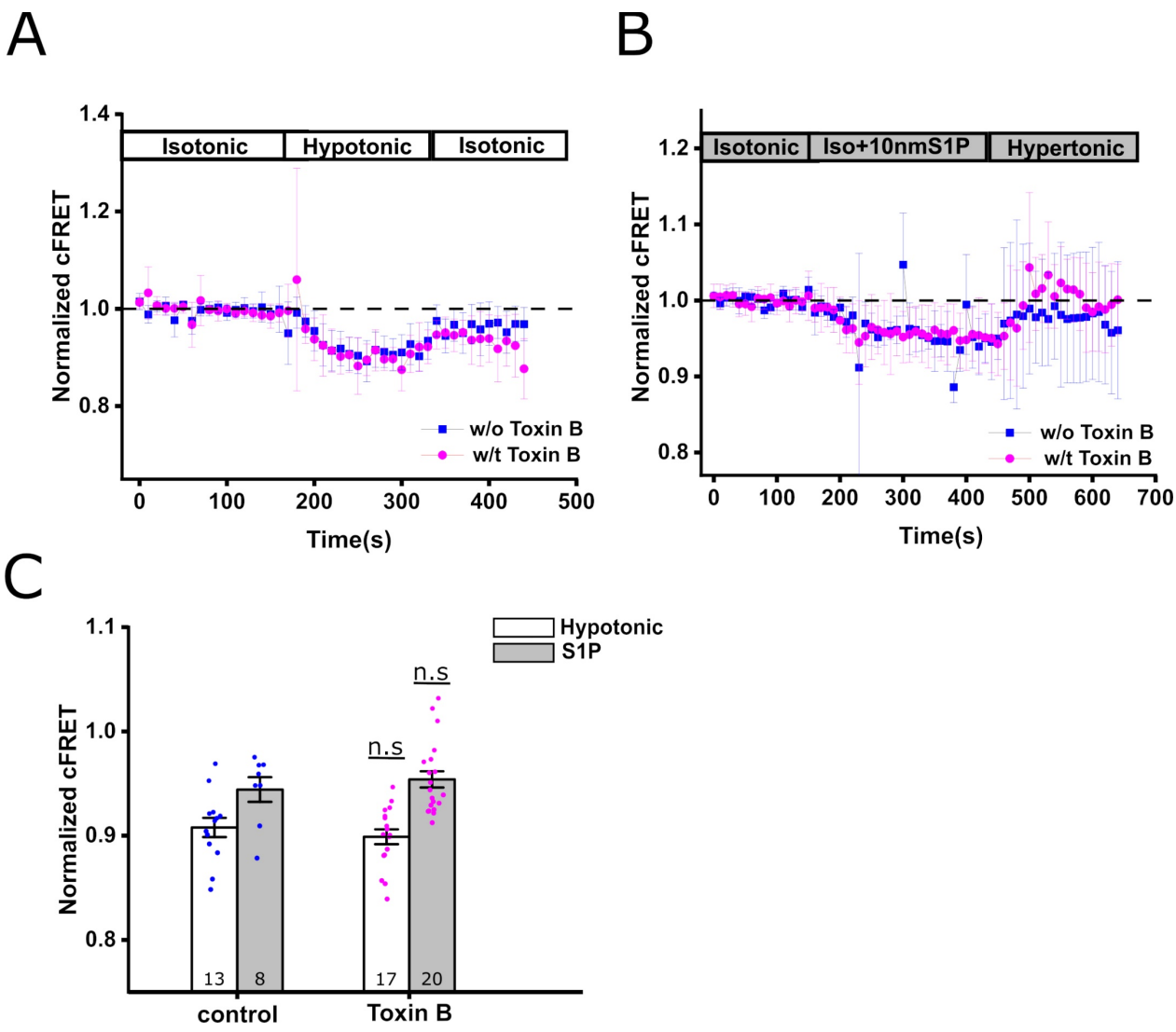

Figure 21. Rho GTPases do not regulate the hypotonicity and S1P-induced VRAC activation. Normalized cFRET of HeLa cells expressing A-CFP/E-YFP during buffer exchange experiments from isotonic to hypotonic medium (A) and isotonic to isotonic+10 nM S1P (B). The blue squares (—■—) (control) depict untreated cells, while the magenta circles (—●—) indicate cells incubated with 1 ng/ml of Clostridium difficile toxin B before FRET measurement. (C) Quantification of normalized cFRET of the treated and untreated HeLa cells challenged with hypotonic and isotonic+10 nM S1P buffer i.e., from (A) and (B). The number in bars indicates the total number of cells for each treatment. Data represents the average cFRET of the last seven time points of individual cells in hypotonic media and the last ten time points in S1P containing isotonic media, and mean of all cells ±s.e.m. n.s., not significant, by Student's t-test compared to control cells.

After analyzing the downstream G-proteins that mediate the S1P signal through S1P receptors, I then examined how S1P receptors contribute to VRAC activation by siRNA-mediated knock-down of receptor expression and a receptor knock-out cell line.

3.2.8. Downregulation of S1PR1 does not affect hypotonic and S1P-induced VRAC activation

Studies on cell surface receptors using antagonists or agonists are critical in understanding the biological responses they mediate; however, they might have additional non-specific targets that lead to ambiguous interpretations of receptor-mediated intracellular signal transduction. Therefore, to further clarify the role of S1P receptors in VRAC activation, I carried out specific siRNA knock-down of S1PR1 in HeLa cells expressing A-CFP/E-YFP heteromeric VRAC. Reduced expression levels of S1PR1 after 24 and 48 hours of siRNA transfection were confirmed by western blotting (Figure 22 A, B). However, I did not observe any significant differences in cFRET reduction caused by S1P or hypotonic extracellular solution due to siRNA-mediated knock-down of S1PR1 (Figure 22 C, D), pointing to the notion that S1PR1 receptor alone does not mediate channel activation. Moreover, the cFRET reduction of an S1PR1 KO HeLa cell line also did not differ significantly from that of wild-type HeLa cells (Figure 23 A, B).

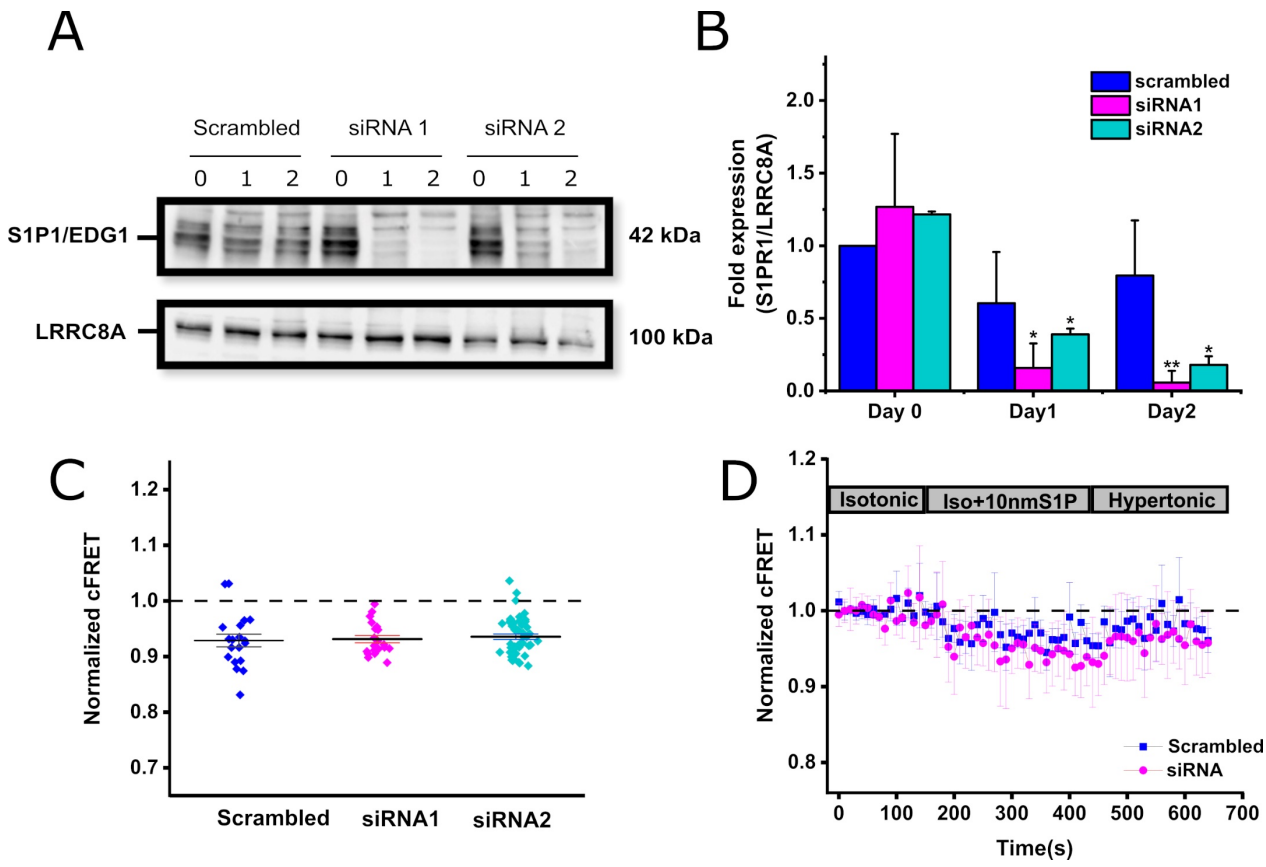

Figure 22. siRNA-mediated knock-down of S1PR1 does not affect S1P and hypotonicity induced VRAC activation. (A) Expression levels of S1PR1 detected by western blot post 24 and 48-hour siRNA transfection. Representative blots are from three independent experiments. LRRC8A was used as a loading control. (B) Quantification of the western blots. Fold changes of S1PR1 expression are normalized to the loading control LRRC8A. Data represents mean ± SD. Statistics: **p<0.005., *p<0.05 by Student's t-test compared to scrambled. (C) Quantification of the cFRET values of HeLa cells transfected with scrambled RNA (blue diamonds) (n=1 dish,19 cells) siRNA1 (magenta diamonds) (n=3 dishes, 20 cells) and siRNA2 (green diamonds) (n=3 dishes,47 cells) in hypotonic buffer. Data represent mean of last ten time points in the hypotonic buffer of individual cells and mean of all cells ± s.e.m. (D). Normalized cFRET of HeLa cells, post siRNA-mediated S1PR1 knock-down, during buffer exchange experiments from isotonic to 10 nM S1P containing isotonic buffer. The blue squares (—■—) represents cells treated with scrambled RNA (n=1 dish,10 cells) and magenta circle represents siRNA transfected cells (—●—) (n=3 dishes, 29 cells).

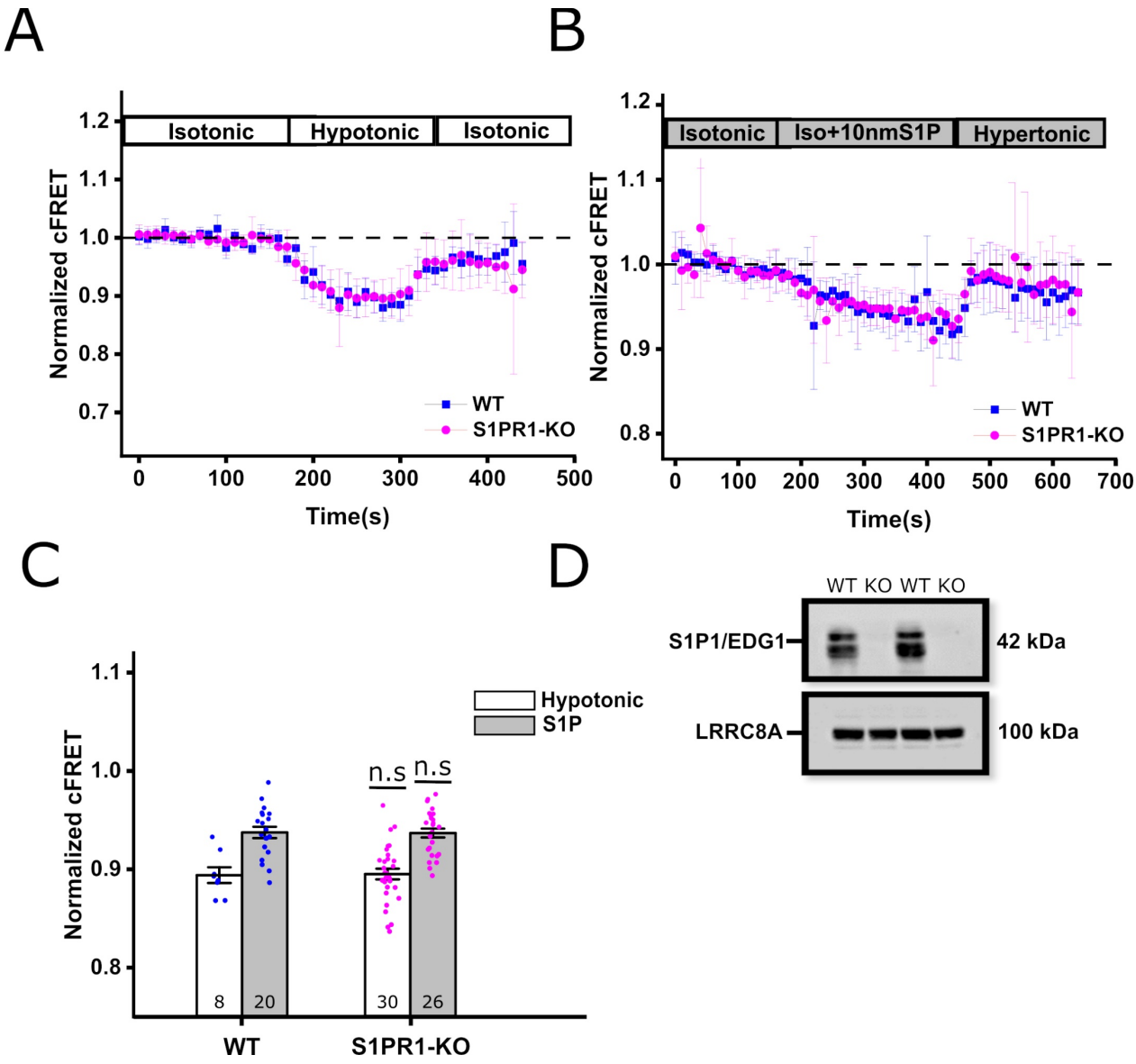

Figure 23. VRAC activation in S1PR1 knock-out and wild-type HeLa cells. Normalized cFRET of HeLa cells expressing A-CFP/E-YFP during buffer exchange experiments from isotonic to hypotonic medium (A) and isotonic to isotonic+10 nM S1P (B). Blue squares (—■—) indicate the wild-type HeLa cells whereas magenta circles (—●—) represent S1PR1 knock-out cells. (C) Quantification of normalized cFRET of the wild-type and S1PR1 KO HeLa cells challenged with hypotonic and isotonic+10 nM S1P buffer i.e., from (A) and (B). The number in bars indicates the total number of cells for each treatment. Data represents the average cFRET of the last seven time points of individual cells in hypotonic media and the last ten time points in S1P containing isotonic media, and mean of all cells ±s.e.m. n.s., not significant, by Student's t-test compared to wild-type cells. (D) Knock-out of S1PR1 was confirmed by western blotting. LRRC8A on the same blot was used as a loading control.

Having observed that, the reduced S1PR1 receptor expression and its genomic knock-out did not affect VRAC activation, I next evaluated the effect of S1PR1 receptor antagonist W123 in the HeLa S1PR1 KO cell line. W123 impaired hypotonicity and S1P-induced VRAC activation as illustrated in section 3.2.5. As long as W123 is only specific for S1PR1, it shouldn't affect the typical cFRET drop observed in S1PR1 KO cells upon channel activation. Following hypotonic buffer application, I could notice the cFRET decrease in both the W123 treated (control) and untreated S1PKO cells (Figure 24 A), however, the magnitude of channel activation was slightly altered in the W123 treated S1PR1-KO cells. Notably, the S1P-induced channel activation was not affected by W123 treatment in the S1PRKO cell line (Figure 24 B).

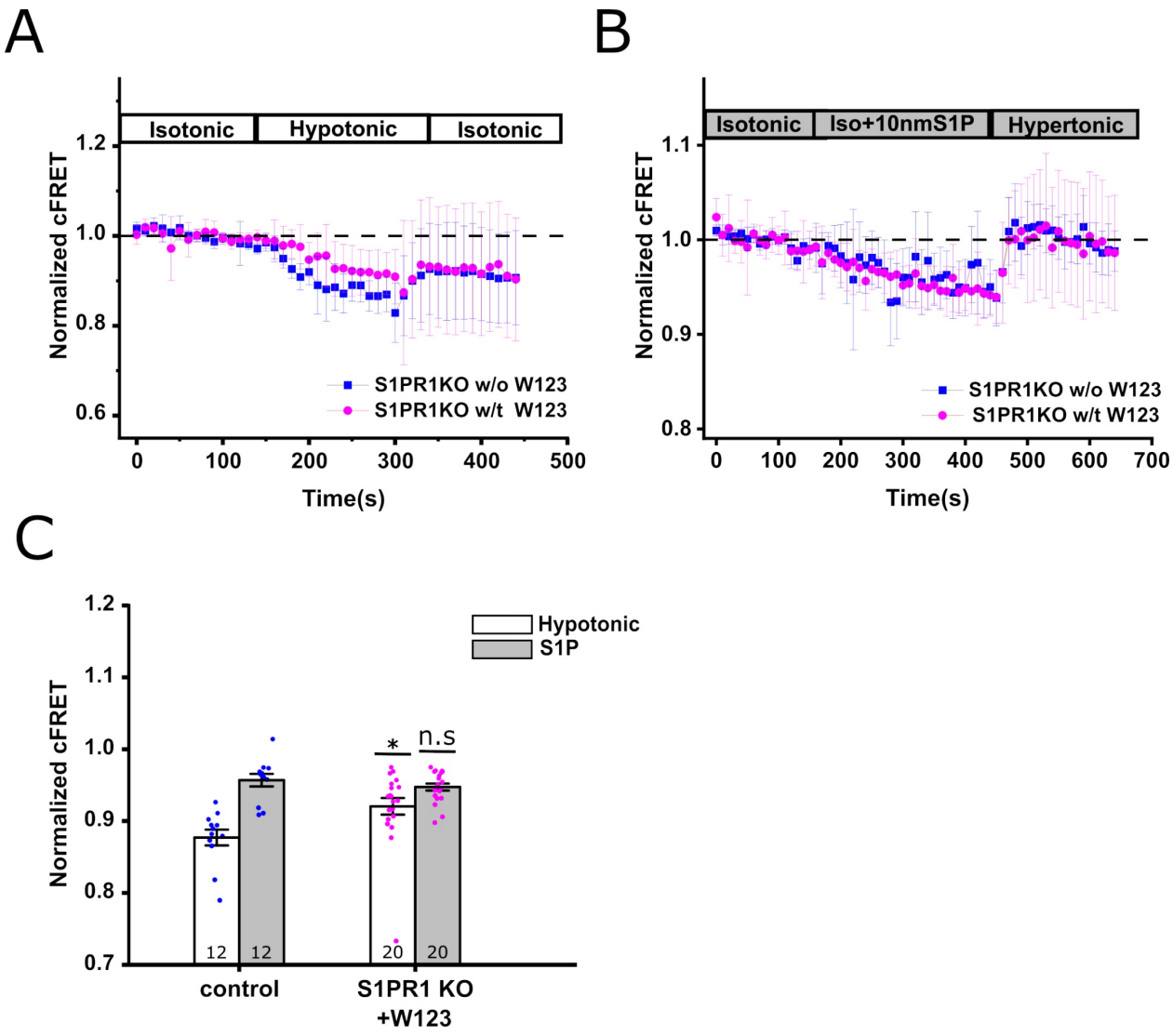

Figure 24. Effect of S1PR1 antagonist in S1PR1 KO cell line. Normalized cFRET of S1PR1 KO HeLa cells expressing A-CFP/E-YFP during buffer exchange experiments from isotonic to hypotonic medium (A) and isotonic to isotonic+10 nM S1P (B). Blue squares (—■—) indicate the

S1PR1 KO HeLa cells without prior incubation with W123; S1PR1 knock-out cells preincubated with 0.1 µM W123 (W123 also in challenging buffers) are represented by magenta circles (—●—). (C) Quantification of normalized cFRET of the S1PR1 KO HeLa cells in the presence and absence of W123 and challenged with different buffers i.e., from (A) and (B). Number in bars indicate the total number of cells for each treatment. Data represents average cFRET of the last seven time points of individual cells in hypotonic media and last ten time points in S1P containing isotonic media, and mean of all cells ±s.e.m. *p<0.05., n.s., not significant, by Student's t-test compared to wild-type cells.

Because the toxin-based results in section 3.2.6.2 indicated that Gq-mediated signaling is critical for S1P-induced channel activation, I tested how knocking down S1PR2/3 receptors would affect S1PR1 KO cells during channel activation.

In the absence of S1PR1, S1P can bind and signal through any of the other receptor subtypes and mediate the S1P signal. siRNA-mediated knock-down of S1PR2 and S1PR3 in S1PR1 KO cells did not affect hypotonicity-induced channel activity (data not shown). Since S1PR2 and S1PR3 signal through Gq, it would be interesting to examine if not the expressed receptor, but the inhibition of its downstream signaling had any biological implications. As shown in Figure 25 A, S1PR1 KO HeLa cells incubated with 1 µM YM-254890 for 5 minutes at 37°C, displayed the usual cFRET reduction with no significant difference as compared to untreated S1PR1 KO cells. Moreover, the cFRET reduction induced by S1P was similar in the S1PR1 KO cells in the presence or absence of the Gq inhibitor (Figure 25 B). This indicates that Gq-coupled S1PR2 and S1PR3 are not sufficient to transduce S1P signal without S1PR1. In addition, the S1PR2 and S1PR3 receptors do not only signal through Gq, but also through Gi and G12/13. Thus, one might expect that these G-proteins could help restore the S1P effect, especially in the absence of S1PR1-coupled signaling. Moreover, there is significant biochemical diversity among the Gq protein family. The cell signaling diversity of the $G\alpha_q$ family of G-proteins is well-reviewed elsewhere (Hubbard & Hepler, 2006).

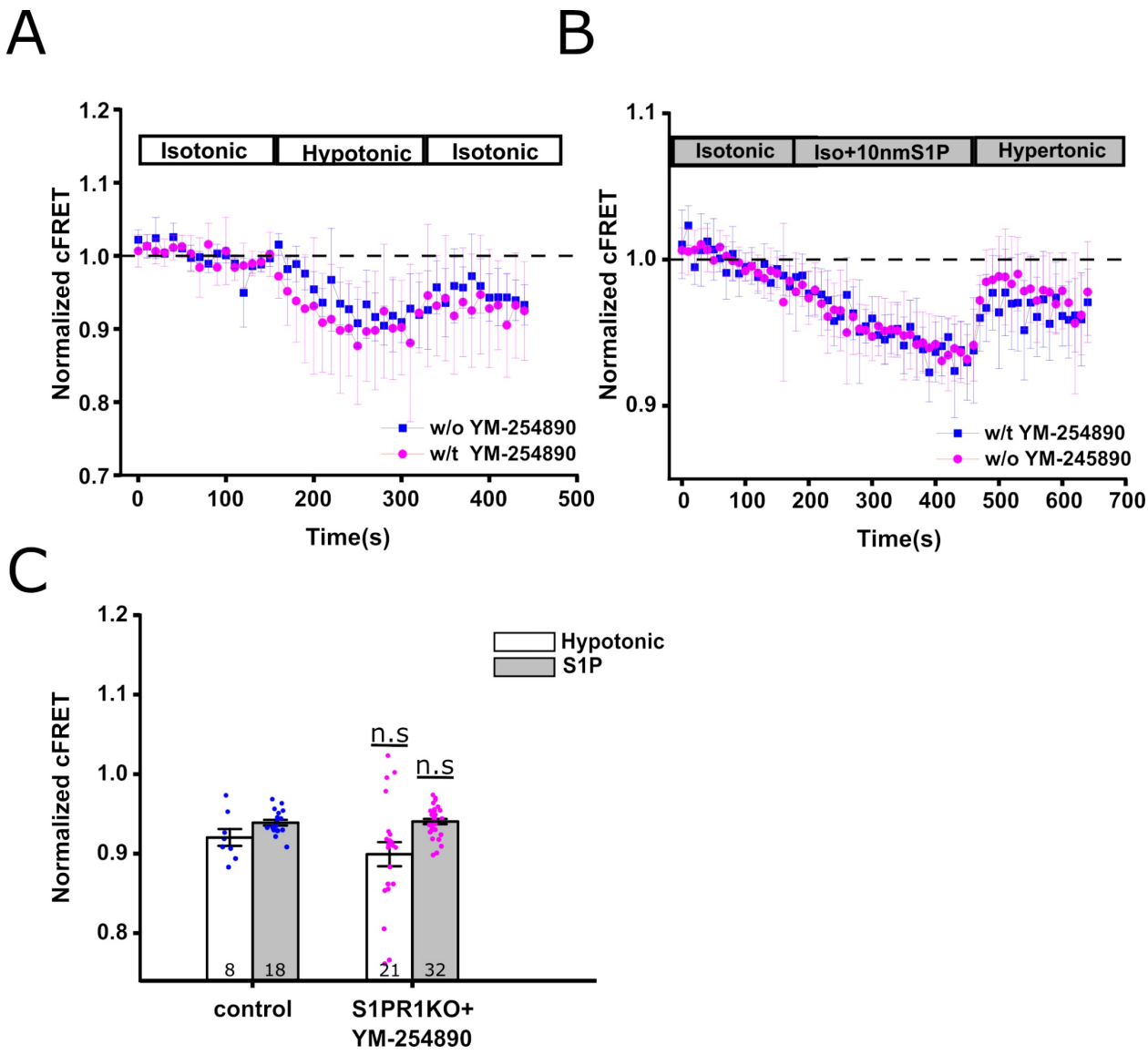

Figure 25. VRAC signaling is not mediated by S1PR2 and S1PR3 in S1PR1 KO cells. Normalized cFRET of HeLa cells expressing A-CFP/E-YFP during buffer exchange experiments from isotonic to hypotonic medium (A) and isotonic to isotonic+10 nM S1P (B). Blue squares (—■—) (control) indicate the untreated S1PR1 KO cells whereas the cells incubated with 1 μM YM-245890 prior to FRET measurements are represented by magenta circles (—●—). (C) Quantification of normalized cFRET of the treated and untreated HeLa cells challenged with hypotonic and isotonic+10 nM S1P buffer i.e., from (A) and (B). The number in bars indicates the total number of cells for each treatment. Data represents the average cFRET of the last seven time points of individual cells in hypotonic media and the last ten time points in S1P containing isotonic media, and mean of all cells ±s.e.m. n.s., not significant, by Student's t-test compared to control cells.

3.3. Effect of phospho-ablative and phospho-mimetic LRRC8A mutations on hypotonicity induced VRAC activation

Many studies have reported phosphorylation events as one of the first responses to swelling (Nilius et al, 1997b; Sadoshima et al, 1996; Tilly et al, 1993). Additionally, protein phosphorylation has been widely implicated in modulating VRAC activity (Bryan-Sisneros et al, 2000; Eggermont et al, 2001; Sadoshima et al, 1996). However, it remains to be investigated whether the phosphorylation target is VRAC itself or another regulatory protein. Therefore, I tested the effect of some potential phosphorylation sites in VRAC. CFP-tagged LRRC8A mutants were kindly provided by Dr. Michael Pusch (CNR, Genova, Italy). These mutants had amino acid substitutions at threonine residues to alanine, serine, and glutamate - T169A, T169S, and T169E, respectively. I next evaluated the effect of these LRRC8-A mutations that act as phospho-mimetic; T169E or phospho-ablative; T169A mutations. HeLa cells were co-transfected with CFP-8A mutants and E-YFP and next day analyzed during FRET measurements in buffer exchange experiments. As shown in Figure 26 A and B, I found that mutation of 8A-T169A failed to activate the channel when cells were bathed with hypotonic extracellular solution, while 8A-T169E was still able to be activated. These results suggest that phosphorylation events may play a role in channel activity.

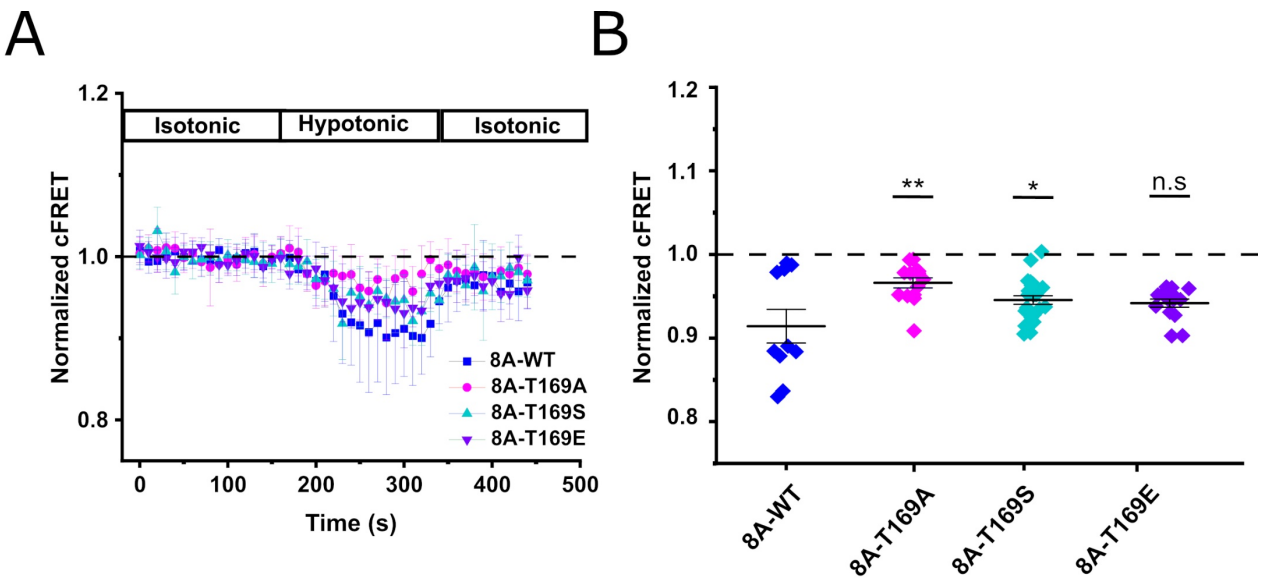

Figure 26. Hypotonic VRAC activation in LRRC8A mutants. Normalized cFRET of HeLa cells expressing 8A-CFP/E-YFP during buffer exchange experiments from isotonic to hypotonic medium. Blue squares (—■—(control) indicate the HeLa cells transfected with WT 8A-CFP/E-YFP (n=1 dish,10 cells); magenta circles (—●—) represents the 8A169ACFP/E-YFP (n=2 dishes, 14 cells); (–▲–) indicate 8AT169S/E-YFP (n=2 dishes, 24 cells) and (—▼—) represents cells with 8A169ECFP/E-YFP (n=2 dishes, 15 cells). (B) Quantification of normalized cFRET of the WT-8A

and 8A mutants HeLa cells challenged with hypotonic buffer i.e., from (A). Data represents the average cFRET of the last seven time points of individual cells in hypotonic media, and mean of all cells ±s.e.m. n.s., not significant, **p<0.005, *p<0.05, by Student's t-test compared to 8A wild-type cells.

3.4. G protein-coupled receptors (GPCR) in glucose-mediated VRAC activation in pancreatic β-cells

GPCRs, being the largest family of transmembrane receptors in the human genome, are important regulators of pancreatic islet function (Amisten et al, 2013). In this context, orphan GPCRs, whose endogenous ligands have not been identified represent an appealing source of undiscovered therapeutic potential. One of the ubiquitously expressed orphan receptors in human islets is the GPCR5B, which belongs to the conserved subgroup of the C family of GPCRs including GPCR5A, GPCR5B, GPCR5C, and GPCR5D. These GPCRs are also called retinoic acid-induced genes (RAIG1-4), as their expression is induced by retinoic acid (Bräuner-Osborne et al, 2001; Robbins et al, 2000; Soni et al, 2013). Several studies indicated that GPCR5B (also known as Raig2) is upregulated in islets of type 2 diabetic patients (Soni et al, 2013). There is also some evidence that its deletion in mice causes glucose intolerance, so it is speculated that it is involved in the pathogenies of diabetes, however, the underlying molecular mechanism is still unclear. It has been long proposed that VRAC contributes to insulin secretion, by depolarizing the β-cells in response to glucose-induced cell swelling (Best et al, 2010; Miley et al, 1999). Recently, Stuhlmann and colleagues confirmed this notion and stated the involvement of VRAC channels in increasing glucose sensitivity and insulin secretion of β-cells. By using a *Lrrc8a* KO mouse, they also suggested an important modulatory role of VRAC in insulin secretion *in vivo* (Stuhlmann et al, 2018). With these observations, I became curious to investigate the role of GPCR5B and VRAC channel activation in response to the glucose induction of pancreatic β-cells. Firstly, I confirmed the swelling induced channel activation in pancreatic β-cells. For this, I used a rat insulinoma cell line INS-1, which is a well-established model for studying the pancreatic islet β-cell function (Asfari et al, 1992). Indeed, co-transfecting the INS-1E cells with CFP tagged LRRC8A and YFP tagged LRRC8E, during buffer exchange experiment from isotonic (340 mOsm) to hypotonic (250 mOsm) solution, enabled cFRET measurements that indicated the activation of A/E containing VRAC heteromers (Figure 27 A). Furthermore, exposure of INS-1E cells to high extracellular glucose (20 mM) also caused the cFRET reduction (compared to the cells buffered with 1 mM glucose) (Figure 27 B), however, the extent of channel activation was smaller than with the large changes of extracellular osmolarity. Notably, the channel activation was irreversible, as the cFRET values did not return to the baseline values, upon hypertonic buffer

application. This is because of the osmotic effects of the intracellular glucose metabolites, which also cause cell swelling (McGlasson et al, 2011; Miley et al, 1997).

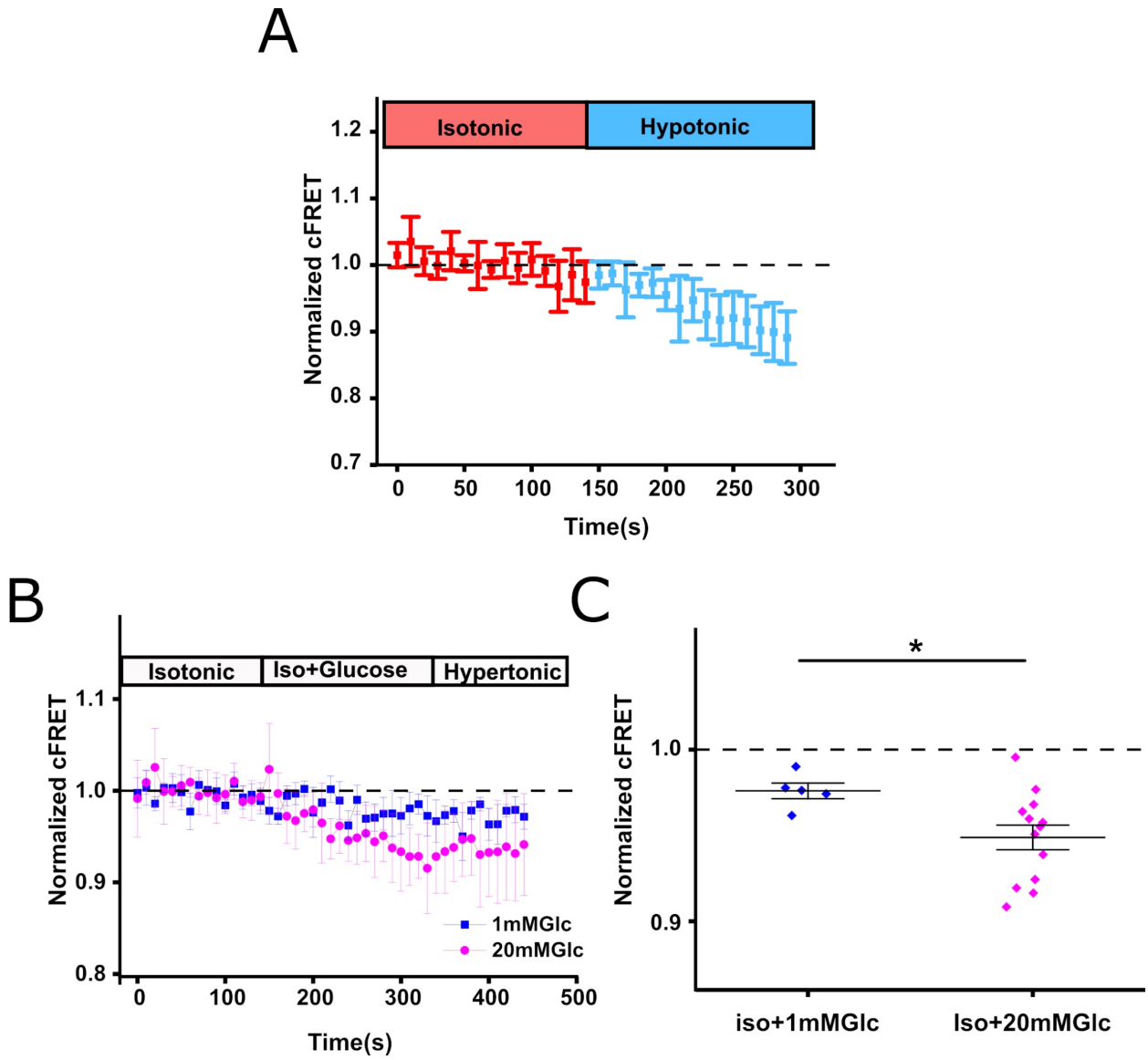

Figure 27. Hypotonicity and high extracellular glucose elicit VRAC activation. (A) Time traces of INS-1E cells expressing A-CFP/E-YFP during buffer exchange experiments from isotonic to hypotonic extracellular buffer. Data represents average cFRET of 9 cells ± SD. (B) Normalized cFRET of INS-1E expressing A-CFP/E-YFP during buffer exchange experiments from 1mM isotonic to 20 mM isotonic buffer Blue squares (—■—)(n= 5 cells) (control) correspond to bath changes without variations in glucose concentration; magenta circles (—●—)(n=13 cells) represents the cells bathed with high extracellular glucose (20 mM glucose). (C) Quantification of normalized cFRET of the INS-1E cells challenged with different glucose-containing isotonic solutions i.e., from (B). Data represents the average cFRET of the last seven time points of individual cells per condition, and mean of all cells ±s.e.m. *p<0.05., by Student's t-test compared to control cells.

3.4.1. Activation of VRAC channels is negatively regulated by GPCR5B

In order to examine, the role of GPCR5B in mediating channel activation in pancreatic β cells, I co-transfected the INS-1E cells with FLAG-tagged GPCR5B mammalian expression vector and the A-CFP and E-YFP FRET vectors, in a ratio of 2:1. This ensures that the FRET-positive cells are also positive for the GPCR5B receptor expression. GPCR5B receptor expression was further confirmed by immunofluorescence staining for the FLAG tag using an anti-FLAG antibody. As shown in Figure 28, the cells expressing the FRET vectors were also found to be positive for the GPCR5B. GPCR5A; which is also a member of the C family of GPCR was used as a control.

The GPCR5B and GPCR5A expressing INS-1E cells were then induced by high extracellular glucose-containing isotonic solution (20 mM glucose) during FRET measurements. Interestingly, I found that the expression of GPCR5B in INS-1E cells caused lower cFRET reduction as compared to the GPCR5A expressing cells (Figure 29 A, B). This indicates that the GPCR5B adversely modulates the VRAC channel activity in pancreatic β cells upon glucose stimulation.

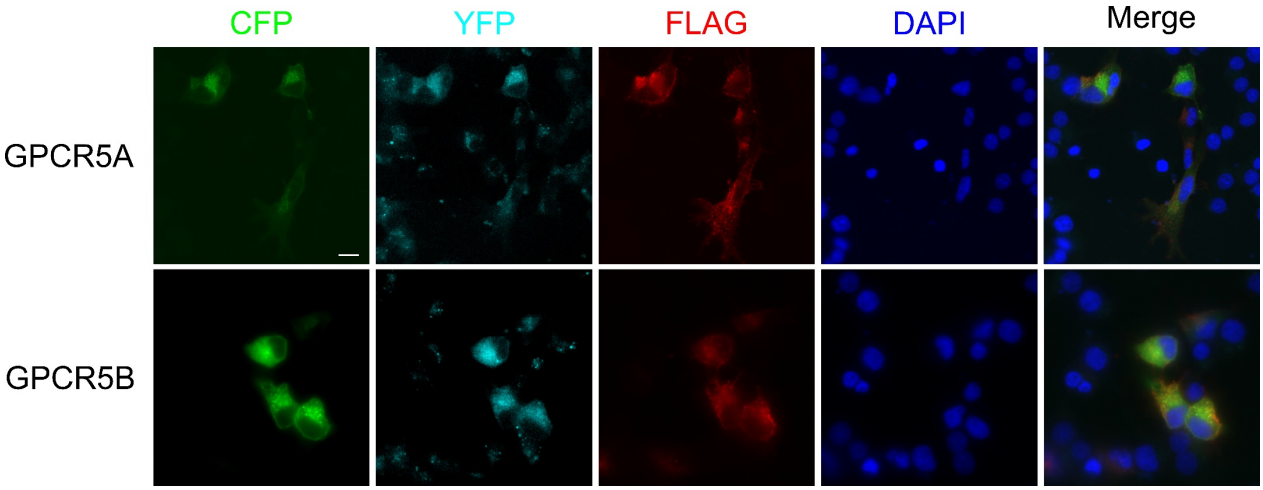

Figure 28. Immunofluorescence of permeabilized HeLa cells transfected with FLAG-tagged GPCR5A/5B. Cells transfected with LRRC8A-CFP (green), LRRC8E-YFP (cyan) and GPCR5A/B plasmid DNA were stained with an anti-FLAG antibody (red) and DAPI (nuclei, blue) after 24h of transfection. Scale bar, 20 μm.

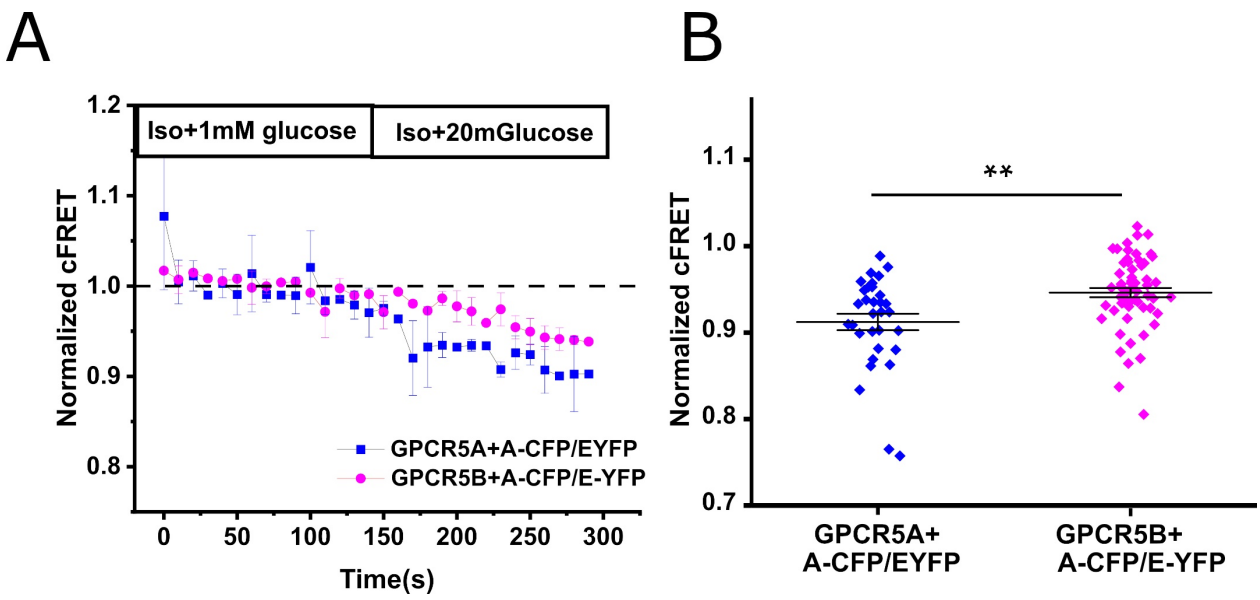

Figure 29. GPCR5B negatively modulates the VRAC channel activation. Time traces of INS-1E cells expressing GPCR5A/B and the FRET pair A-CFP/E-YFP stimulated with high extracellular glucose-containing isotonic solution (Iso+20 mM glucose). Blue squares (—■—) (control) (n=2 dishes, 32 cells) correspond to cells expressing GPCR5A and FRET pair; magenta circles (—●—) represents the GPCR5B positive cells (n=7 dishes, 61 cells). Data represents the average cFRET of all the cells ± SD. (B) Quantification of normalized cFRET of the GPCR5A/B expressing INS-1E cells challenged with 20 mM glucose-containing isotonic solution i.e., from (A). Data represents average cFRET of the last seven time points of individual cells per condition, and mean of all cells ±s.e.m. **p<0.005., by Student's t-test compared to GPCR5A expressing cells.

4. Discussion

With the discovery of the LRRC8 family of proteins, LRRC8A-LRRC8E, constituting the volume-regulated anion channel, several speculations about VRAC's molecular identity were put to rest (Qiu et al, 2014; Voss et al, 2014). Notably, Voss and colleagues showed that the multi-span transmembrane protein LRRC8A requires heteromerization with at least one other family member of the LRRC8 family i.e. LRRC8B-E, which was later on confirmed in various independent studies (Gaitán-Peñas et al, 2016; Syeda et al, 2016). Furthermore, siRNA-mediated knock-down of LRRC8A in patch-clamp experiments reduced $ICl_{(swell)}$ in multiple cell lines (Qiu et al, 2014; Voss et al, 2014). On the one hand, $ICl_{(swell)}$ could be restored by heterologous expression of LRRC8A in genome-edited LRRC8A- deficient HEK293 and HCT116 cell lines (but not in quintuple KO cells), indicating that LRRC8A is indispensable for VRAC activity (Voss et al, 2014) while on the other hand, its overexpression did not increase, but rather decreased $ICl_{(swell),}$ indicating that LRRC8A is part of a heteromeric complex (Qiu et al, 2014; Voss et al, 2014). Heteromerization of LRRC8A with other LRRC8 family members (LRRC8B-E) has been confirmed by co-immunoprecipitation (Lee et al, 2014; Syeda et al, 2016; Voss et al, 2014). Additionally, LRRC8A localizes to the plasma membrane in native cells (Voss et al, 2014) and when exogenously expressed (Qiu et al, 2014; Voss et al, 2014) while other LRRC8 proteins (LRRC8B-E) require co-expression with LRRC8A for plasma membrane delivery. High-resolution cryo-EM structures of LRRC8A and LRRC8D homomers (Nakamura et al, 2020) and LRRC8A/C heteromers further validated the hexameric nature of the native VRAC complexes (Deneka et al, 2018; Kasuya et al, 2018; Kefauver et al, 2018; Kern et al, 2019).

Interestingly, VRACs display a variable subunit stoichiometry that is dependent on the relative expression levels of the subunits (Gaitán-Peñas et al, 2016). Moreover, it has been reported that LRRC8A can combine with more than one other subunit within one complex (Lutter et al, 2017). So, it is tempting to speculate that an enormous and unknown amount of VRACs with different functional hexameric configurations can exist. What would be the impact of such variable stoichiometry? Indeed, it has been reported that the subunit compositions can affect physiologically relevant properties of VRAC, e.g., depolarization dependent inactivation, single-channel conductance, the extent of rectification, response to the regulatory factors, and substrate specificity (König & Stauber, 2019).

4.1. Native VRAC complexes contain low levels of LRRC8A subunit

In view of the fact that subunit stoichiometry is dependent on relative expression levels, it is important to know the expression profiles of the VRAC subunits in native complexes. In this thesis, I developed a method to quantify the protein levels of the five different LRRC8 VRAC subunits in cells and tissues by using recombinantly expressed and purified LRRC8 fragments to calibrate the signal in immunoblots. Based on the appropriate dilution of the recombinant proteins (tested by trial and error in preliminary experiments), the protein amounts in the tested lysate (obtained from cells and organs) lied within the dilution range, which could be linearly fitted. With this method, I could both compare the expression of LRRC8 protein between tissues and also compare the expression of all LRRC8 paralogues within one organ or cell line. Despite LRRC8A being the essential subunit for VRAC activity, I discovered that, except for 3T3, it accounts for only about one-sixth of all LRRC8 proteins in any of the tissues tested, or often even less. Moreover, except for 3T3 and spleen, I found at least one other subunit that is present in significantly higher amounts than LRRC8A. A previous study also reported reduced expression of LRRC8A, at least at the mRNA levels, e.g., in Jurkat cells, LRRC8A was expressed at less than one-sixth of all the LRRC8 RNA molecules (Gradogna et al, 2017b). In rat astrocytes, LRRC8A mRNA was shown to be expressed at equally low levels (Hyzinski-García et al, 2014) or similar levels to each of LRRC8B-D (Schober et al, 2017). It remained uncertain whether the abundance of mRNA would indeed mirror protein levels, nonetheless these results align well with the protein levels found here. I also found relatively low levels of LRRC8A compared to other LRRC8 proteins in co-immunoprecipitation experiments. All of these data hint towards a very low number of LRRC8A subunits in a VRAC hexamer. A requirement of only a few LRRC8A subunits per hexamer may explain the larger currents upon dilution of the LRRC8A subunits in LRRC8A/C co-expression (Yamada et al, 2016) and the strong suppression of endogenous VRAC currents upon overexpression of LRRC8A (Voss et al, 2014) that would interfere with the low ratio of LRRC8A per VRAC complex. Recently, two studies highlighted the biological consequences of high levels of LRRC8A expression in cancer. Elevated expression of LRRC8A may promote cancer cell growth, metastasis in colon and osteosarcoma cells, and poor survival of colon cancer patients (Zhang et al, 2018; Zhang et al, 2021). The results should be viewed with caution as LRRC8A expression was not quantified at the protein level in osteosarcoma, and sample sizes were not sufficient to support the notion in both of the studies.

I found a variable expression profile of the non-LRRC8A subunits (LRRC8B-E) in the tested cell lines and tissues. It remains to be investigated whether they have preferences for certain

interactions or whether they mix randomly depending on abundance. It is beyond the scope of this thesis to evaluate how the expression pattern relates to the physiological responses of VRAC. Nonetheless, Lipple-Wienhues and colleagues reported non-inactivating current characteristics of VRAC in T-cells, which is a typical feature of the LRRC8C subunit (Gaitán-Peñas et al, 2016; Voss et al, 2014), furthermore, VRAC currents in Jurkat cells were inhibited by oxidation, and the LRRC8E subunit, which would be expected to confer an activating effect of oxidation is the least expressed (Gradogna et al, 2017b).

Future studies would reveal whether the non-LRRC8A subunits mix randomly or if they prefer certain combinations. I cannot exclude the presence of non-LRRC8A containing complexes, which would mean that, despite relatively low levels of LRRC8A, it could be the major subunit of LRRC8 heteromers. Since all of the LRRC8B-E require co-expression of LRRC8A to localize to the plasma membrane, the complexes without LRRC8A would be more likely to stuck in ER and may be subjected to ER- associated degradation.

Since I knew the number of cells used in the protein lysate preparations, I could estimate the number of VRAC complexes per cell if one LRRC8A is present in each hexameric VRAC. Therefore, I roughly calculated the presence of ~6,000 for 3T3 cells and ~60,000 VRAC complexes for C2C12 cells. An earlier study, which measured the single-channel conductance of VRAC, estimated the expression of 10,000 functional VRACs per cell in T-lymphocytes (Lewis et al, 1993) and is in good agreement with my finding.

To summarize, the method I used enabled the measurements of absolute protein levels of the five LRRC8 VRAC subunits in any cell line and tissue type. With this method in hand, I observed a relatively low abundance of essential LRRC8A subunit, which hints towards the presence of only one LRRC8A per hexameric VRAC. Although this method has several uncertainties, it should provide a good lead for the true protein amount, provided it is viewed with caution. Nonetheless, the present method helps identify the tissue-specific roles of VRAC and determining the specific roles of the non-LRRC8A subunits.

4.2. VRAC activation mechanisms: a revisited perspective

The activation mechanisms for VRAC are still unclear. Over the last decades, a plethora of studies indicated different signaling pathways and molecules – reviewed in (Chen et al, 2019b; Okada, 1997; Strange et al, 2019). However, the essential molecular mechanism underlying the activation by hypotonicity and other triggers remains obscure. It would be worthwhile to review the methods

used to analyze the signal transduction to the plasma membrane when the channel is activated. Monitoring channel activity using electrophysiology has been widely practiced in this context. Indeed, it is the most used and powerful technique to study VRAC, however, it suffers from some drawbacks. The whole-cell configuration patch-clamp which is the most used configuration to study VRACs challenges the native composition of the cytosol against the pipette solution. Furthermore, it creates an artificial environment, with unpredictable influences on cellular signaling events underlying the regulation of VRAC. Additionally, VRAC apart from conducting Cl^- also conducts (net) uncharged osmolytes such as taurine and *myo*-inositol, however, electrophysiological measurements can only detect the flow of charged species, so these uncharged osmolytes conducted by VRAC cannot be recorded as currents. Compared to classical approaches, optical methods have several advantages in studying the conformational dynamics of ion channels in viable cells. Subunit-specific labeling will enable us to track their relevant physiological functions. Furthermore, the optical methods would offer spatio-temporal information about the channels and a less invasive approach compared to electrophysiological measurements. In this regard, FRET represents a powerful tool for monitoring the interactions whereby a donor fluorophore transfers energy to a close acceptor. The FRET measurements not only provide high throughput but also a non-invasive and longtime recording of live cells. In the past, FRET microscopy has been used to study conformational changes of chloride channels. Slow gating of ClC-0 has been an enigma until spectra FRET resolved the molecular mechanism and revealed large backbone movements in the C-terminus of the channel (Bykova et al, 2006).

The sensitized-emission FRET (seFRET) technique is the most widely used approach for non-destructive, live-cell FRET imaging. The sensitized fluorescence of the acceptor is detected through an optical FRET filter set selecting the acceptor emission during the donor excitation. The recent cryo-EM resolution of LRRC8 structures has suggested that the cytoplasmic LRRDs have a certain degree of flexibility, leading to the assumption that they may undergo structural reorganization during channel activation. This is the same as what I and the lab's previous study (König et al, 2019) found using the cFRET method, in which the cFRET modifications reflect C-termini movement in VRAC complexes during osmotic swelling as well as other activating signals.

4.2.1. Isosmotic VRAC activation is regulated by PKD signaling

AVD is an early-phase event leading to apoptotic cell death, and is driven by osmolyte efflux resulting from the activation of K^+ and Cl^- conductances (Gómez-Angelats & Cidlowski, 2002; Okada et al, 2001). Cl^- currents were even reported to be activated following apoptosis in some

studies (Schumann et al, 1993; Szabò et al, 1998a). A decade later, this Cl^- conductance was reported to occur via the VRAC, whereby death receptor-mediated apoptosis inducers, Fas-ligand and TNF-α in combination with cycloheximide are able to stimulate VRAC Cl^- channels (Shimizu et al, 2004). Consistent with this, using the FRET-based approach I found rapid (within minutes) activation of LRRC8A/E containing VRAC heteromers following stimulation of death receptor-mediated apoptotic pathway. It is also tempting to speculate that activation of VRAC is an early prerequisite for apoptosis in HeLa cells treated with death-receptor ligands (TNF-α+CHX).

Reactive oxygen species act as upstream signals in the activation of VRAC channels by mitochondrion-mediated apoptosis inducers, but most of the details remain unknown concerning death receptor-mediated apoptosis. One of the studies reported the involvement of Src-like tyrosine kinase, p56Lck, in lymphocytes stimulated with Fas-ligand. In the past, several studies suggested that the protein kinase C family and its paralogs are involved in modulating and activating the VRAC (Hermoso et al, 2004; König et al, 2019; Rudkouskaya et al, 2008; Senju et al, 2015) - not to mention that there is an equal amount of data set indicating an inhibiting effect (von Weikersthal et al, 1999). The protein kinase C family consists of several paralogs with a variety of cellular functions that they accomplish by phosphorylating their substrates at serine or threonine resides. They are activated and recruited to the plasma membrane by DAG. DAG is produced by the cleavage of PIP2 to DAG and IP3. The protein kinase family called protein kinase D (PKD), consists of PKD1 (formerly called PKCμ (Johannes et al, 1994) PKD2 and PKD3, that could be recruited by DAG to the plasma membrane. Many agents activate PKD1 *in vivo* through the activation of PKC for example, DAG analogs (Van Lint et al, 1995), neuropeptides, platelet-derived growth factors, and oxidative stress (Waldron & Rozengurt, 2000). Additionally, PKD1 can also be activated by TNF-α (Endo et al, 2000). Consistently, I observed that TNF-α+CHX-induced early VRAC channel activation was modulated by the PKD inhibitor CRT0066101. In an earlier study, pharmacological inhibition of PKD, but not PKC, impaired hypotonicity-induced VRAC activation (König et al, 2019). This inhibition by the PKD but not by PKC can be explained by the fact that PKD1 can be activated by different upstream mechanisms, mainly transphosphorylation of Ser744 and autophosphorylation of Ser748 in its activation loop (Jacamo et al, 2008; Sinnett-Smith et al, 2009b). The translocation, multi-site phosphorylation, and regulation of the catalytic activity of PKD have been excellently reviewed elsewhere (Rozengurt et al, 2005). Conclusively, PKD is a point of convergence and integration of multiple stimuli that is rapidly activated through PKCs, and persistently through PKC-dependent or PKC-independent pathways. Since DAG recruits and activates novel and conventional PKCs and PKDs at the plasma membrane (Kolczynska et al, 2020). So, it is intriguing to speculate that the application of

TNF-α or hypotonicity might recruit PKDs to the cell surface and activated PKDs potentially directly phosphorylate plasma membrane-localized VRAC. In the case of death receptor-mediated apoptosis, PKD might be the upstream signal in the channel activation. Further studies are needed to clarify the components upstream of PKD recruitment for VRAC activation triggered by apoptotic stimuli.

4.2.2. GPCR and $G\alpha_q$ G-proteins in DAG-mediated VRAC activation

Apart from PLCs, G-proteins are also implicated in DAG-mediated VRAC activation. Some of the isoforms of PKD can be activated by multiple growth-promoting GPCR agonists (that act through the Gq, G12, and Gi), indicating that PKD functions in mediating mitogenic signaling (Yuan et al, 2000; Yuan et al, 2003; Yuan et al, 2001; Zugaza et al, 1997). For example, in Swiss3T3 fibroblasts, GPCR agonist-induced overexpression of either PKD1 or PKD2, through an early PKC-dependent and late PKC-independent mechanisms causes ERK activation, DNA synthesis, and cell proliferation (Sinnett-Smith et al, 2009b; Sinnett-Smith et al, 2007; Zhukova et al, 2001). The lipid lysophosphatidic acid (LPA) potentiates a rapid and striking activation of PKD2 in human colonic epithelial NCM460 cells (Chiu et al, 2007). S1P represents an important signaling bioactive lipid, which signals through the five S1P receptors that are members of the lysophospholipid receptor family. Activation of VRAC has been reported by S1P (Burow et al, 2015). In the present study, I could also monitor the S1P-induced VRAC activation using the FRET optical sensor. All of the five S1P receptors signal through small heterotrimeric G-proteins, additionally there is a handful amount of data showing the involvement of heterotrimeric and monomeric G protein families in VRAC activation (Doroshenko & Neher, 1992; Estevez et al, 2001; Nilius et al, 1999; Voets et al, 1998). I investigated the involved S1P-induced signaling cascade in mediating VRAC activation using S1PR antagonist, S1PR knock-down and knock-out, and toxin-based inhibition of the receptor-coupled small heterotrimeric and monomeric G-proteins. I discovered that the S1PR1 receptor antagonist W123 prevented channel activation upon hypotonicity or S1P ligand binding. However, I found a slight antagonistic effect of W123 in the S1PR1 knock-out HeLa cell after hypotonic VRAC activation. This may be due to an offsite antagonizing effect of W123 on other S1P receptors that could mediate the hypotonicity-induced activation signal. S1P-induced VRAC activation did not differ significantly in the S1PR1 knock-out cell line in the presence or absence of W123, meaning that the S1P effect is mediated by other S1P receptors, and so W123 cannot suppress channel activation without S1PR1. This notion is further supported by the results obtained from receptor antagonist inhibition of the S1PR2. By using JTE-013 that is reported to be specific for S1PR2 (Arikawa et al, 2003; Osada et al, 2002),

I found no effect on channel activation induced by hypotonic extracellular solution or by S1P. This suggests a cooperative role of S1P receptors in mediating channel activity. Such an example of coordinated S1PR signaling has been reported for murine tumor growth, metastasis, and regulation of tumor vascular phenotype. Endothelial cells express S1PR2 and S1PR3 in addition to S1PR1 (Lee et al, 1999). While S1PR1 and S1PR2 stimulate opposing cellular functions, S1PR2 can activate redundant signaling pathways in the absence of S1PR1 (Adada et al, 2013; Sanchez et al, 2007). Moreover, both S1PR2 and S1PR3 were capable of signaling redundantly as S1PR1, for example via the Gi-pathway (Cartier et al, 2020). The hypotonic and S1P-induced VRAC activation in S1PR1 KO HeLa cells also indicates that S1PR1 alone is not sufficient to media the activation of VRAC. It is important to mention that Burrow and colleagues did not notice an inhibitory effect of W123 on hypotonicity-induced VRAC currents in RAW macrophages. However, in consistence with my finding, they also noted that S1P-induced VRAC currents were abolished by S1PR1 antagonist W123 but not by S1PR2 blocker JTE-013 (Burow et al, 2015).

Using toxin-mediated inhibition of different heterotrimeric G-proteins, I could show that S1P-induced VRAC activation was modulated by PTX-insensitive signaling involving the Gq family of G-proteins. A significant amount of studies suggested a possible role of the Gq family of heterotrimeric G-proteins for VRAC. For example, Gq/11-coupled receptors are thought to be sensors of mechanical membrane stretch and would therefore logically appeal to be the upstream activators of VRAC (Mederos y Schnitzler et al, 2008; Waldo et al, 2010), also because β-isoforms of PLC are the canonical effector molecules of activated, GTP-bound Gα subunits of Gq family (Harden et al, 2011). Importantly, nearly 40% of all the GPCRs rely upon the Gq alpha family members to stimulate the inositol lipid signaling (Watson & Girdlestone, 1994) and maximal PKD activation by cellular stimuli requires phosphorylation of the two activation loop resides of PKD Ser744 and Ser748. Multiple lines of evidence indicate the Gq family as central mediators of the rapid induction of PKC-mediated PKD phosphorylation. Interestingly, more recent studies indicate many agonists of Gq-coupled receptors induce a biphasic PKD activation in a variety of cell types, characterized by rapid PKC dependent followed by PKC independent PKD activation involving Ser748 autophosphorylation (Sinnett-Smith et al, 2009a; Sinnett-Smith et al, 2011; Waldron et al, 2012). This PKC-independent PKD activation further strengthens the notion that PKCs are dispensable for (hypotonic) VRAC activation (König et al, 2019) and favors the DAG-PKD mediated VRAC activation, in which the Gq family might serve as central upstream mediators of the signaling. Lastly, S1PR2 and S1PR3 receptors are coupled to the Gq family, and of the S1PR family, the S1PR2,3 and 4 were shown to activate PLC, again supporting the notion that the Gq family is involved in S1P-mediated VRAC activation.

Another interesting finding of the present study was the melittin-based inhibition of S1P-induced VRAC activation. Melittin has remarkably diverse effects on cells, and its functional effects are essentially unpredictable. It inhibits intrinsic Gs and stimulates Gi activity. Interestingly, melittin inhibited the S1P-induced channel activation, suggesting that the Gi family of G-proteins stimulate the channel under basal conditions. In addition to differentially regulating the activity of Gs and Gi proteins, melittin also inhibits PKC activity (Raynor et al, 1991) One of the studies reported the melittin-based inhibition of PDGF receptor beta-tyrosine phosphorylation and its downstream PLCγ1 phosphorylation (Son et al, 2007). PLCγ1 is involved in the hydrolysis of membrane PIP2 resulting in the production of intracellular second messengers DAG and IP3. This again points towards the involvement of DAG-PKD mediated VRAC activation, through melittin-based inhibition of PLC γ1.

Signaling downstream of the S1P receptors is intricate, with numerous synergistic and antagonistic cross-talks that play a critical role in signal transmission, integration, and distribution. Nonetheless, the Gq family of G-proteins coupled to S1PR2 and S1PR3, suggest possible candidates for DAG-PKD mediated VRAC activation. To sum up, I substantiated that S1P recruited and activated PTX-insensitive Gq protein-coupled S1P receptors and then stimulated PKC-independent activation of PKD which leads to VRAC activation. Additionally, I speculated that PKD might activate VRAC by phosphorylating it, in the scenario described above. Phosphorylation is still being debated as crucial for VRAC activation. In the past, several other chloride channels have been reported to be modulated by phosphorylation events e.g., the cytosolic regulatory domain (R) of the cystic fibrosis transmembrane conductance regulator (CFTR) is phosphorylated by the cAMP-dependent protein kinase (PKA) and results in channel activation (Cohn et al, 1992; Tabcharani et al, 1991). Importantly, except for LRRC8E, LRRC8A, B, C, and D were detected in phospho-proteome screen (Dephoure et al, 2008; Olsen et al, 2006; Zhou et al, 2013), and interestingly, all these phosphorylation sites were located in the intracellular loop (IL-1). Additionally, a PKD motif can also be found in each of the five LRRC8 proteins, mostly in the LRRD. As this thesis was being compiled, we received some CFP-tagged LRRC8A mutants in which threonine was replaced by serine, alanine, and glutamate, at positions T169S, T169A, and T169E. Mutation of threonine to alanine might result in a loss of function if this residue is important for activation while mutating threonine to glutamic acid or aspartic acid can mimic phosphorylation of the protein at these sites. Since LRRC8E was found to have no conserved PKD motif, nor was it ever detected in a phospho-proteome screen, co-expressing CFP-tagged 8A mutants with E-YFP and testing the VRAC activation by hypotonic or other activation triggers would reveal the potential role of phosphorylation. Indeed, I found that mutation of 8A-T169A

failed to activate the channel upon cell swelling, while 8A-T169E was still able to be activated upon hypotonic swelling. Mutating threonine residue to glutamic acid could render the channel constitutively open, in this case, it is difficult to detect the channel activity as cFRET is measured as a relative change from a before measured baseline cFRET value. So, the constitutively open channels cannot be distinguished from the closed ones, and one might expect very low FRET or no change in cFRET. Nevertheless, the 8A-T169E exhibited a lower cFRET drop as compared to WT 8A/8E and the 8A-T169A mutant during FRET measurements. This difference between phospho-mimetic (8A-T169E) and phospho-ablative (8A-T169A) mutation suggested that the protein is phosphorylated at these sites during channel activation. However, locking the protein in its phosphorylated state neglects to contribute much to the physiological environment of the cell, in which dynamic phosphorylation/dephosphorylation may occur (Gelens & Saurin, 2018). In short, the hypothesis outlined here is only one possible signaling pathway underlying the activation of VRAC, and will undoubtedly grow through further research.

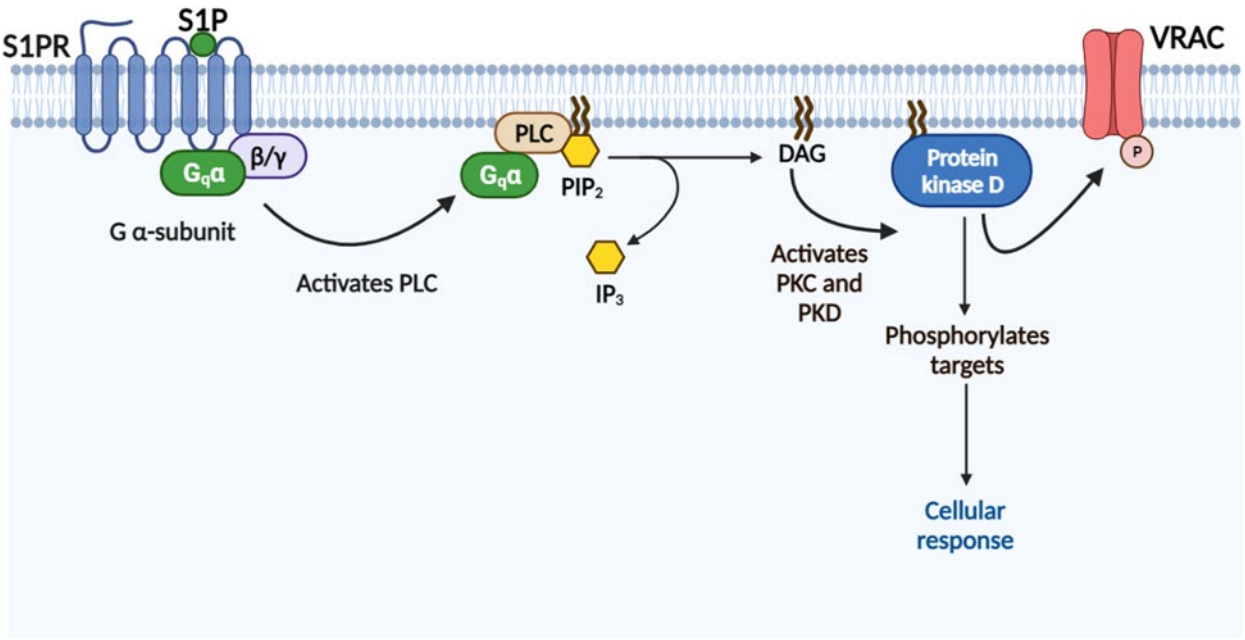

Figure 30. Theoretical model of VRAC activation. Shown is the proposed signaling pathway for activation of the VRAC by S1P/S1PR. The molecules are sphingosine-1 phosphate (S1P); sphingosine-1 phosphate receptor (S1PR); Gαq protein family and its βγ subunit; phospholipase C (PLC), phoshphatidyl inositol 4,5-bisphosphate (PIP2); Inositol triphosphate (IP3); diacylglycerol (DAG); protein kinase C (PKC); protein kinase D (PKD). Ligand-induced stimulation of S1PR leads to the activation of the Gq family of G-proteins, activated Gq proteins dissociate from the βγ subunit and activates PLC. PLC hydrolyzes PIP2 to DAG and IP3. DAG recruits and activates PKD. Activated PKD might directly phosphorylate VRAC thus activating it. Due to their

unclear roles in VRAC regulation, some of the effector molecules are omitted from the diagram for clarity.

4.3. VRAC modulation by orphan GPCRs

The classical GPCR signaling mechanisms have been long studied and established for many years. However, it has been increasingly clear that GPCR signaling biology is remarkably more complex than originally thought. Traditionally the G protein-coupled receptors are categorized into five classes based on homology, though recent studies suggested the classification based on ligand type (Pawson et al, 2014). Regardless, of the classification method, all groups of GPCRs include a subgroup referred to as “orphans”, which are GPCRs that have been identified using molecular cloning or bioinformatics, but yet do not have a known endogenous ligand (Kolar et al, 2017). GPCR5B, alternatively called RAIG2, represents an important orphan GPCR belonging to GPCR family C, group 5. There are almost 300 GPCRs expressed in pancreatic islets, that offer multiple opportunities to modulate insulin, glucagon, and somatostatin secretion (Amisten et al, 2013; Regard et al, 2008), though most of the receptors are still considered orphans. It is well established that many GPCRs do not retain a wide expression pattern, but rather are restricted to a specific cell/tissue, thus exerting the activity only in that given cell/tissue (Hakak et al, 2003). These restricted expression profiles of GPCRs enabled the identification of their functions in several physiological mechanisms (Insel et al, 2015) and in the regulation of glucose homeostasis (Sebastiani et al, 2018). The orphan receptor GPCR5B is highly expressed in mouse and human islets (Soni et al, 2013), brain (Robbins et al, 2002), and white adipose tissue (Kim et al, 2012). There is also evidence that it is highly up-regulated in islets from donors with type 2 diabetes (Soni et al, 2013) and its deletion in mice causes glucose intolerance (Kim et al, 2012), which hints towards its involvement in the pathogenies of diabetes. So far, in one study the authors (Soni et al, 2013) suggested GPCR5B to be a negative modulator of insulin secretion. Considering that GPCR5B negatively modulates insulin secretion and islet cell survival, and VRAC increases the sensitivity of β-cells to glucose (Stuhlmann et al, 2018), it is tempting to speculate that GPCR5B negatively modulates VRAC as well. This is exactly what I have observed in the present study. Using the FRET-based approach, I observed that GPCR5B negatively modulates the LRRC8A/LRRC8E heteromeric channel, therefore overexpressing GPCR5B prevented glucose-induced channel activation. A recent study has identified several ion/transport channels as well as GPCRs particularly GPCR5B in the GlialCAM interactome from the mouse brain and analyzed its interaction with GlialCAM and MLC1 (Alonso-Gardón et al, 2021). Mutations in *MLC1* or *GLIALCAM* cause megalencephalic leukoencephalopathy with cysts (MLC) which is a rare type

of leukodystrophy (van der Knaap et al, 2012). Moreover, these proteins have been linked to the regulation of different chloride channels such as ClC-2 and VRAC. VRAC has been speculated to be involved in cell volume alterations of astrocytes in MLC. Astrocytes depleted of GPCR5B showed a dramatic reduction in VRAC currents under hypotonic conditions (Alonso-Gardón et al, 2021) contrary to what I observed in FRET measurements of pancreatic β-cells upon glucose stimulation.

It is obvious that future studies are needed to elucidate the precise mechanism and the second messenger responses by which GPCR5B regulates VRAC activation and insulin secretion, also because pancreatic islets consist of several cell types and GPCRs can couple to more than one G protein family, so the results obtained in pancreatic cell lines do not always match the response in primary cells or intact cells. Conclusively, antagonizing the activity of GPCR5B (by genetic or pharmacological means) could be an intriguing way to modulate insulin secretion and VRAC activation in type-2 diabetes.

4.4. Conclusion and outlook

In the present study, I uncovered a novel role of GPCRs and the associated heterotrimeric G-proteins as upstream regulators in the DAG-PKD mediated activation of VRAC. Utilizing a FRET-based sensor, I could show that isosmotic VRAC activation by S1P involves signaling through Gq coupled S1PR receptors. I proposed that the signal is transduced *via* a PKC-independent PKD activation. Stimulated PKD might phosphorylate VRAC, thus activating it. The notion is further strengthened by the observation that the phospho-ablative mutation of LRRC8A at T169A, resulted in the loss of channel activity during hypotonic swelling. Thus, phosphorylation might be crucial for VRAC activation, and in the presented hypothesis might be carried out by PKDs. Additionally, I discussed the role of an orphan GPCR, GPCR5B in regulating β-cell function and insulin secretion via modulating VRAC activity.

Subsequent studies should examine the effect of S1P on channel activity by considering the S1P-S1PR alliance and using peptidic, chemical inhibitors, siRNA-mediated or genomic knock-out of different receptor combinations. The participation of specific G-proteins in *in vivo* signal transduction can then be elucidated by using G protein-deficient mouse models or by knock-down of Gα and Gβ subunits through small interfering RNA. More sophisticated tools such as bioluminescence resonance energy transform (BRET) and dynamic mass redistribution (DMR) can be used to measure the cellular responses to GPCR activation. For a G protein-coupled

receptor (e.g., S1PR) that couples to multiple G-proteins signaling pathways, inhibition of a specific G protein will block some, but not all pathways. Although the present study evaluates most of the S1PR coupled G protein pathways, the contribution from other classes of G-proteins can be addressed in the future. The $G\alpha_q$-mediated activation of downstream signaling molecules can be assessed by specifically inhibiting its well-known effector molecules the phospholipase C, (PLC-β), and the Rho guanine nucleotide exchange factors (RhoGEFs). It would be also interesting to monitor the effect of PMA, pharmacological inhibition of PKD or PKC during the S1P, and hypotonicity-induced activation of the phospho-mimetic and phospho-ablative mutants. The negative modulation of VRAC activity by GPCR5B in pancreatic β-cells needs to be clarified, and the underlying second messenger pathways should be identified. Importantly, the FRET approach used in this study is subunit-specific, mostly with CFP tagged LRRC8A and YFP tagged LRRC8E. On the one hand, key results should be corroborated by classical electrophysiological means. On the other hand, it will be interesting to label and test other LRRC8 members together with LRRC8A by FRET. This will not only allow the validation of the proposed signaling pathway for VRAC activation using different subunit combinations, but will also enlighten the cell type-specific regulatory mechanisms.

5. Material and Methods

5.1. Materials

5.1.1. Cell lines

Table 2. Cell lines

Name	Source/Reference	Description/ Additional Information
C2C12	CVCL_0188	Mouse myoblast/ Kindly provided by P. Knaus (Freie Universität Berlin, Germany)
3T3-L1	CVCL_0123	Mouse fibroblast/ Kindly provided by P. Knaus (Freie Universität Berlin, Germany)
HCT116	CVCL_0291	Human colon cancer/ Obtained from Leibniz Forschungsinstitut DSMZ
LRRC8A-E KO (HCT116)	(Voss et al, 2014)	HCT116 cells with quintuple LRRC8 protein depleted/ Kindly provided by T.J. Jentsch (FMP and MDC, Berlin, Germany)
HEK293	CVCL_0045	Human embryonic kidney/ obtained from Leibniz Forschungsinstitut DSMZ
LRRC8A-E KO (HEK293)	(Lutter et al, 2017)	HEK293 cells with quintuple LRRC8 protein depleted/ Kindly provided by T.J. Jentsch (FMP and MDC, Berlin, Germany)
HeLa	CVCL_0030	Mammalian cervix carcinoma/ Obtained from Leibniz Forschungsinstitut DSMZ
S1PR1 KO (HeLa)	ab265936	Human S1PR1 (S1P1/EDG1) knock-out HeLa cell line/abcam

INS-1E	CVCL_0351	Rat insulinoma cancerous cell line/ Kindly provided by T.J. Jentsch (FMP and MDC, Berlin, Germany)
RAW 2647.1	CVCL_0493	Murine macrophage cell line/ Kindly provided by P. Knaus (Freie Universität Berlin, Germany)

5.1.2. Cell culture media and transfection reagents

Table 3. Cell culture medium components

Name	Company	Product/Catalog Number
Dulbecco's modified eagle medium (DMEM)	PAN-Biotech	P04-03550
McCoy's 5A medium	PAN-Biotech	P04-05500
RPMI 1640 medium	PAN-Biotech	P04-16515
Fetal bovine serum (FBS)	PAN-Biotech	P30-3302
Penicillin-Streptomycin	PAN-Biotech	P06-07100
Trypsin/EDTA	PAN-Biotech	P10-029500
Trypsin 0.25% in PBS	PAN-Biotech	P10-021100
Dulbecco's phosphate-buffered saline (DPBS)	PAN-Biotech	P04-36500
2-mercaptoethanol	ThermoFisher	31350010
HEPES	ThermoFisher	15630080
Sodium Pyruvate	ThermoFisher	11360070
Opti-MEM	Gibco	31985070
Fugene 6	Promega	E2691
Lipofectamine™ RNAiMAX	ThermoFisher	13778075
Lipofectamine 2000	ThermoFisher	11668030

5.1.3. Chemicals and drugs

Unless otherwise stated, all chemicals used in this thesis were purchased from Sigma-Aldrich or Carl Roth.

Table 4. Chemicals and drugs

Name	Company	Product/Catalog Number

Dimethyl sulfoxide (DMSO)	PAN-Biotech	P60-36720100
CRT 0066101	Tocris, Bio-Techne	0484
Sphingosine 1-phosphate	Sigma-Aldrich	73914
Tumor necrosis factor-alpha (TNF-α)	Sigma-Aldrich	94948-59-1
Cycloheximide (CHX)	Sigma-Aldrich	66-81-9
W123	Cayman chemical	10010992
SEW 2871	Tocris, Bio-Techne	2284
JTE 013	Tocris, Bio-Techne	2392
Pertussis toxin	Tocris, Bio-Techne	3097
Cholera toxin	Sigma-Aldrich	C8052-1MG
Clostridium difficile toxin B	Sigma-Aldrich	SML1153-2UG
Gallein	Tocris, Bio-Techne	3090
Mellitin	Tocris, Bio-Techne	1193
YM-254890	Biomol GmbH	AG-CN2-0509

5.1.4. siRNAs

Table 5. Used siRNAs and their sequence

Name	**Sequence**	**Company/Product number**
Scrambled siRNA	A non-targeting negative control siRNA	ThermoFisher/4390844
S1PR1 siRNA 1	sense: GCACCACGGUCUUCACUCUtt	ThermoFisher/s4447
S1PR1 siRNA 2	sense: AGACCGUAAUUAUCGUCCUtt	ThermoFisher/s4449

5.1.5. Plasmids

Table 6. Plasmids

Name	**Vector backbone**	**Number in internal database**	**Description/Reference**
LRRC8A-Cerulean	pECFP-N1	105	(König et al, 2019)
LRRC8E-Venus	pEYFP-N1	106	(König et al, 2019)
LRRC8A-Venus	pEYFP-N1	108	(König et al, 2019)
GPCR5A-Tango	empty Tango	100	GPRC5A-Tango was a gift from Bryan Roth

			(Addgene plasmid # 66382)(Kroeze et al, 2015)
GPCR5B-Tango	empty Tango	101	GPRC5B-Tango was a gift from Bryan Roth (Addgene plasmid # 66383)(Kroeze et al, 2015)

5.1.6. Antibodies

Table 7. Antibodies

Name	Company/Supplier	Product number/Reference	Dilution
Rabbit anti-LRRC8A (5a)	Kindly provided by T.J. Jentsch (FMP and MDC, Berlin, Germany)	(Planells-Cases et al, 2015; Voss et al, 2014)	1:1000
Rabbit anti-LRRC8B (5b)			
Rabbit anti-LRRC8C (ct)			
Rabbit anti-LRRC8D (ct)			
Rabbit anti-LRRC8E (ct)			
Rabbit anti-GAPDH	Cell Signaling Technology	clone 14C10/2118	1:2500
Mouse anti- Na^+, K^+ ATPase α1	Merck	clone C464.6/05-369	1:1000
Mouse anti-GM-130	BD Biosciences	clone 35/610822	1:300
Rabbit anti-GST	Cell Signaling	5475	1:1000
Mouse-anti-beta-actin HRP	abcam	ab49900	1:10,000
Horseradish peroxidase (HRP)-conjugated goat anti-rabbit	Jackson ImmmunoResearch	aB_2307391	1:5000
Horseradish peroxidase (HRP)-conjugated goat anti-mouse	Jackson ImmmunoResearch	aB_10015289	1:5000
Recombinant Anti-S1P1/EDG1 antibody	Abcam	ab233386	1:1000

Alexa Fluor 633-goat anti-mouse Ig	Molecular probes	A-21052	1:1000

5.1.7. Primers

Table 8. Primers

Name	Species	Sequence
LRRC8A fw	Mouse	5'-GGAATTCGAGGAGAGTGACCCCAA-3'
LRRC8A rev	Mouse	5'-CCGCTCGAGTTACTTCGCCTGCTCCCCT-3'
LRRC8B fw	Mouse	5'-GGAATTCCTCTCCAAGTCCAAAAC-3'
LRRC8B rev	Mouse	5'-CCGCTCGAGTTACTTGGCTTGTTCGCC-3'
LRRC8C fw	Mouse	5'-GGAATTCTTTGAAGTCCTCCCTCC-3'
LRRC8C rev	Mouse	5'-CCGCTCGAGTTAGTCTGCTTTCAT-3'
LRRC8D fw	Mouse	5'-GGAATTCCAGTGTCGGATGCT-3'
LRRC8D rev	Mouse	5'-CCGCTCGAGTCAAATCCCGTTTGC-3'
LRRC8E fw	Mouse	5'-GGAATTCCTCAGCCGTCTGGAGCT-3'
LRRC8E rev	Mouse	5'-CTCGAGCGGTCATTCCTCCTCCAT-3'

5.2. Methods

5.2.1. Cell culture

All the cell lines used, unless stated otherwise, were maintained in growth medium (DMEM supplemented with 10% FBS, 100 units/ml penicillin and 100 µg/ml streptomycin) at 37°C under a humidified atmosphere with 5% CO_2. Wild-type and LRRC8A-E KO HCT116 cell lines were maintained in McCoy's 5A medium with 10% FBS, 100 units/ml penicillin, and 100 µg/ml streptomycin, at 37°C in a humidified atmosphere with 5% CO_2. INS-1E cells were cultured in RPMI 1640 medium supplemented with 10% FBS, 10 mM HEPES, 1mM sodium pyruvate, 50 µM 2-merceptoethanol, and 100 units/ml penicillin and 100 µg/ml streptomycin.

5.2.2. Cloning, expression and purification of recombinant GST fusion proteins

All the LRRC8 fragments were PCR amplified using the primers listed in Table 8 on genomic DNA which was purified from mouse tissue with an Invisorb kit (Invitek Molecular, Berlin, Germany)

and cloned into pGEX-5X-1 with EcoRI/XhoI. The fusion construct of GST with the amino-terminal 80 amino acids of CLC-6 (C6N) has been reported previously (Stauber & Jentsch, 2010).

The GST-tagged fusion proteins were expressed in BL21 for 3 h at 37°C after induction with 0.5 mM IPTG at an OD600 of 0.8-1.0. The bacteria were then harvested by centrifugation, resuspended in lysis buffer (50 mM Tris pH 7.5, 300 mM NaCl, 5% glycerol (v/v), supplemented with complete and AEBSF (0.5 mg/ml)) and lysed by sonication. Afterward, Triton X-100 was added to a final concentration of 1% and cell debris was removed by centrifugation (40 min, 19,500 x g, 4 °C). For purifying the GST fusion proteins, glutathione sepharose in binding buffer (50 mM Tris pH 7.5, 300 mM NaCl, 5% glycerol (v/v), 0.1% Triton X-100 (v/v)) was added to the cell lysate and incubated under agitation for 1 h at 4°C. Subsequently, the sepharose-lysate mix was centrifuged for 5 min at 500 x g at 4°C to get the flow-through fraction. The slurry was then washed five times with binding buffer supplemented with a complete protease inhibitor cocktail and AEBSF (0.5 mg/ml), after which the bound protein was eluted from the sepharose using elution buffer (50 mM Tris-HCl, 10 mM reduced glutathione, pH 8.0). A BCA-assay kit (Thermo Fisher Scientific, Darmstadt, Germany) was used to measure the protein concentration. The proteins were then flash-frozen in liquid nitrogen and kept at -80 °C for later use.

5.2.3. Generation of knock-out cell lines

The C2C12 and 3T3 LRRC8A knock-out cell lines used in this thesis have been described previously (Liu & Stauber, 2019; Pervaiz et al, 2019). Wild-type and LRRC8A-E KO HCT116 and HEK293 cell lines, reported in (Lutter et al, 2017; Voss et al, 2014) were kindly provided by T.J Jentsch, FMP and MDC Berlin, Germany.

5.2.4. Preparation of tissue and cell lysates

For preparing tissue lysates, 8 weeks old male C57BL/6 wild-type mice were sacrificed by cerebral dislocation. The mouse organs (brain, kidney, lung, heart, and spleen) were then homogenized with Triple-Pure High Impact Zirconium Beads with a 1.5mm diameter in RIPA buffer using a BeadBug 6 Position Homogenizer (Benchmark Scientific, USA). The samples were then centrifuged for 10 min at 1,000x g at 4°C (Heraeus Fresco 21, Thermo Fisher Scientific, Darmstadt, Germany) and the cell debris was removed. The supernatant contained the whole-organ lysate and its protein concentration was measured using the Pierce BCA protein Assay kit (Thermo Fisher Scientific, Darmstadt, Germany).

The cells were collected by scraping on ice, pelleted down at 2000x g for 5 min and resuspended in pre-cooled RIPA buffer (150 mM NaCl, 50 mM Tris pH 8.0, 5 mM EDTA pH 8.0, 1% NP-40, 0.5% sodium deoxycholate, 0.1% SDS) containing proteinase inhibitor cocktail (Roche, Basel, Switzerland). The resuspension was then vortexed and incubated on ice for 30 min with being vortexed every 10 min, centrifuged at 10,000 x g at 4°C for 10 min. The resulting supernatant was then mixed with SDS sample buffer heated at 95°C for 5 min. Total protein amounts were determined using the Pierce BCA protein Assay kit (Thermo Fisher Scientific, Darmstadt, Germany).

5.2.5. SDS-PAGE and immunoblotting

GST-tagged recombinant proteins and cell and tissue lysates were separated by 10% SDS-PAGE and transferred to nitrocellulose membranes (Macherey Nagel, Düren, Germany) at 200 mA for 80 min. After the transfer, the membranes were blocked with 5%-skim milk (in TBS-T) (20 mM Tris pH 7.6, 150 mM NaCl and 0.02% Tween-20) for 1 h at room temperature and incubated with the respective primary antibodies overnight at 4°C. The primary antibodies against LRRC8A-E were kindly provided by T.J. Jentsch and have been described previously (Planells-Cases et al, 2015; Voss et al, 2014). For generating the antibodies, the epitope peptides (Table1) were coupled through N-terminally added cysteines to keyhole limpet hemocyanin and then injected into rabbits. The polyclonal antibodies were then affinity-purified from rabbit sera with the respective peptides and their concentration was determined using the Pierce BCA protein Assay kit (Thermo Fisher Scientific, Darmstadt, Germany).

After, overnight incubation with the primary antibodies and subsequent three washes with TBS-T, for 30 min (10 min each wash) the membranes were incubated with horseradish peroxidase (HRP)-conjugated secondary antibody for 1 h at room temperature, washed with TBST-T and finally developed by enhanced chemiluminescence reagent (HRP juice; PJK GmbH, Kleinblittersdorf, Germany) and a ChemiSmart 5000 digital imaging system (Vilber-Lourmat, Collègien, France). Proteins were quantified using Fiji software (Schindelin et al, 2012).

5.2.6. Co-immunoprecipitation

C2C12 and 3T3 cells were lysed in 300 µl of lysis buffer (150 mM NaCl, 50 mM Tris-HCl pH 7.5, 1% NP-40, 0.5% sodium deoxycholate) containing 4 mM Pefabloc (Carl Roth, Karlsruhe, Germany) and proteinase inhibitor cocktail (Roche, Basel, Switzerland) for 10 min on ice. The

lysate was then precleared by centrifugation at 14.000 rpm for 10 min at 4°C and then spun at 30.000 g for 30 min at 4°C. The protein concentration of the lysate was determined using the Pierce BCA protein Assay kit (Thermo Fisher Scientific, Darmstadt, Germany). After then, 15 µg of the LRRC8A antibody was added to the cleared lysate containing 2.5 mg of the total protein and rotated for 1-2 h at 4°C. The rotation was then continued overnight after the addition of 50 µl of Protein A Dynabeads (Thermo Fisher Scientific, Darmstadt, Germany). The next day, after four washes with 500 µl wash buffer (same as lysis buffer, but with 0.1% NP-40 and 0.05% sodium deoxycholate), precipitates were eluted in 100 µl of Lämmli sample buffer, separated by SDS-PAGE and analyzed by immunoblot as indicated. Experiments were repeated 3 times.

5.2.7. Calculation of protein amounts

For each immunoblot, a calibration curve was generated with the recombinant proteins (Figure 31 B). Having the signal of the protein of interest in the cell or tissue lysate (quantified using Fiji software) (Schindelin et al, 2012) within the linear range of the calibration curve, the amount of protein in 60 µg of the protein (the amount loaded in the gels) can be calculated by multiplying the equivalent value of GST fusion protein with the ratio between the molecular weight of the LRRC8 protein (LRRC8A, 100 kDa; LRRC8B, 95 kDa; LRRC8C, 100 kDa; LRRC8D, 110 kDa; LRRC8E, 100 kDa) and the GST fusion protein (34 kDa). With the molecular weight, the molar amount per 1 µg total protein was calculated. Two lysates were tested per calibration curve and all experiments were performed three times, so there were six values per protein and cell type/organ.

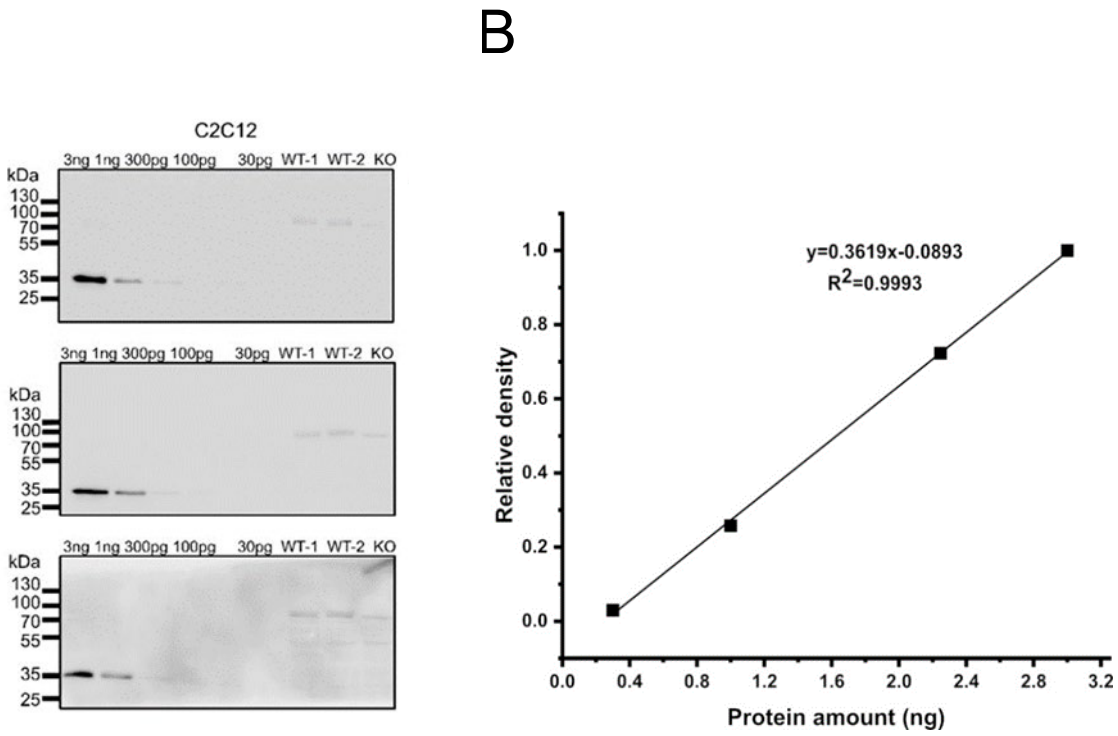

Figure 31. Example for the calibration of protein amounts.

(A) Shown here are three representative blots for LRRC8B in C2C12 cells. The band intensities of the LRRC8B in the cell lysates appear to be in the range between 300 pg and 1 ng of the recombinant protein. Measurement of the band intensities by software and calculation of the protein amount reveals the signal equivalent to ~450 pg of recombinant protein. Multiplying this with 2.79 (the ratio between the molecular weight of the LRRC8B protein (95 kDa) and the GST fusion protein (34 kDa)) gives ~1.25 ng LRRC8B in 60 µg total protein; so, 0.02 ng/µg. With the molar mass of 95 kDa, this is 0.21 fmol/ µg (as shown in Figure 5). (B) one out of the three calibration curves for LRRC8B in C2C12 cells. The measured signal is plotted as a function of the amount of recombinant protein loaded. The measured values of LRRC8B from the cell lysates lie within this linear range and thus the protein amount can be calculated.

5.2.8. Transfection of cells

For siRNA transfection, HeLa cells were seeded at a density of 1 x 10^5 in 35 mm glass-bottom dishes (MatTek) and the next day transfected with 15 nM siRNA using the Lipofectamine RNAiMAX (Invitrogen) according to the manufacturer's instructions. For FRET measurements, the cells were transfected with plasmids (LRRC8A-CFP, LRRC8E-YFP post 24 h of siRNA transfection.

For the FRET experiments, HeLa cells (1 x 10^5) were co-transfected with LRRC8A-Cerulean and LRRC8E-Venus (Table 6) using FuGENE 6 (Promega) according to the manufacturer's

instructions. 500 ng of each plasmid DNA were used, and cells were measured 24 h post-transfection. INS-1E cells were seeded (3 x 10^5) in 0.01% poly-L-lysine coated MatTek dishes. Transient transfection of INS-1E cells was performed using the Lipofectamine 2000 reagent (Invitrogen) according to the manufacturer's instructions. The DNA/lipofectamine ratio was 1/3. The transfection medium was replaced with regular growth medium after 5h, and cells were measured 24 h post-transfection. RAW 264.7 cells were transfected using the Neon electroporation transfection system (Invitrogen) according to the manufacturer's instructions and using the electroporation parameters; Pulse voltage (v): 1680, Pulse width (ms): 20, Pulse number :1, and 10µl Neon tip.

For overexpression, 2 µg of GPCR5A/GPCR5B and 1 µg of the LRRC8A-Cerulean LRRC8E-venus (500 ng each) were co-transfected in INS-1E cells using Lipofectamine 2000 reagent as stated above.

5.2.9. Immunofluorescence staining

For immunofluorescence staining of the INS-1E cells, the cells growing on MatTek dishes were transfected with the GPCR5A/B and the FRET vectors, after 24 h transfection the dishes were rinsed with PBS and fixed in 4% paraformaldehyde for 15 min at room temperature. Cells were subsequently blocked in 30 mM Glycine for 15 min and permeabilized in 0.01% saponin in 3% BSA for 15 min. After that cells were incubated with a mouse monoclonal anti-FLAG antibody in blocking buffer for 90 min. After three times washing with PBS cells were incubated with Alexa Fluor 633-labeled goat anti-mouse Ig (1:1000) for 1 h at room temperature, stained with DAPI (1:5000 in PBS; Sigma-Aldrich) for 5 min. Images were acquired with a DMi8 fluorescence microscope using a 20x or 40x objective (Leica Microsystems).

5.2.10. Imaging buffers

All the imaging buffers were prepared with sterile filtered stock solutions. Isotonic imaging buffer (340 mOsm) contained (in mM): 150 NaCl, 6 KCl, 1 MgCl2, 1.5 CaCl2,10 glucose,10 HEPES, pH 7.4 (adjusted with NaOH). Hypotonic imaging buffer (250 mOsm) was the same as isotonic, but with 105mM NaCl. Hypertonic imaging buffers (500 mOsm) were as isotonic buffers supplemented with 160 mM mannitol. For FRET measurements of INS-1E cells, the isotonic imaging buffer (320 mOsm) contained (in mM): 130 NaCl, 5 KCl, 1 MgCl2, 2.5 CaCl2,20 HEPES, and 20 Mannitol, pH 7.4 (adjusted with NaOH). For the Hypotonic buffer (250 mOsm) the concentration of NaCl was adjusted to 105 mM NaCl, further osmolarity is adjusted by omitting

Mannitol. For glucose stimulation experiments, cells were bathed with 1 mM glucose-containing isosmotic solution, that contained (in mM): 120 NaCl, 5 KCl, 1 MgCl2, 2.5 CaCl2,1 glucose,19 HEPES for 1.5 min and then exposed to 20 mM glucose isotonic solution, that contained (in mM): 120 NaCl, 5 KCl, 1 MgCl2, 2.5 CaCl2, 20 glucose.

5.2.11. FRET measurements

FRET experiments were performed as previously described (König et al, 2019). All the images were collected on a high-speed setup of Leica Microsystems (Dmi6000B stage, 63x/1.4 oil objective, high-speed external Leica wheels with Leica FRET set filters (11522073), EL6000 light source, DFC360 FX camera, controlled by Las AF software platform). All experiments were conducted at room temperature. Before imaging, the growth medium was removed and cells were washed three times with isotonic imaging buffer. seFRET images were acquired in the donor, acceptor, and FRET channels. Acquisition parameters remained the same for all the channels (8x8 binning, gain1, 100ms exposure time, illumination intensity 2). cFRET values were calculated according to the following equation (Jiang & Sorkin, 2002)

$$cFRET = \frac{I^{DA} - I^{DD}.\beta - I^{AA}.\gamma}{I^{AA}}$$

(I^{DD}) is the emission intensity of the donor channel; (I^{AA}) is for the acceptor channel and (I^{DA}) for the FRET channel. β and γ are the correction factors for the donor bleed through and acceptor cross excitation. The calculation of correction factors was described previously (König et al, 2019). cFRET maps were determined by hand-drawn regions of interest (ROIs) and were processed with the PixFRET plugin (Feige et al, 2005) (threshold set to 1, Gaussian blur to 2) with a self-written macro. The absolute FRET values varied between individual cells, so the cFRET values of individual cells were normalized to their mean cFRET in the isotonic buffer.

5.2.12. Statistical analysis

The quantitative data for the protein amounts is represented as the mean of the six measurements ±SD. *p* values were determined by a one-way analysis of variance (ANOVA) with Bonferroni's *post hoc* test. For FRET measurements, normalized cFRET values are depicted as mean of n (number of individual cells) ± SD. *p* values between two groups were determined by a two-tailed Student's *t*-test. In all the figures, *p* values are indicated according to convention: *$P < 0.05$, **$P < 0.01$, ***$P < 0.001$, n.s. = not significant.

6. References

Abascal, F. & Zardoya, R. (2012) LRRC8 proteins share a common ancestor with pannexins, and may form hexameric channels involved in cell-cell communication. *Bioessays*, 34(7), 551-60.

Adada, M., Canals, D., Hannun, Y. A. & Obeid, L. M. (2013) Sphingosine-1-phosphate receptor 2. *The FEBS journal*, 280(24), 6354-6366.

Akita, T., Fedorovich, S. V. & Okada, Y. (2011) Ca2+ nanodomain-mediated component of swelling-induced volume-sensitive outwardly rectifying anion current triggered by autocrine action of ATP in mouse astrocytes. *Cell Physiol Biochem*, 28(6), 1181-90.

Akita, T. & Okada, Y. (2014) Characteristics and roles of the volume-sensitive outwardly rectifying (VSOR) anion channel in the central nervous system. *Neuroscience*, 275, 211-31.

Aktories, K., Schmidt, G. & Just, I. (2000) Rho GTPases as targets of bacterial protein toxins. *Biol Chem*, 381(5-6), 421-6.

Alonso-Gardón, M., Elorza-Vidal, X., Castellanos, A., La Sala, G., Armand-Ugon, M., Gilbert, A., Di Pietro, C., Pla-Casillanis, A., Ciruela, F., Gasull, X., Nunes, V., Martínez, A., Schulte, U., Cohen-Salmon, M., Marazziti, D. & Estévez, R. (2021) Identification of the GlialCAM interactome: the G protein-coupled receptors GPRC5B and GPR37L1 modulate megalencephalic leukoencephalopathy proteins. *Human Molecular Genetics*.

Amisten, S., Salehi, A., Rorsman, P., Jones, P. M. & Persaud, S. J. (2013) An atlas and functional analysis of G-protein coupled receptors in human islets of Langerhans. *Pharmacol Ther*, 139(3), 359-91.

Arikawa, K., Takuwa, N., Yamaguchi, H., Sugimoto, N., Kitayama, J., Nagawa, H., Takehara, K. & Takuwa, Y. (2003) Ligand-dependent Inhibition of B16 Melanoma Cell Migration and Invasion via Endogenous S1P2 G Protein-coupled Receptor: REQUIREMENT OF INHIBITION OF CELLULAR RAC ACTIVITY*. *Journal of Biological Chemistry*, 278(35), 32841-32851.

Asfari, M., Janjic, D., Meda, P., Li, G., Halban, P. A. & Wollheim, C. B. (1992) Establishment of 2-mercaptoethanol-dependent differentiated insulin-secreting cell lines. *Endocrinology*, 130(1), 167-178.

Ashcroft, F. M. & Rorsman, P. (2013) K(ATP) channels and islet hormone secretion: new insights and controversies. *Nat Rev Endocrinol*, 9(11), 660-9.

Bach, M. D., Sørensen, B. H. & Lambert, I. H. (2018) Stress-induced modulation of volume-regulated anions channels in human alveolar carcinoma cells. *Physiol Rep*, 6(19), e13869.

Bao, J., Perez, C. J., Kim, J., Zhang, H., Murphy, C. J., Hamidi, T., Jaubert, J., Platt, C. D., Chou, J., Deng, M., Zhou, M. H., Huang, Y., Gaitán-Peñas, H., Guénet, J. L., Lin, K., Lu, Y., Chen, T., Bedford, M. T., Dent, S. Y., Richburg, J. H., Estévez, R., Pan, H. L., Geha, R. S., Shi, Q. & Benavides, F. (2018) Deficient LRRC8A-dependent volume-regulated anion channel activity is associated with male infertility in mice. *JCI Insight*, 3(16).

Ben Soussia, I., Mies, F., Naeije, R. & Shlyonsky, V. (2012) Melatonin down-regulates volume-sensitive chloride channels in fibroblasts. *Pflugers Arch*, 464(3), 273-85.

Benfenati, V., Caprini, M., Nicchia, G. P., Rossi, A., Dovizio, M., Cervetto, C., Nobile, M. & Ferroni, S. (2009) Carbenoxolone inhibits volume-regulated anion conductance in cultured rat cortical astroglia. *Channels (Austin)*, 3(5), 323-36.

Bertelli, S., Remigante, A., Zuccolini, P., Barbieri, R., Ferrera, L., Picco, C., Gavazzo, P. & Pusch, M. (2021) Mechanisms of Activation of LRRC8 Volume Regulated Anion Channels. *Cell Physiol Biochem*, 55(S1), 41-56.

Best, L. & Brown, P. D. (2009) Studies of the mechanism of activation of the volume-regulated anion channel in rat pancreatic beta-cells. *J Membr Biol*, 230(2), 83-91.

Best, L., Brown, P. D., Sener, A. & Malaisse, W. J. (2010) Electrical activity in pancreatic islet cells: The VRAC hypothesis. *Islets*, 2(2), 59-64.

Blom, T., Bergelin, N., Meinander, A., Löf, C., Slotte, J. P., Eriksson, J. E. & Törnquist, K. (2010) An autocrine sphingosine-1-phosphate signaling loop enhances NF-κB-activation and survival. *BMC Cell Biology*, 11(1), 45.

Bond, T., Basavappa, S., Christensen, M. & Strange, K. (1999) ATP dependence of the ICl,swell channel varies with rate of cell swelling. Evidence for two modes of channel activation. *J Gen Physiol*, 113(3), 441-56.

Bortner, C. D. & Cidlowski, J. A. (1998) A necessary role for cell shrinkage in apoptosis. *Biochem Pharmacol*, 56(12), 1549-59.

Bräuner-Osborne, H., Jensen, A. A., Sheppard, P. O., Brodin, B., Krogsgaard-Larsen, P. & O'Hara, P. (2001) Cloning and characterization of a human orphan family C G-protein coupled receptor GPRC5D. *Biochim Biophys Acta*, 1518(3), 237-48.

Bryan-Sisneros, A., Sabanov, V., Thoroed, S. M. & Doroshenko, P. (2000) Dual role of ATP in supporting volume-regulated chloride channels in mouse fibroblasts. *Biochimica et Biophysica Acta (BBA) - Biomembranes*, 1468(1), 63-72.

Burow, P., Klapperstück, M. & Markwardt, F. (2015) Activation of ATP secretion via volume-regulated anion channels by sphingosine-1-phosphate in RAW macrophages. *Pflugers Arch*, 467(6), 1215-26.

Bykova, E. A., Zhang, X. D., Chen, T. Y. & Zheng, J. (2006) Large movement in the C terminus of CLC-0 chloride channel during slow gating. *Nat Struct Mol Biol*, 13(12), 1115-9.

Cahalan, M. D. & Lewis, R. S. (1988) Role of potassium and chloride channels in volume regulation by T lymphocytes. *Soc Gen Physiol Ser*, 43, 281-301.

Cannon, C. L., Basavappa, S. & Strange, K. (1998) Intracellular ionic strength regulates the volume sensitivity of a swelling-activated anion channel. *Am J Physiol*, 275(2), C416-22.

Cartier, A., Leigh, T., Liu, C. H. & Hla, T. (2020) Endothelial sphingosine 1-phosphate receptors promote vascular normalization and antitumor therapy. *Proceedings of the National Academy of Sciences*, 117(6), 3157.

Catacuzzeno, L., Michelucci, A., Sforna, L., Aiello, F., Sciaccaluga, M., Fioretti, B., Castigli, E. & Franciolini, F. (2014) Identification of key signaling molecules involved in the activation of the swelling-activated chloride current in human glioblastoma cells. *J Membr Biol*, 247(1), 45-55.

Chang, F. H. & Bourne, H. R. (1989) Cholera Toxin Induces cAMP-independent Degradation of Gs. *Journal of Biological Chemistry*, 264(10), 5352-5357.

Chen, L., Becker, T. M., Koch, U. & Stauber, T. (2019a) The LRRC8/VRAC anion channel facilitates myogenic differentiation of murine myoblasts by promoting membrane hyperpolarization. *J Biol Chem*, 294(39), 14279-14288.

Chen, L., König, B., Liu, T., Pervaiz, S., Razzaque, Y. S. & Stauber, T. (2019b) More than just a pressure relief valve: physiological roles of volume-regulated LRRC8 anion channels. *Biological Chemistry*, 400(11), 1481-1496.

Chen, M. & Simard, J. M. (2001) Cell swelling and a nonselective cation channel regulated by internal Ca2+ and ATP in native reactive astrocytes from adult rat brain. *The Journal of neuroscience : the official journal of the Society for Neuroscience*, 21(17), 6512-6521.

Chi, H. (2011) Sphingosine-1-phosphate and immune regulation: trafficking and beyond. *Trends Pharmacol Sci*, 32(1), 16-24.

Chiu, T. T., Leung, W. Y., Moyer, M. P., Strieter, R. M. & Rozengurt, E. (2007) Protein kinase D2 mediates lysophosphatidic acid-induced interleukin 8 production in nontransformed human colonic epithelial cells through NF-kappaB. *Am J Physiol Cell Physiol*, 292(2), C767-77.

Choi, H., Ettinger, N., Rohrbough, J., Dikalova, A., Nguyen, H. N. & Lamb, F. S. (2016) LRRC8A channels support TNFα-induced superoxide production by Nox1 which is required for receptor endocytosis. *Free Radic Biol Med*, 101, 413-423.

Christensen, O. & Hoffmann, E. K. (1992) Cell swelling activates K+ and Cl− channels as well as nonselective, stretch-activated cation channels in ehrlich ascites tumor cells. *The Journal of Membrane Biology*, 129(1), 13-36.

Citro, S., Malik, S., Oestreich, E. A., Radeff-Huang, J., Kelley, G. G., Smrcka, A. V. & Brown, J. H. (2007) Phospholipase Cε is a nexus for Rho and Rap-mediated G protein-coupled receptor-induced astrocyte proliferation. *Proceedings of the National Academy of Sciences*, 104(39), 15543.

Clapham, D. E. & Neer, E. J. (1997) G PROTEIN βγ SUBUNITS. *Annual Review of Pharmacology and Toxicology*, 37(1), 167-203.

Cohn, J. A., Nairn, A. C., Marino, C. R., Melhus, O. & Kole, J. (1992) Characterization of the cystic fibrosis transmembrane conductance regulator in a colonocyte cell line. *Proceedings of the National Academy of Sciences of the United States of America*, 89(6), 2340-2344.

Cuvillier, O. (2012) [Sphingosine 1-phosphate receptors: from biology to physiopathology]. *Med Sci (Paris)*, 28(11), 951-7.

Davis, T. L., Bonacci, T. M., Sprang, S. R. & Smrcka, A. V. (2005) Structural and Molecular Characterization of a Preferred Protein Interaction Surface on G Protein βγ Subunits. *Biochemistry*, 44(31), 10593-10604.

de Oliveira, P. G., Ramos, M. L. S., Amaro, A. J., Dias, R. A. & Vieira, S. I. (2019) G(i/o)-Protein Coupled Receptors in the Aging Brain. *Frontiers in aging neuroscience*, 11, 89-89.

Deneka, D., Sawicka, M., Lam, A. K. M., Paulino, C. & Dutzler, R. (2018) Structure of a volume-regulated anion channel of the LRRC8 family. *Nature*, 558(7709), 254-259.

Dephoure, N., Zhou, C., Villén, J., Beausoleil, S. A., Bakalarski, C. E., Elledge, S. J. & Gygi, S. P. (2008) A quantitative atlas of mitotic phosphorylation. *Proc Natl Acad Sci U S A*, 105(31), 10762-7.

Doroshenko, P. (1998) Pervanadate inhibits volume-sensitive chloride current in bovine chromaffin cells. *Pflugers Arch*, 435(2), 303-9.

Doroshenko, P. & Neher, E. (1992) Volume-sensitive chloride conductance in bovine chromaffin cell membrane. *J Physiol*, 449, 197-218.

Doroshenko, P., Sabanov, V. & Doroshenko, N. (2001) Cell cycle-related changes in regulatory volume decrease and volume-sensitive chloride conductance in mouse fibroblasts. *J Cell Physiol*, 187(1), 65-72.

dos Remedios, C. G., Miki, M. & Barden, J. A. (1987) Fluorescence resonance energy transfer measurements of distances in actin and myosin. A critical evaluation. *J Muscle Res Cell Motil*, 8(2), 97-117.

Droogmans, G., Maertens, C., Prenen, J. & Nilius, B. (1999) Sulphonic acid derivatives as probes of pore properties of volume-regulated anion channels in endothelial cells. *Br J Pharmacol*, 128(1), 35-40.

Eggermont, J., Trouet, D., Carton, I. & Nilius, B. (2001) Cellular function and control of volume-regulated anion channels. *Cell Biochem Biophys*, 35(3), 263-74.

Elder, A. D., Domin, A., Kaminski Schierle, G. S., Lindon, C., Pines, J., Esposito, A. & Kaminski, C. F. (2009) A quantitative protocol for dynamic measurements of protein interactions by Förster resonance energy transfer-sensitized fluorescence emission. *Journal of The Royal Society Interface*, 6(suppl_1), S59-S81.

Elmore, S. (2007) Apoptosis: a review of programmed cell death. *Toxicologic pathology*, 35(4), 495-516.

Elorza-Vidal, X., Gaitán-Peñas, H. & Estévez, R. (2019) Chloride Channels in Astrocytes: Structure, Roles in Brain Homeostasis and Implications in Disease. *International journal of molecular sciences*, 20(5), 1034.

Endo, K., Oki, E., Biedermann, V., Kojima, H., Yoshida, K., Johannes, F.-J., Kufe, D. & Datta, R. (2000) Proteolytic Cleavage and Activation of Protein Kinase C μ by Caspase-3 in the Apoptotic Response of Cells to 1-β-d-Arabinofuranosylcytosine and Other Genotoxic Agents *. *Journal of Biological Chemistry*, 275(24), 18476-18481.

Ernest, N. J., Habela, C. W. & Sontheimer, H. (2008) Cytoplasmic condensation is both necessary and sufficient to induce apoptotic cell death. *J Cell Sci*, 121(Pt 3), 290-7.

Estevez, A. Y., Bond, T. & Strange, K. (2001) Regulation of I(Cl,swell) in neuroblastoma cells by G protein signaling pathways. *Am J Physiol Cell Physiol*, 281(1), C89-98.

Farrugia, G. & Rae, J. (1993) Effect of volume changes on a potassium current in rabbit corneal epithelial cells. *Am J Physiol*, 264(5 Pt 1), C1238-45.

Feige, J. N., Sage, D., Wahli, W., Desvergne, B. & Gelman, L. (2005) PixFRET, an ImageJ plug-in for FRET calculation that can accommodate variations in spectral bleed-throughs. *Microsc Res Tech*, 68(1), 51-8.

Feustel, P. J., Jin, Y. & Kimelberg, H. K. (2004) Volume-regulated anion channels are the predominant contributors to release of excitatory amino acids in the ischemic cortical penumbra. *Stroke*, 35(5), 1164-8.

Fukushima, N., Kohno, M., Kato, T., Kawamoto, S., Okuda, K., Misu, Y. & Ueda, H. (1998) Melittin, a metabostatic peptide inhibiting Gs activity. *Peptides*, 19(5), 811-9.

Gaitán-Peñas, H., Gradogna, A., Laparra-Cuervo, L., Solsona, C., Fernández-Dueñas, V., Barrallo-Gimeno, A., Ciruela, F., Lakadamyali, M., Pusch, M. & Estévez, R. (2016) Investigation of LRRC8-Mediated Volume-Regulated Anion Currents in Xenopus Oocytes. *Biophysical Journal*, 111(7), 1429-1443.

Gandy, K. A., Canals, D., Adada, M., Wada, M., Roddy, P., Snider, A. J., Hannun, Y. A. & Obeid, L. M. (2013) Sphingosine 1-phosphate induces filopodia formation through S1PR2 activation of ERM proteins. *Biochem J*, 449(3), 661-72.

Gelens, L. & Saurin, A. T. (2018) Exploring the Function of Dynamic Phosphorylation-Dephosphorylation Cycles. *Developmental Cell*, 44(6), 659-663.

Ghosh, A., Khandelwal, N., Kumar, A. & Bera, A. K. (2017) Leucine-rich repeat-containing 8B protein is associated with the endoplasmic reticulum Ca²⁺ leak in HEK293 cells. *Journal of Cell Science*, 130(22), 3818.

Gómez-Angelats, M. & Cidlowski, J. A. (2002) Cell volume control and signal transduction in apoptosis. *Toxicol Pathol*, 30(5), 541-51.

Gosling, M., Smith, J. W. & Poyner, D. R. (1995) Characterization of a volume-sensitive chloride current in rat osteoblast-like (ROS 17/2.8) cells. *The Journal of physiology*, 485 (Pt 3)(Pt 3), 671-682.

Gradogna, A., Gaitán-Peñas, H., Boccaccio, A., Estévez, R. & Pusch, M. (2017a) Cisplatin activates volume sensitive LRRC8 channel mediated currents in Xenopus oocytes. *Channels (Austin, Tex.)*, 11(3), 254-260.

Gradogna, A., Gavazzo, P., Boccaccio, A. & Pusch, M. (2017b) Subunit-dependent oxidative stress sensitivity of LRRC8 volume-regulated anion channels. *J Physiol*, 595(21), 6719-6733.

Haas, B. R. & Sontheimer, H. (2010) Inhibition of the Sodium-Potassium-Chloride Cotransporter Isoform-1 reduces glioma invasion. *Cancer research*, 70(13), 5597-5606.

Hakak, Y., Shrestha, D., Goegel, M. C., Behan, D. P. & Chalmers, D. T. (2003) Global analysis of G-protein-coupled receptor signaling in human tissues. *FEBS Letters*, 550(1), 11-17.

Hand, M., Morrison, R. & Strange, K. (1997) Characterization of volume-sensitive organic osmolyte efflux and anion current in Xenopus oocytes. *The Journal of Membrane Biology*, 157(1), 9-16.

Hannun, Y. A. & Obeid, L. M. (2008) Principles of bioactive lipid signalling: lessons from sphingolipids. *Nat Rev Mol Cell Biol*, 9(2), 139-50.

Hannun, Y. A. & Obeid, L. M. (2018) Sphingolipids and their metabolism in physiology and disease. *Nat Rev Mol Cell Biol*, 19(3), 175-191.

Harden, T. K., Waldo, G. L., Hicks, S. N. & Sondek, J. (2011) Mechanism of activation and inactivation of Gq/phospholipase C-β signaling nodes. *Chemical reviews*, 111(10), 6120-6129.

Harrigan, T. J., Abdullaev, I. F., Jourd'heuil, D. & Mongin, A. A. (2008) Activation of microglia with zymosan promotes excitatory amino acid release via volume-regulated anion channels: the role of NADPH oxidases. *J Neurochem*, 106(6), 2449-62.

Hasegawa, Y., Shimizu, T., Takahashi, N. & Okada, Y. (2012) The apoptotic volume decrease is an upstream event of MAP kinase activation during Staurosporine-induced apoptosis in HeLa cells. *International journal of molecular sciences*, 13(7), 9363-9379.

Hazama, A. & Okada, Y. (1988) Ca2+ sensitivity of volume-regulatory K+ and Cl- channels in cultured human epithelial cells. *J Physiol*, 402, 687-702.

He, D., Luo, X., Wei, W., Xie, M., Wang, W. & Yu, Z. (2012) DCPIB, a specific inhibitor of volume-regulated anion channels (VRACs), inhibits astrocyte proliferation and cell cycle progression via G1/S arrest. *J Mol Neurosci*, 46(2), 249-57.

Hermoso, M., Olivero, P., Torres, R., Riveros, A., Quest, A. F. & Stutzin, A. (2004) Cell volume regulation in response to hypotonicity is impaired in HeLa cells expressing a protein kinase Calpha mutant lacking kinase activity. *J Biol Chem*, 279(17), 17681-9.

Hisano, Y., Nishi, T. & Kawahara, A. (2012) The functional roles of S1P in immunity. *J Biochem*, 152(4), 305-11.

Hoffmann, E. K., Lambert, I. H. & Pedersen, S. F. (2009) Physiology of Cell Volume Regulation in Vertebrates. *Physiological Reviews*, 89(1), 193-277.

Hoffmann, E. K. & Simonsen, L. O. (1989) Membrane mechanisms in volume and pH regulation in vertebrate cells. *Physiol Rev*, 69(2), 315-82.

Hubbard, K. B. & Hepler, J. R. (2006) Cell signalling diversity of the Gqalpha family of heterotrimeric G proteins. *Cell Signal*, 18(2), 135-50.

Hurowitz, E. H., Melnyk, J. M., Chen, Y.-J., Kouros-Mehr, H., Simon, M. I. & Shizuya, H. (2000) Genomic Characterization of the Human Heterotrimeric G Protein α, β, and γ Subunit Genes. *DNA Research*, 7(2), 111-120.

Hyzinski-García, M. C., Rudkouskaya, A. & Mongin, A. A. (2014) LRRC8A protein is indispensable for swelling-activated and ATP-induced release of excitatory amino acids in rat astrocytes. *J Physiol*, 592(22), 4855-62.

Ikeda, S. R. (1996) Voltage-dependent modulation of N-type calcium channels by G-protein β γsubunits. *Nature*, 380(6571), 255-258.

Inoue, H., Ohtaki, H., Nakamachi, T., Shioda, S. & Okada, Y. (2007) Anion channel blockers attenuate delayed neuronal cell death induced by transient forebrain ischemia. *J Neurosci Res*, 85(7), 1427-35.

Insel, P. A., Wilderman, A., Zambon, A. C., Snead, A. N., Murray, F., Aroonsakool, N., McDonald, D. S., Zhou, S., McCann, T., Zhang, L., Sriram, K., Chinn, A. M., Michkov, A. V., Lynch, R. M., Overland, A. C. & Corriden, R. (2015) G Protein-Coupled Receptor (GPCR) Expression in Native Cells: "Novel" endoGPCRs as Physiologic Regulators and Therapeutic Targets. *Molecular pharmacology*, 88(1), 181-187.

Ise, T., Shimizu, T., Lee, E. L., Inoue, H., Kohno, K. & Okada, Y. (2005) Roles of volume-sensitive Cl- channel in cisplatin-induced apoptosis in human epidermoid cancer cells. *J Membr Biol*, 205(3), 139-45.

Jacamo, R., Sinnett-Smith, J., Rey, O., Waldron, R. T. & Rozengurt, E. (2008) Sequential protein kinase C (PKC)-dependent and PKC-independent protein kinase D catalytic activation via Gq-coupled receptors: differential regulation of activation loop Ser(744) and Ser(748) phosphorylation. *J Biol Chem*, 283(19), 12877-87.

Jackson, P. S., Churchwell, K., Ballatori, N., Boyer, J. L. & Strange, K. (1996) Swelling-activated anion conductance in skate hepatocytes: regulation by cell Cl- and ATP. *American Journal of Physiology-Cell Physiology*, 270(1), C57-C66.

Jackson, P. S., Morrison, R. & Strange, K. (1994) The volume-sensitive organic osmolyte-anion channel VSOAC is regulated by nonhydrolytic ATP binding. *Am J Physiol*, 267(5 Pt 1), C1203-9.

Jackson, P. S. & Strange, K. (1993) Volume-sensitive anion channels mediate swelling-activated inositol and taurine efflux. *Am J Physiol*, 265(6 Pt 1), C1489-500.

Jackson, P. S. & Strange, K. (1995) Characterization of the voltage-dependent properties of a volume-sensitive anion conductance. *Journal of General Physiology*, 105(5), 661-676.

Jentsch, T. J. (1996) Chloride channels: a molecular perspective. *Current Opinion in Neurobiology*, 6(3), 303-310.

Jiang, X. & Sorkin, A. (2002) Coordinated Traffic of Grb2 and Ras during Epidermal Growth Factor Receptor Endocytosis Visualized in Living Cells. *Molecular Biology of the Cell*, 13(5), 1522-1535.

Jo, E., Sanna, M. G., Gonzalez-Cabrera, P. J., Thangada, S., Tigyi, G., Osborne, D. A., Hla, T., Parrill, A. L. & Rosen, H. (2005) S1P1-selective in vivo-active agonists from high-throughput screening: off-the-shelf chemical probes of receptor interactions, signaling, and fate. *Chem Biol*, 12(6), 703-15.

Johannes, F. J., Prestle, J., Eis, S., Oberhagemann, P. & Pfizenmaier, K. (1994) PKCu is a novel, atypical member of the protein kinase C family. *J Biol Chem*, 269(8), 6140-8.

Kang, C., Gunasekar, S. K., Mishra, A., Xie, L., Zhang, Y., Pai, S., Gao, Y., Norris, A. W., Stephens, S. B. & Sah, R. (2017) SWELL1 is a glucose sensor required for β-cell excitability and insulin secretion. *bioRxiv*, 155093.

Kang, C., Xie, L., Gunasekar, S. K., Mishra, A., Zhang, Y., Pai, S., Gao, Y., Kumar, A., Norris, A. W., Stephens, S. B. & Sah, R. (2018) SWELL1 is a glucose sensor regulating β-cell excitability and systemic glycaemia. *Nat Commun*, 9(1), 367.

Kang, Y. S., Ko, Y. G. & Seo, J. S. (2000) Caveolin internalization by heat shock or hyperosmotic shock. *Exp Cell Res*, 255(2), 221-8.

Kasuya, G., Nakane, T., Yokoyama, T., Jia, Y., Inoue, M., Watanabe, K., Nakamura, R., Nishizawa, T., Kusakizako, T., Tsutsumi, A., Yanagisawa, H., Dohmae, N., Hattori, M., Ichijo, H., Yan, Z., Kikkawa, M., Shirouzu, M., Ishitani, R. & Nureki, O. (2018) Cryo-EM structures of the human volume-regulated anion channel LRRC8. *Nature Structural & Molecular Biology*, 25(9), 797-804.

Kefauver, J. M., Saotome, K., Dubin, A. E., Pallesen, J., Cottrell, C. A., Cahalan, S. M., Qiu, Z., Hong, G., Crowley, C. S., Whitwam, T., Lee, W. H., Ward, A. B. & Patapoutian, A. (2018) Structure of the human volume regulated anion channel. *Elife*, 7.

Kelley, G. G., Kaproth-Joslin, K. A., Reks, S. E., Smrcka, A. V. & Wojcikiewicz, R. J. H. (2006) G-protein-coupled receptor agonists activate endogenous phospholipase Cepsilon and phospholipase Cbeta3 in a temporally distinct manner. *The Journal of biological chemistry*, 281(5), 2639-2648.

Kern, D. M., Oh, S., Hite, R. K. & Brohawn, S. G. (2019) Cryo-EM structures of the DCPIB-inhibited volume-regulated anion channel LRRC8A in lipid nanodiscs. *eLife*, 8, e42636.

Kim, Y. J., Sano, T., Nabetani, T., Asano, Y. & Hirabayashi, Y. (2012) GPRC5B activates obesity-associated inflammatory signaling in adipocytes. *Sci Signal*, 5(251), ra85.

Kimelberg, H. K., Goderie, S. K., Higman, S., Pang, S. & Waniewski, R. A. (1990) Swelling-induced release of glutamate, aspartate, and taurine from astrocyte cultures. *J Neurosci*, 10(5), 1583-91.

Kirk, K., Ellory, J. C. & Young, J. D. (1992) Transport of organic substrates via a volume-activated channel. *Journal of Biological Chemistry*, 267(33), 23475-23478.

Kittl, M., Dobias, H., Beyreis, M., Kiesslich, T., Mayr, C., Gaisberger, M., Ritter, M., Kerschbaum, H. & Jakab, M. (2018) Glycine Induces Migration of Microglial BV-2 Cells via SNAT-Mediated Cell Swelling. *Cellular Physiology and Biochemistry*, 50, 1460 - 1473.

Klausen, T. K., Bergdahl, A., Hougaard, C., Christophersen, P., Pedersen, S. F. & Hoffmann, E. K. (2007) Cell cycle-dependent activity of the volume- and Ca2+-activated anion currents in Ehrlich lettre ascites cells. *J Cell Physiol*, 210(3), 831-42.

Klausen, T. K., Hougaard, C., Hoffmann, E. K. & Pedersen, S. F. (2006) Cholesterol modulates the volume-regulated anion current in Ehrlich-Lettre ascites cells via effects on Rho and F-actin. *Am J Physiol Cell Physiol*, 291(4), C757-71.

Kolar, G. R., Grote, S. M. & Yosten, G. L. C. (2017) Targeting orphan G protein-coupled receptors for the treatment of diabetes and its complications: C-peptide and GPR146. *Journal of Internal Medicine*, 281(1), 25-40.

Kolczynska, K., Loza-Valdes, A., Hawro, I. & Sumara, G. (2020) Diacylglycerol-evoked activation of PKC and PKD isoforms in regulation of glucose and lipid metabolism: a review. *Lipids in Health and Disease*, 19(1), 113.

König, B., Hao, Y., Schwartz, S., Plested, A. J. R. & Stauber, T. (2019) A FRET sensor of C-terminal movement reveals VRAC activation by plasma membrane DAG signaling rather than ionic strength. *eLife*, 8, e45421.

König, B. & Stauber, T. (2019) Biophysics and Structure-Function Relationships of LRRC8-Formed Volume-Regulated Anion Channels. *Biophysical Journal*, 116(7), 1185-1193.

Kroeze, W. K., Sassano, M. F., Huang, X. P., Lansu, K., McCorvy, J. D., Giguère, P. M., Sciaky, N. & Roth, B. L. (2015) PRESTO-Tango as an open-source resource for interrogation of the druggable human GPCRome. *Nat Struct Mol Biol*, 22(5), 362-9.

Kubo, M. & Okada, Y. (1992) Volume-regulatory Cl- channel currents in cultured human epithelial cells. *The Journal of physiology*, 456, 351-371.

Kumar, L., Chou, J., Yee, C. S. K., Borzutzky, A., Vollmann, E. H., von Andrian, U. H., Park, S.-Y., Hollander, G., Manis, J. P., Poliani, P. L. & Geha, R. S. (2014) Leucine-rich repeat containing 8A (LRRC8A) is essential for T lymphocyte development and function. *The Journal of experimental medicine*, 211(5), 929-942.

Lahey, L. J., Mardjuki, R. E., Wen, X., Hess, G. T., Ritchie, C., Carozza, J. A., Böhnert, V., Maduke, M., Bassik, M. C. & Li, L. (2020) LRRC8A:C/E Heteromeric Channels Are Ubiquitous Transporters of cGAMP. *Molecular Cell*, 80(4), 578-591.e5.

Lai, T. W., Zhang, S. & Wang, Y. T. (2014) Excitotoxicity and stroke: identifying novel targets for neuroprotection. *Prog Neurobiol*, 115, 157-88.

Lalouette, A., Lablack, A., Guenet, J. L., Montagutelli, X. & Segretain, D. (1996) Male sterility caused by sperm cell-specific structural abnormalities in ebouriffé, a new mutation of the house mouse. *Biol Reprod*, 55(2), 355-63.

Lang, F. & Hoffmann, E. K. (2012) Role of ion transport in control of apoptotic cell death. *Compr Physiol*, 2(3), 2037-61.

Lang, F., Shumilina, E., Ritter, M., Gulbins, E., Vereninov, A. & Huber, S. M. (2006) Ion channels and cell volume in regulation of cell proliferation and apoptotic cell death. *Contrib Nephrol*, 152, 142-160.

Lee, C. C., Freinkman, E., Sabatini, D. M. & Ploegh, H. L. (2014) The protein synthesis inhibitor blasticidin s enters mammalian cells via leucine-rich repeat-containing protein 8D. *J Biol Chem*, 289(24), 17124-31.

Lee, E. L., Shimizu, T., Ise, T., Numata, T., Kohno, K. & Okada, Y. (2007) Impaired activity of volume-sensitive Cl- channel is involved in cisplatin resistance of cancer cells. *J Cell Physiol*, 211(2), 513-21.

Lee, M.-J., Van Brocklyn, J. R., Thangada, S., Liu, C. H., Hand, A. R., Menzeleev, R., Spiegel, S. & Hla, T. (1998) Sphingosine-1-Phosphate as a Ligand for the G Protein-Coupled Receptor EDG-1. *Science*, 279(5356), 1552.

Lee, M. J., Thangada, S., Claffey, K. P., Ancellin, N., Liu, C. H., Kluk, M., Volpi, M., Sha'afi, R. I. & Hla, T. (1999) Vascular endothelial cell adherens junction assembly and morphogenesis induced by sphingosine-1-phosphate. *Cell*, 99(3), 301-12.

Lehmann, D. M., Seneviratne, A. M. & Smrcka, A. V. (2008) Small molecule disruption of G protein beta gamma subunit signaling inhibits neutrophil chemotaxis and inflammation. *Mol Pharmacol*, 73(2), 410-8.

Lepple-Wienhues, A., Szabò, I., Laun, T., Kaba, N. K., Gulbins, E. & Lang, F. (1998) The tyrosine kinase p56lck mediates activation of swelling-induced chloride channels in lymphocytes. *J Cell Biol*, 141(1), 281-6.

Levitan, I., Christian, A. E., Tulenko, T. N. & Rothblat, G. H. (2000) Membrane cholesterol content modulates activation of volume-regulated anion current in bovine endothelial cells. *J Gen Physiol*, 115(4), 405-16.

Lewis, R. S., Ross, P. E. & Cahalan, M. D. (1993) Chloride channels activated by osmotic stress in T lymphocytes. *Journal of General Physiology*, 101(6), 801-826.

Liang, W., Huang, L., Zhao, D., He, J. Z., Sharma, P., Liu, J., Gramolini, A. O., Ward, M. E., Cho, H. C. & Backx, P. H. (2014) Swelling-activated Cl- currents and intracellular CLC-3 are involved in proliferation of human pulmonary artery smooth muscle cells. *J Hypertens*, 32(2), 318-30.

Lin, J. & Redies, C. (2012) Histological evidence: housekeeping genes beta-actin and GAPDH are of limited value for normalization of gene expression. *Dev Genes Evol*, 222(6), 369-76.

Liu, H.-T., Akita, T., Shimizu, T., Sabirov, R. Z. & Okada, Y. (2009) Bradykinin-induced astrocyte-neuron signalling: glutamate release is mediated by ROS-activated volume-sensitive outwardly rectifying anion channels. *The Journal of physiology*, 587(Pt 10), 2197-2209.

Liu, H. T., Tashmukhamedov, B. A., Inoue, H., Okada, Y. & Sabirov, R. Z. (2006) Roles of two types of anion channels in glutamate release from mouse astrocytes under ischemic or osmotic stress. *Glia*, 54(5), 343-57.

Liu, T. & Stauber, T. (2019) The Volume-Regulated Anion Channel LRRC8/VRAC Is Dispensable for Cell Proliferation and Migration. *Int J Mol Sci*, 20(11).

Logothetis, D. E., Kurachi, Y., Galper, J., Neer, E. J. & Clapham, D. E. (1987) The βγ subunits of GTP-binding proteins activate the muscarinic K+ channel in heart. *Nature*, 325(6102), 321-326.

Lück, J. C., Puchkov, D., Ullrich, F. & Jentsch, T. J. (2018) LRRC8/VRAC anion channels are required for late stages of spermatid development in mice. *Journal of Biological Chemistry*, 293(30), 11796-11808.

Lutter, D., Ullrich, F., Lueck, J. C., Kempa, S. & Jentsch, T. J. (2017) Selective transport of neurotransmitters and modulators by distinct volume-regulated LRRC8 anion channels. *J Cell Sci*, 130(6), 1122-1133.

Maceyka, M., Harikumar, K. B., Milstien, S. & Spiegel, S. (2012) Sphingosine-1-phosphate signaling and its role in disease. *Trends in cell biology*, 22(1), 50-60.

Maeda, S., Nakagawa, S., Suga, M., Yamashita, E., Oshima, A., Fujiyoshi, Y. & Tsukihara, T. (2009) Structure of the connexin 26 gap junction channel at 3.5 A resolution. *Nature*, 458(7238), 597-602.

Maeno, E., Ishizaki, Y., Kanaseki, T., Hazama, A. & Okada, Y. (2000) Normotonic cell shrinkage because of disordered volume regulation is an early prerequisite to apoptosis. *Proceedings of the National Academy of Sciences*, 97(17), 9487.

Maertens, C., Droogmans, G., Chakraborty, P. & Nilius, B. (2001) Inhibition of volume-regulated anion channels in cultured endothelial cells by the anti-oestrogens clomiphene and nafoxidine. *Br J Pharmacol*, 132(1), 135-42.

Mangmool, S. & Kurose, H. (2011) G(i/o) protein-dependent and -independent actions of Pertussis Toxin (PTX). *Toxins*, 3(7), 884-899.

Mao, J., Wang, L., Fan, A., Wang, J., Xu, B., Jacob, T. J. & Chen, L. (2007) Blockage of volume-activated chloride channels inhibits migration of nasopharyngeal carcinoma cells. *Cell Physiol Biochem*, 19(5-6), 249-58.

McGlasson, L., Best, L. & Brown, P. D. (2011) The glucokinase activator GKA50 causes an increase in cell volume and activation of volume-regulated anion channels in rat pancreatic β-cells. *Mol Cell Endocrinol*, 342(1-2), 48-53.

Mederos y Schnitzler, M., Storch, U., Meibers, S., Nurwakagari, P., Breit, A., Essin, K., Gollasch, M. & Gudermann, T. (2008) Gq-coupled receptors as mechanosensors mediating myogenic vasoconstriction. *Embo j*, 27(23), 3092-103.

Miley, H. E., Brown, P. D. & Best, L. (1999) Regulation of a volume-sensitive anion channel in rat pancreatic beta-cells by intracellular adenine nucleotides. *J Physiol*, 515 (Pt 2)(Pt 2), 413-7.

Miley, H. E., Sheader, E. A., Brown, P. D. & Best, L. (1997) Glucose-induced swelling in rat pancreatic beta-cells. *The Journal of physiology*, 504 (Pt 1)(Pt 1), 191-198.

Min, X. J., Li, H., Hou, S. C., He, W., Liu, J., Hu, B. & Wang, J. (2011) Dysfunction of volume-sensitive chloride channels contributes to cisplatin resistance in human lung adenocarcinoma cells. *Exp Biol Med (Maywood)*, 236(4), 483-91.

Mizuno, N. & Itoh, H. (2009) Functions and regulatory mechanisms of Gq-signaling pathways. *Neurosignals*, 17(1), 42-54.

Mongin, A. A. (2016) Volume-regulated anion channel--a frenemy within the brain. *Pflugers Archiv : European journal of physiology*, 468(3), 421-441.

Mongin, A. A. & Kimelberg, H. K. (2002) ATP potently modulates anion channel-mediated excitatory amino acid release from cultured astrocytes. *American Journal of Physiology-Cell Physiology*, 283(2), C569-C578.

Morishima, S., Shimizu, T., Kida, H. & Okada, Y. (2000) Volume expansion sensitivity of swelling-activated Cl(-) channel in human epithelial cells. *Jpn J Physiol*, 50(2), 277-80.

Nakamura, R., Numata, T., Kasuya, G., Yokoyama, T., Nishizawa, T., Kusakizako, T., Kato, T., Hagino, T., Dohmae, N., Inoue, M., Watanabe, K., Ichijo, H., Kikkawa, M., Shirouzu, M., Jentsch,

T. J., Ishitani, R., Okada, Y. & Nureki, O. (2020) Cryo-EM structure of the volume-regulated anion channel LRRC8D isoform identifies features important for substrate permeation. *Communications Biology*, 3(1), 240.

Netti, V., Pizzoni, A., Pérez-Domínguez, M., Ford, P., Pasantes-Morales, H., Ramos-Mandujano, G. & Capurro, C. (2018) Release of taurine and glutamate contributes to cell volume regulation in human retinal Müller cells: differences in modulation by calcium. *J Neurophysiol*, 120(3), 973-984.

Neves, S. R., Ram, P. T. & Iyengar, R. (2002) G protein pathways. *Science*, 296(5573), 1636-9.

Nilius, B. & Droogmans, G. (2003) Amazing chloride channels: an overview. *Acta Physiol Scand*, 177(2), 119-47.

Nilius, B., Eggermont, J., Voets, T., Buyse, G., Manolopoulos, V. & Droogmans, G. (1997a) Properties of volume-regulated anion channels in mammalian cells. *Progress in Biophysics and Molecular Biology*, 68(1), 69-119.

Nilius, B., Eggermont, J., Voets, T., Buyse, G., Manolopoulos, V. & Droogmans, G. (1997b) Properties of volume-regulated anion channels in mammalian cells. *Prog Biophys Mol Biol*, 68(1), 69-119.

Nilius, B., Sehrer, J., Viana, F., De Greef, C., Raeymaekers, L., Eggermont, J. & Droogmans, G. (1994) Volume-activated Cl- currents in different mammalian non-excitable cell types. *Pflugers Arch*, 428(3-4), 364-71.

Nilius, B., Voets, T., Prenen, J., Barth, H., Aktories, K., Kaibuchi, K., Droogmans, G. & Eggermont, J. (1999) Role of Rho and Rho kinase in the activation of volume-regulated anion channels in bovine endothelial cells. *The Journal of physiology*, 516 (Pt 1)(Pt 1), 67-74.

Oiki, S., Kubo, M. & Okada, Y. (1994) Mg2+ and ATP-dependence of volume-sensitive Cl- channels in human epithelial cells. *Jpn J Physiol*, 44 Suppl 2, S77-9.

Okada, Y. (1997) Volume expansion-sensing outward-rectifier Cl- channel: fresh start to the molecular identity and volume sensor. *Am J Physiol*, 273(3 Pt 1), C755-89.

Okada, Y., Maeno, E., Shimizu, T., Dezaki, K., Wang, J. & Morishima, S. (2001) Receptor-mediated control of regulatory volume decrease (RVD) and apoptotic volume decrease (AVD). *The Journal of physiology*, 532(Pt 1), 3-16.

Okada, Y., Okada, T., Sato-Numata, K., Islam, M. R., Ando-Akatsuka, Y., Numata, T., Kubo, M., Shimizu, T., Kurbannazarova, R. S., Marunaka, Y. & Sabirov, R. Z. (2019) Cell Volume-Activated and Volume-Correlated Anion Channels in Mammalian Cells: Their Biophysical, Molecular, and Pharmacological Properties. *Pharmacol Rev*, 71(1), 49-88.

Okada, Y., Shimizu, T., Maeno, E., Tanabe, S., Wang, X. & Takahashi, N. (2006) Volume-sensitive chloride channels involved in apoptotic volume decrease and cell death. *J Membr Biol*, 209(1), 21-9.

Okamoto, H., Takuwa, N., Gonda, K., Okazaki, H., Chang, K., Yatomi, Y., Shigematsu, H. & Takuwa, Y. (1998) EDG1 is a functional sphingosine-1-phosphate receptor that is linked via a Gi/o to multiple signaling pathways, including phospholipase C activation, Ca2+ mobilization,

Ras-mitogen-activated protein kinase activation, and adenylate cyclase inhibition. *J Biol Chem*, 273(42), 27104-10.

Okumura, N., Imai, S., Toyoda, F., Isoya, E., Kumagai, K., Matsuura, H. & Matsusue, Y. (2009) Regulatory role of tyrosine phosphorylation in the swelling-activated chloride current in isolated rabbit articular chondrocytes. *The Journal of physiology*, 587(Pt 15), 3761-3776.

Oldham, W. M. & Hamm, H. E. (2008) Heterotrimeric G protein activation by G-protein-coupled receptors. *Nature Reviews Molecular Cell Biology*, 9(1), 60-71.

Olsen, J. V., Blagoev, B., Gnad, F., Macek, B., Kumar, C., Mortensen, P. & Mann, M. (2006) Global, in vivo, and site-specific phosphorylation dynamics in signaling networks. *Cell*, 127(3), 635-48.

Orlov, S. N., Platonova, A. A., Hamet, P. & Grygorczyk, R. (2013) Cell volume and monovalent ion transporters: their role in cell death machinery triggering and progression. *Am J Physiol Cell Physiol*, 305(4), C361-72.

Orre, L. M., Vesterlund, M., Pan, Y., Arslan, T., Zhu, Y., Fernandez Woodbridge, A., Frings, O., Fredlund, E. & Lehtiö, J. (2019) SubCellBarCode: Proteome-wide Mapping of Protein Localization and Relocalization. *Mol Cell*, 73(1), 166-182.e7.

Osada, M., Yatomi, Y., Ohmori, T., Ikeda, H. & Ozaki, Y. (2002) Enhancement of sphingosine 1-phosphate-induced migration of vascular endothelial cells and smooth muscle cells by an EDG-5 antagonist. *Biochemical and Biophysical Research Communications*, 299(3), 483-487.

Oshima, A., Tani, K. & Fujiyoshi, Y. (2016) Atomic structure of the innexin-6 gap junction channel determined by cryo-EM. *Nature Communications*, 7(1), 13681.

Patel, A. J., Lauritzen, I., Lazdunski, M. & Honoré, E. (1998) Disruption of Mitochondrial Respiration Inhibits Volume-Regulated Anion Channels and Provokes Neuronal Cell Swelling. *The Journal of Neuroscience*, 18(9), 3117.

Pawson, A. J., Sharman, J. L., Benson, H. E., Faccenda, E., Alexander, S. P., Buneman, O. P., Davenport, A. P., McGrath, J. C., Peters, J. A., Southan, C., Spedding, M., Yu, W. & Harmar, A. J. (2014) The IUPHAR/BPS Guide to PHARMACOLOGY: an expert-driven knowledgebase of drug targets and their ligands. *Nucleic Acids Res*, 42(Database issue), D1098-106.

Pedersen, S. F., Beisner, K. H., Hougaard, C., Willumsen, B. M., Lambert, I. H. & Hoffmann, E. K. (2002) Rho family GTP binding proteins are involved in the regulatory volume decrease process in NIH3T3 mouse fibroblasts. *J Physiol*, 541(Pt 3), 779-96.

Pedersen, S. F., Hoffmann, E. K. & Novak, I. (2013) Cell volume regulation in epithelial physiology and cancer. *Front Physiol*, 4, 233.

Pedersen, S. F., Okada, Y. & Nilius, B. (2016) Biophysics and Physiology of the Volume-Regulated Anion Channel (VRAC)/Volume-Sensitive Outwardly Rectifying Anion Channel (VSOR). *Pflügers Archiv - European Journal of Physiology*, 468(3), 371-383.

Pervaiz, S., Kopp, A., von Kleist, L. & Stauber, T. (2019) Absolute Protein Amounts and Relative Abundance of Volume-regulated Anion Channel (VRAC) LRRC8 Subunits in Cells and Tissues Revealed by Quantitative Immunoblotting. *International Journal of Molecular Sciences*, 20(23).

Planells-Cases, R., Lutter, D., Guyader, C., Gerhards, N. M., Ullrich, F., Elger, D. A., Kucukosmanoglu, A., Xu, G., Voss, F. K., Reincke, S. M., Stauber, T., Blomen, V. A., Vis, D. J., Wessels, L. F., Brummelkamp, T. R., Borst, P., Rottenberg, S. & Jentsch, T. J. (2015) Subunit composition of VRAC channels determines substrate specificity and cellular resistance to Pt-based anti-cancer drugs. *Embo j*, 34(24), 2993-3008.

Platt, C. D., Chou, J., Houlihan, P., Badran, Y. R., Kumar, L., Bainter, W., Poliani, P. L., Perez, C. J., Dent, S. Y. R., Clapham, D. E., Benavides, F. & Geha, R. S. (2017) Leucine-rich repeat containing 8A (LRRC8A)-dependent volume-regulated anion channel activity is dispensable for T-cell development and function. *J Allergy Clin Immunol*, 140(6), 1651-1659.e1.

Pohlman, T. H. & Harlan, J. M. (1989) Human endothelial cell response to lipopolysaccharide, interleukin-1, and tumor necrosis factor is regulated by protein synthesis. *Cellular Immunology*, 119(1), 41-52.

Poulsen, K. A., Andersen, E. C., Hansen, C. F., Klausen, T. K., Hougaard, C., Lambert, I. H. & Hoffmann, E. K. (2009) Deregulation of apoptotic volume decrease and ionic movements in multidrug-resistant tumor cells: role of chloride channels. *American Journal of Physiology-Cell Physiology*, 298(1), C14-C25.

Pulli, I., Asghar, M. Y., Kemppainen, K. & Törnquist, K. (2018) Sphingolipid-mediated calcium signaling and its pathological effects. *Biochimica et Biophysica Acta (BBA) - Molecular Cell Research*, 1865(11, Part B), 1668-1677.

Qiu, Z., Dubin, Adrienne E., Mathur, J., Tu, B., Reddy, K., Miraglia, Loren J., Reinhardt, J., Orth, Anthony P. & Patapoutian, A. (2014) SWELL1, a Plasma Membrane Protein, Is an Essential Component of Volume-Regulated Anion Channel. *Cell*, 157(2), 447-458.

Raynor, R. L., Zheng, B. & Kuo, J. F. (1991) Membrane interactions of amphiphilic polypeptides mastoparan, melittin, polymyxin B, and cardiotoxin. Differential inhibition of protein kinase C, Ca2+/calmodulin-dependent protein kinase II and synaptosomal membrane Na,K-ATPase, and Na+ pump and differentiation of HL60 cells. *J Biol Chem*, 266(5), 2753-8.

Regard, J. B., Sato, I. T. & Coughlin, S. R. (2008) Anatomical profiling of G protein-coupled receptor expression. *Cell*, 135(3), 561-71.

Robbins, M. J., Charles, K. J., Harrison, D. C. & Pangalos, M. N. (2002) Localisation of the GPRC5B receptor in the rat brain and spinal cord. *Molecular Brain Research*, 106(1), 136-144.

Robbins, M. J., Michalovich, D., Hill, J., Calver, A. R., Medhurst, A. D., Gloger, I., Sims, M., Middlemiss, D. N. & Pangalos, M. N. (2000) Molecular cloning and characterization of two novel retinoic acid-inducible orphan G-protein-coupled receptors (GPRC5B and GPRC5C). *Genomics*, 67(1), 8-18.

Rorsman, P. & Braun, M. (2013) Regulation of insulin secretion in human pancreatic islets. *Annu Rev Physiol*, 75, 155-79.

Roy, G. (1995) Amino acid current through anion channels in cultured human glial cells. *The Journal of Membrane Biology*, 147(1), 35-44.

Rozengurt, E., Rey, O. & Waldron, R. T. (2005) Protein Kinase D Signaling*. *Journal of Biological Chemistry*, 280(14), 13205-13208.

Rubino, S., Bach, M. D., Schober, A. L., Lambert, I. H. & Mongin, A. A. (2018) Downregulation of Leucine-Rich Repeat-Containing 8A Limits Proliferation and Increases Sensitivity of Glioblastoma to Temozolomide and Carmustine. *Front Oncol*, 8, 142.

Rudkouskaya, A., Chernoguz, A., Haskew-Layton, R. E. & Mongin, A. A. (2008) Two conventional protein kinase C isoforms, alpha and beta I, are involved in the ATP-induced activation of volume-regulated anion channel and glutamate release in cultured astrocytes. *J Neurochem*, 105(6), 2260-70.

Sabirov, R. Z., Prenen, J., Tomita, T., Droogmans, G. & Nilius, B. (2000) Reduction of ionic strength activates single volume-regulated anion channels (VRAC) in endothelial cells. *Pflugers Arch*, 439(3), 315-20.

Sadoshima, J., Qiu, Z., Morgan, J. P. & Izumo, S. (1996) Tyrosine kinase activation is an immediate and essential step in hypotonic cell swelling-induced ERK activation and c-fos gene expression in cardiac myocytes. *Embo j*, 15(20), 5535-46.

Sanchez, T., Skoura, A., Wu, M. T., Casserly, B., Harrington, E. O. & Hla, T. (2007) Induction of vascular permeability by the sphingosine-1-phosphate receptor-2 (S1P2R) and its downstream effectors ROCK and PTEN. *Arterioscler Thromb Vasc Biol*, 27(6), 1312-8.

Sandford, C. A., Sweiry, J. H. & Jenkinson, D. H. (1992) Properties of a cell volume-sensitive potassium conductance in isolated guinea-pig and rat hepatocytes. *J Physiol*, 447, 133-48.

Sanna, M. G., Liao, J., Jo, E., Alfonso, C., Ahn, M. Y., Peterson, M. S., Webb, B., Lefebvre, S., Chun, J., Gray, N. & Rosen, H. (2004) Sphingosine 1-phosphate (S1P) receptor subtypes S1P1 and S1P3, respectively, regulate lymphocyte recirculation and heart rate. *J Biol Chem*, 279(14), 13839-48.

Sawada, A., Takihara, Y., Kim, J. Y., Matsuda-Hashii, Y., Tokimasa, S., Fujisaki, H., Kubota, K., Endo, H., Onodera, T., Ohta, H., Ozono, K. & Hara, J. (2003) A congenital mutation of the novel gene LRRC8 causes agammaglobulinemia in humans. *J Clin Invest*, 112(11), 1707-13.

Schindelin, J., Arganda-Carreras, I., Frise, E., Kaynig, V., Longair, M., Pietzsch, T., Preibisch, S., Rueden, C., Saalfeld, S., Schmid, B., Tinevez, J.-Y., White, D. J., Hartenstein, V., Eliceiri, K., Tomancak, P. & Cardona, A. (2012) Fiji: an open-source platform for biological-image analysis. *Nature Methods*, 9(7), 676-682.

Schober, A. L., Wilson, C. S. & Mongin, A. A. (2017) Molecular composition and heterogeneity of the LRRC8-containing swelling-activated osmolyte channels in primary rat astrocytes. *J Physiol*, 595(22), 6939-6951.

Schumann, M. A., Gardner, P. & Raffin, T. A. (1993) Recombinant human tumor necrosis factor alpha induces calcium oscillation and calcium-activated chloride current in human neutrophils. The role of calcium/calmodulin-dependent protein kinase. *Journal of Biological Chemistry*, 268(3), 2134-2140.

Schwab, A., Fabian, A., Hanley, P. J. & Stock, C. (2012) Role of Ion Channels and Transporters in Cell Migration. *Physiological Reviews*, 92(4), 1865-1913.

Schwiebert, E. M., Mills, J. W. & Stanton, B. A. (1994) Actin-based cytoskeleton regulates a chloride channel and cell volume in a renal cortical collecting duct cell line. *J Biol Chem*, 269(10), 7081-9.

Sebastiani, G., Ceccarelli, E., Castagna, M. G. & Dotta, F. (2018) G-protein-coupled receptors (GPCRs) in the treatment of diabetes: Current view and future perspectives. *Best Practice & Research Clinical Endocrinology & Metabolism*, 32(2), 201-213.

Sekar, R. B. & Periasamy, A. (2003) Fluorescence resonance energy transfer (FRET) microscopy imaging of live cell protein localizations. *The Journal of cell biology*, 160(5), 629-633.

Senju, Y., Rosenbaum, E., Shah, C., Hamada-Nakahara, S., Itoh, Y., Yamamoto, K., Hanawa-Suetsugu, K., Daumke, O. & Suetsugu, S. (2015) Phosphorylation of PACSIN2 by protein kinase C triggers the removal of caveolae from the plasma membrane. *Journal of Cell Science*, 128(15), 2766.

Shen, M. R., Droogmans, G., Eggermont, J., Voets, T., Ellory, J. C. & Nilius, B. (2000) Differential expression of volume-regulated anion channels during cell cycle progression of human cervical cancer cells. *The Journal of physiology*, 529 Pt 2(Pt 2), 385-394.

Shimizu, T., Morishima, S. & Okada, Y. (2000) Ca2+-sensing receptor-mediated regulation of volume-sensitive Cl- channels in human epithelial cells. *J Physiol*, 528(Pt 3), 457-72.

Shimizu, T., Numata, T. & Okada, Y. (2004) A role of reactive oxygen species in apoptotic activation of volume-sensitive Cl(-) channel. *Proc Natl Acad Sci U S A*, 101(17), 6770-3.

Shimizu, T., Ohtake, H., Fujii, T., Tabuchi, Y. & Sakai, H. (2015) Volume-sensitive outwardly rectifying Cl(-) channels contribute to butyrate-triggered apoptosis of murine colonic epithelial MCE301 cells. *J Physiol Sci*, 65(2), 151-7.

Siehler, S. & Manning, D. R. (2002) Pathways of transduction engaged by sphingosine 1-phosphate through G protein-coupled receptors. *Biochim Biophys Acta*, 1582(1-3), 94-9.

Simons, K. & Toomre, D. (2000) Lipid rafts and signal transduction. *Nature Reviews Molecular Cell Biology*, 1(1), 31-39.

Singer, W. D., Brown, H. A. & Sternweis, P. C. (1997) Regulation of eukaryotic phosphatidylinositol-specific phospholipase C and phospholipase D. *Annu Rev Biochem*, 66, 475-509.

Sinnett-Smith, J., Jacamo, R., Kui, R., Wang, Y. M., Young, S. H., Rey, O., Waldron, R. T. & Rozengurt, E. (2009a) Protein Kinase D Mediates Mitogenic Signaling by G_q-coupled Receptors through Protein Kinase C-independent Regulation of Activation Loop Ser⁷⁴⁴ and Ser⁷⁴⁸ Phosphorylation *. *Journal of Biological Chemistry*, 284(20), 13434-13445.

Sinnett-Smith, J., Jacamo, R., Kui, R., Wang, Y. M., Young, S. H., Rey, O., Waldron, R. T. & Rozengurt, E. (2009b) Protein kinase D mediates mitogenic signaling by Gq-coupled receptors through protein kinase C-independent regulation of activation loop Ser744 and Ser748 phosphorylation. *J Biol Chem*, 284(20), 13434-13445.

Sinnett-Smith, J., Rozengurt, N., Kui, R., Huang, C. & Rozengurt, E. (2011) Protein Kinase D1 Mediates Stimulation of DNA Synthesis and Proliferation in Intestinal Epithelial IEC-18 Cells and in Mouse Intestinal Crypts *. *Journal of Biological Chemistry*, 286(1), 511-520.

Sinnett-Smith, J., Zhukova, E., Rey, O. & Rozengurt, E. (2007) Protein kinase D2 potentiates MEK/ERK/RSK signaling, c-Fos accumulation and DNA synthesis induced by bombesin in Swiss 3T3 cells. *J Cell Physiol*, 211(3), 781-90.

Sirianant, L., Wanitchakool, P., Ousingsawat, J., Benedetto, R., Zormpa, A., Cabrita, I., Schreiber, R. & Kunzelmann, K. (2016) Non-essential contribution of LRRC8A to volume regulation. *Pflügers Archiv - European Journal of Physiology*, 468(5), 805-816.

Siripurapu, P., Kankanamge, D., Ratnayake, K., Senarath, K. & Karunarathne, A. (2017) Two independent but synchronized Gβγ subunit-controlled pathways are essential for trailing-edge retraction during macrophage migration. *J Biol Chem*, 292(42), 17482-17495.

Smith, C. A., Farrah, T. & Goodwin, R. G. (1994) The TNF receptor superfamily of cellular and viral proteins: activation, costimulation, and death. *Cell*, 76(6), 959-62.

Smrcka, A. V. (2008) G protein βγ subunits: Central mediators of G protein-coupled receptor signaling. *Cellular and Molecular Life Sciences*, 65(14), 2191-2214.

Son, D. J., Kang, J., Kim, T. J., Song, H.-S., Sung, K.-J., Yun, D. Y. & Hong, J. T. (2007) Melittin, A Major Bioactive Component of Bee Venom Toxin, Inhibits PDGF Receptor Beta-tyrosine Phosphorylation and Downstream Intracellular Signal Transduction in Rat Aortic Vascular Smooth Muscle Cells. *Journal of Toxicology and Environmental Health, Part A*, 70(15-16), 1350-1355.

Soni, A., Amisten, S., Rorsman, P. & Salehi, A. (2013) GPRC5B a putative glutamate-receptor candidate is negative modulator of insulin secretion. *Biochemical and Biophysical Research Communications*, 441(3), 643-648.

Sorota, S. (1995) Tyrosine protein kinase inhibitors prevent activation of cardiac swelling-induced chloride current. *Pflügers Archiv*, 431(2), 178-185.

Stauber, T. & Jentsch, T. J. (2010) Sorting motifs of the endosomal/lysosomal CLC chloride transporters. *J Biol Chem*, 285(45), 34537-48.

Stehno-Bittel, L., Krapivinsky, G., Krapivinsky, L., Perez-Terzic, C. & Clapham, D. E. (1995) The G protein beta gamma subunit transduces the muscarinic receptor signal for Ca2+ release in Xenopus oocytes. *J Biol Chem*, 270(50), 30068-74.

Stephens, L., Smrcka, A., Cooke, F. T., Jackson, T. R., Sternweis, P. C. & Hawkins, P. T. (1994) A novel phosphoinositide 3 kinase activity in myeloid-derived cells is activated by G protein βγ subunits. *Cell*, 77(1), 83-93.

Strange, K., Emma, F. & Jackson, P. S. (1996) Cellular and molecular physiology of volume-sensitive anion channels. *Am J Physiol*, 270(3 Pt 1), C711-30.

Strange, K., Yamada, T. & Denton, J. S. (2019) A 30-year journey from volume-regulated anion currents to molecular structure of the LRRC8 channel. *Journal of General Physiology*, 151(2), 100-117.

Stroka, Kimberly M., Jiang, H., Chen, S.-H., Tong, Z., Wirtz, D., Sun, Sean X. & Konstantopoulos, K. (2014) Water Permeation Drives Tumor Cell Migration in Confined Microenvironments. *Cell*, 157(3), 611-623.

Stryer, L. & Haugland, R. P. (1967) Energy transfer: a spectroscopic ruler. *Proceedings of the National Academy of Sciences*, 58(2), 719.

Stuhlmann, T., Planells-Cases, R. & Jentsch, T. J. (2018) LRRC8/VRAC anion channels enhance β-cell glucose sensing and insulin secretion. *Nature Communications*, 9(1), 1974.

Syeda, R., Qiu, Z., Dubin, Adrienne E., Murthy, Swetha E., Florendo, Maria N., Mason, Daniel E., Mathur, J., Cahalan, Stuart M., Peters, Eric C., Montal, M. & Patapoutian, A. (2016) LRRC8 Proteins Form Volume-Regulated Anion Channels that Sense Ionic Strength. *Cell*, 164(3), 499-511.

Syrovatkina, V., Alegre, K. O., Dey, R. & Huang, X. Y. (2016) Regulation, Signaling, and Physiological Functions of G-Proteins. *J Mol Biol*, 428(19), 3850-68.

Szabò, I., Lepple-Wienhues, A., Kaba, K. N., Zoratti, M., Gulbins, E. & Lang, F. (1998a) Tyrosine kinase-dependent activation of a chloride channel in CD95-induced apoptosis in T lymphocytes. *Proc Natl Acad Sci U S A*, 95(11), 6169-74.

Szabò, I., Lepple-Wienhues, A., Kaba, K. N., Zoratti, M., Gulbins, E. & Lang, F. (1998b) Tyrosine kinase-dependent activation of a chloride channel in CD95-induced apoptosis in T lymphocytes. *Proceedings of the National Academy of Sciences*, 95(11), 6169.

Szücs, G., Heinke, S., De Greef, C., Raeymaekers, L., Eggermont, J., Droogmans, G. & Nilius, B. (1996) The volume-activated chloride current in endothelial cells from bovine pulmonary artery is not modulated by phosphorylation. *Pflügers Archiv*, 431(4), 540-548.

Tabcharani, J. A., Chang, X. B., Riordan, J. R. & Hanrahan, J. W. (1991) Phosphorylation-regulated Cl- channel in CHO cells stably expressing the cystic fibrosis gene. *Nature*, 352(6336), 628-31.

Takasaki, J., Saito, T., Taniguchi, M., Kawasaki, T., Moritani, Y., Hayashi, K. & Kobori, M. (2004) A novel Galphaq/11-selective inhibitor. *J Biol Chem*, 279(46), 47438-45.

Takuwa, Y., Okamoto, Y., Yoshioka, K. & Takuwa, N. (2012) Sphingosine-1-phosphate signaling in physiology and diseases. *Biofactors*, 38(5), 329-37.

Ternovsky, V. I., Okada, Y. & Sabirov, R. Z. (2004) Sizing the pore of the volume-sensitive anion channel by differential polymer partitioning. *FEBS Lett*, 576(3), 433-6.

Thoroed, S. M., Bryan-Sisneros, A. & Doroshenko, P. (1999) Protein phosphotyrosine phosphatase inhibitors suppress regulatory volume decrease and the volume-sensitive Cl- conductance in mouse fibroblasts. *Pflugers Arch*, 438(2), 133-40.

Tilly, B. C., Edixhoven, M. J., Tertoolen, L. G., Morii, N., Saitoh, Y., Narumiya, S. & de Jonge, H. R. (1996) Activation of the osmo-sensitive chloride conductance involves P21rho and is accompanied by a transient reorganization of the F-actin cytoskeleton. *Mol Biol Cell*, 7(9), 1419-27.

Tilly, B. C., van den Berghe, N., Tertoolen, L. G., Edixhoven, M. J. & de Jonge, H. R. (1993) Protein tyrosine phosphorylation is involved in osmoregulation of ionic conductances. *J Biol Chem*, 268(27), 19919-22.

Tominaga, K., Kondo, C., Kagata, T., Hishida, T., Nishizuka, M. & Imagawa, M. (2004) The novel gene fad158, having a transmembrane domain and leucine-rich repeat, stimulates adipocyte differentiation. *J Biol Chem*, 279(33), 34840-8.

Trothe, J., Ritzmann, D., Lang, V., Scholz, P., Pul, Ü., Kaufmann, R., Buerger, C. & Ertongur-Fauth, T. (2018) Hypotonic stress response of human keratinocytes involves LRRC8A as component of volume-regulated anion channels. *Exp Dermatol*, 27(12), 1352-1360.

Ullrich, F., Reincke, S. M., Voss, F. K., Stauber, T. & Jentsch, T. J. (2016) Inactivation and Anion Selectivity of Volume-regulated Anion Channels (VRACs) Depend on C-terminal Residues of the First Extracellular Loop *. *Journal of Biological Chemistry*, 291(33), 17040-17048.

Vakili, A., Hosseinzadeh, S. A. & Khorasani, M. Z. (2009) Peripheral administration of carbenoxolone reduces ischemic reperfusion injury in transient model of cerebral ischemia. *J Stroke Cerebrovasc Dis*, 18(2), 81-5.

van der Knaap, M. S., Boor, I. & Estévez, R. (2012) Megalencephalic leukoencephalopathy with subcortical cysts: chronic white matter oedema due to a defect in brain ion and water homoeostasis. *Lancet Neurol*, 11(11), 973-85.

Van Lint, J., Sinnett-Smith, J. & Rozengurt, E. (1995) Expression and Characterization of PKD, a Phorbol Ester and Diacylglycerol-stimulated Serine Protein Kinase (∗). *Journal of Biological Chemistry*, 270(3), 1455-1461.

Vandenberg, J. I., Yoshida, A., Kirk, K. & Powell, T. (1994) Swelling-activated and isoprenaline-activated chloride currents in guinea pig cardiac myocytes have distinct electrophysiology and pharmacology. *J Gen Physiol*, 104(6), 997-1017.

Varela, D., Simon, F., Riveros, A., Jørgensen, F. & Stutzin, A. (2004) NAD(P)H oxidase-derived H(2)O(2) signals chloride channel activation in cell volume regulation and cell proliferation. *J Biol Chem*, 279(14), 13301-4.

Voets, T., Droogmans, G. & Nilius, B. (1997) Modulation of Voltage-dependent Properties of a Swelling-activated Cl− Current. *Journal of General Physiology*, 110(3), 313-325.

Voets, T., Droogmans, G., Raskin, G., Eggermont, J. & Nilius, B. (1999) Reduced intracellular ionic strength as the initial trigger for activation of endothelial volume-regulated anion channels. *Proceedings of the National Academy of Sciences*, 96(9), 5298.

Voets, T., Manolopoulos, V., Eggermont, J., Ellory, C., Droogmans, G. & Nilius, B. (1998) Regulation of a swelling-activated chloride current in bovine endothelium by protein tyrosine phosphorylation and G proteins. *J Physiol*, 506 (Pt 2)(Pt 2), 341-52.

Voets, T., Szücs, G., Droogmans, G. & Nilius, B. (1995) Blockers of volume-activated Cl- currents inhibit endothelial cell proliferation. *Pflugers Arch*, 431(1), 132-4.

Volonté, D., Galbiati, F., Pestell, R. G. & Lisanti, M. P. (2001) Cellular stress induces the tyrosine phosphorylation of caveolin-1 (Tyr(14)) via activation of p38 mitogen-activated protein kinase and

c-Src kinase. Evidence for caveolae, the actin cytoskeleton, and focal adhesions as mechanical sensors of osmotic stress. *J Biol Chem*, 276(11), 8094-103.

von Weikersthal, S. F., Barrand, M. A. & Hladky, S. B. (1999) Functional and molecular characterization of a volume-sensitive chloride current in rat brain endothelial cells. *The Journal of physiology*, 516 (Pt 1), 75-84.

Voss, F. K., Ullrich, F., Münch, J., Lazarow, K., Lutter, D., Mah, N., Andrade-Navarro, M. A., von Kries, J. P., Stauber, T. & Jentsch, T. J. (2014) Identification of LRRC8 Heteromers as an Essential Component of the Volume-Regulated Anion Channel VRAC. *Science*, 344(6184), 634.

Waldo, G. L., Ricks, T. K., Hicks, S. N., Cheever, M. L., Kawano, T., Tsuboi, K., Wang, X., Montell, C., Kozasa, T., Sondek, J. & Harden, T. K. (2010) Kinetic scaffolding mediated by a phospholipase C-beta and Gq signaling complex. *Science*, 330(6006), 974-80.

Waldron, R. T., Innamorati, G., Torres-Marquez, M. E., Sinnett-Smith, J. & Rozengurt, E. (2012) Differential PKC-dependent and -independent PKD activation by G protein α subunits of the Gq family: Selective stimulation of PKD Ser748 autophosphorylation by Gαq. *Cellular Signalling*, 24(4), 914-921.

Waldron, R. T. & Rozengurt, E. (2000) Oxidative stress induces protein kinase D activation in intact cells. Involvement of Src and dependence on protein kinase C. *J Biol Chem*, 275(22), 17114-21.

Wallach, D., Varfolomeev, E. E., Malinin, N. L., Goltsev, Y. V., Kovalenko, A. V. & Boldin, M. P. (1999) TUMOR NECROSIS FACTOR RECEPTOR AND Fas SIGNALING MECHANISMS. *Annual Review of Immunology*, 17(1), 331-367.

Wang, E., He, X. & Zeng, M. (2019a) The Role of S1P and the Related Signaling Pathway in the Development of Tissue Fibrosis. *Frontiers in Pharmacology*, 9(1504).

Wang, P., Yuan, Y., Lin, W., Zhong, H., Xu, K. & Qi, X. (2019b) Roles of sphingosine-1-phosphate signaling in cancer. *Cancer Cell International*, 19(1), 295.

Wang, R., Lu, Y., Gunasekar, S., Zhang, Y., Benson, C. J., Chapleau, M. W., Sah, R. & Abboud, F. M. (2017) The volume-regulated anion channel (LRRC8) in nodose neurons is sensitive to acidic pH. *JCI Insight*, 2(5), e90632.

Wang, Y., Ren, F., Chen, P., Liu, S., Song, Z. & Ma, X. (2018) Identification of a six-gene signature with prognostic value for patients with endometrial carcinoma. *Cancer Med*, 7(11), 5632-5642.

Watson, S. & Girdlestone, D. (1994) TiPS receptor and ion channel nomenclature supplement 1994. *Trends in Pharmacological Sciences*, 15, 1-51.

Watters, R. J., Wang, H.-G., Sung, S.-S., Loughran, T. P. & Liu, X. (2011a) Targeting sphingosine-1-phosphate receptors in cancer. *Anti-cancer agents in medicinal chemistry*, 11(9), 810-817.

Watters, R. J., Wang, H. G., Sung, S. S., Loughran, T. P. & Liu, X. (2011b) Targeting sphingosine-1-phosphate receptors in cancer. *Anticancer Agents Med Chem*, 11(9), 810-7.

Wong, R., Chen, W., Zhong, X., Rutka, J. T., Feng, Z. P. & Sun, H. S. (2018) Swelling-induced chloride current in glioblastoma proliferation, migration, and invasion. *J Cell Physiol*, 233(1), 363-370.

Xia, P., Wang, L., Gamble, J. R. & Vadas, M. A. (1999) Activation of sphingosine kinase by tumor necrosis factor-alpha inhibits apoptosis in human endothelial cells. *J Biol Chem*, 274(48), 34499-505.

Xiao, L., Zhou, Y., Friis, T., Beagley, K. & Xiao, Y. (2019) S1P-S1PR1 Signaling: the “Sphinx” in Osteoimmunology. *Frontiers in Immunology*, 10(1409).

Xue, Y., Li, H., Zhang, Y., Han, X., Zhang, G., Li, W., Zhang, H., Lin, Y., Chen, P., Sun, X., Liu, Y., Chu, L., Zhang, J., Zhang, M. & Zhang, X. (2018) Natural and synthetic flavonoids, novel blockers of the volume-regulated anion channels, inhibit endothelial cell proliferation. *Pflugers Arch*, 470(10), 1473-1483.

Yamada, T. & Strange, K. (2018) Intracellular and extracellular loops of LRRC8 are essential for volume-regulated anion channel function. *Journal of General Physiology*, 150(7), 1003-1015.

Yamada, T., Wondergem, R., Morrison, R., Yin, V. P. & Strange, K. (2016) Leucine-rich repeat containing protein LRRC8A is essential for swelling-activated Cl- currents and embryonic development in zebrafish. *Physiol Rep*, 4(19).

Yamamoto, S., Ichishima, K. & Ehara, T. (2008) Regulation of volume-regulated outwardly rectifying anion channels by phosphatidylinositol 3,4,5-trisphosphate in mouse ventricular cells. *Biomed Res*, 29(6), 307-15.

Yang, J., Vitery, M. D. C., Chen, J., Osei-Owusu, J., Chu, J. & Qiu, Z. (2019) Glutamate-Releasing SWELL1 Channel in Astrocytes Modulates Synaptic Transmission and Promotes Brain Damage in Stroke. *Neuron*, 102(4), 813-827.e6.

Yeung, C. H., Barfield, J. P. & Cooper, T. G. (2006) Physiological volume regulation by spermatozoa. *Mol Cell Endocrinol*, 250(1-2), 98-105.

Yuan, J., Slice, L., Walsh, J. H. & Rozengurt, E. (2000) Activation of protein kinase D by signaling through the alpha subunit of the heterotrimeric G protein G(q). *J Biol Chem*, 275(3), 2157-64.

Yuan, J., Slice, L. W., Gu, J. & Rozengurt, E. (2003) Cooperation of Gq, Gi, and G12/13 in protein kinase D activation and phosphorylation induced by lysophosphatidic acid. *J Biol Chem*, 278(7), 4882-91.

Yuan, J., Slice, L. W. & Rozengurt, E. (2001) Activation of protein kinase D by signaling through Rho and the alpha subunit of the heterotrimeric G protein G13. *J Biol Chem*, 276(42), 38619-27.

Zachariassen, L. G., Katchan, L., Jensen, A. G., Pickering, D. S., Plested, A. J. R. & Kristensen, A. S. (2016) Structural rearrangement of the intracellular domains during AMPA receptor activation. *Proceedings of the National Academy of Sciences*, 113(27), E3950.

Zahiri, D., Burow, P., Großmann, C., Müller, C. E., Klapperstück, M. & Markwardt, F. (2021) Sphingosine-1-phosphate induces migration of microglial cells via activation of volume-sensitive anion channels, ATP secretion and activation of purinergic receptors. *Biochimica et Biophysica Acta (BBA) - Molecular Cell Research*, 1868(2), 118915.

Zhang, H., Deng, Z., Zhang, D., Li, H., Zhang, L., Niu, J., Zuo, W., Fu, R., Fan, L., Ye, J. H. & She, J. (2018) High expression of leucine-rich repeat-containing 8A is indicative of a worse outcome of colon cancer patients by enhancing cancer cell growth and metastasis. *Oncol Rep*, 40(3), 1275-1286.

Zhang, J. & Lieberman, M. (1996) Chloride conductance is activated by membrane distention of cultured chick heart cells. *Cardiovascular Research*, 32(1), 168-179.

Zhang, N., Deng, Z., Li, W., Zou, Y., Xiong, J., Duan, L. & Wang, D. (2021) Expression of LRRC8A is elevated in the cytoplasm of osteosarcoma tissues: An immunohistochemical study with tissue microarrays. *Exp Ther Med*, 21(1), 71.

Zhang, Y., Xie, L., Gunasekar, S. K., Tong, D., Mishra, A., Gibson, W. J., Wang, C., Fidler, T., Marthaler, B., Klingelhutz, A., Abel, E. D., Samuel, I., Smith, J. K., Cao, L. & Sah, R. (2017) SWELL1 is a regulator of adipocyte size, insulin signalling and glucose homeostasis. *Nat Cell Biol*, 19(5), 504-517.

Zhang, Y., Zhang, H., Feustel, P. J. & Kimelberg, H. K. (2008) DCPIB, a specific inhibitor of volume regulated anion channels (VRACs), reduces infarct size in MCAo and the release of glutamate in the ischemic cortical penumbra. *Exp Neurol*, 210(2), 514-20.

Zholos, A., Beck, B., Sydorenko, V., Lemonnier, L., Bordat, P., Prevarskaya, N. & Skryma, R. (2005) Ca(2+)- and volume-sensitive chloride currents are differentially regulated by agonists and store-operated Ca2+ entry. *J Gen Physiol*, 125(2), 197-211.

Zhou, C., Chen, X., Planells-Cases, R., Chu, J., Wang, L., Cao, L., Li, Z., López-Cayuqueo, K. I., Xie, Y., Ye, S., Wang, X., Ullrich, F., Ma, S., Fang, Y., Zhang, X., Qian, Z., Liang, X., Cai, S.-Q., Jiang, Z., Zhou, D., Leng, Q., Xiao, T. S., Lan, K., Yang, J., Li, H., Peng, C., Qiu, Z., Jentsch, T. J. & Xiao, H. (2020) Transfer of cGAMP into Bystander Cells via LRRC8 Volume-Regulated Anion Channels Augments STING-Mediated Interferon Responses and Anti-viral Immunity. *Immunity*, 52(5), 767-781.e6.

Zhou, H., Di Palma, S., Preisinger, C., Peng, M., Polat, A. N., Heck, A. J. R. & Mohammed, S. (2013) Toward a Comprehensive Characterization of a Human Cancer Cell Phosphoproteome. *Journal of Proteome Research*, 12(1), 260-271.

Zhukova, E., Sinnett-Smith, J. & Rozengurt, E. (2001) Protein kinase D potentiates DNA synthesis and cell proliferation induced by bombesin, vasopressin, or phorbol esters in Swiss 3T3 cells. *J Biol Chem*, 276(43), 40298-305.

Zugaza, J. L., Waldron, R. T., Sinnett-Smith, J. & Rozengurt, E. (1997) Bombesin, vasopressin, endothelin, bradykinin, and platelet-derived growth factor rapidly activate protein kinase D through a protein kinase C-dependent signal transduction pathway. *J Biol Chem*, 272(38), 23952-60.